INVESTIGATIONS INTO SIGMA FACTOR C REGULATION AND COENZYME B_{12} SYNTHESIS IN MYCOBACTERIUM TUBERCULOSIS

by

SAMANTHA LYNN TUCKER

(Under the Direction of Russell Karls)

ABSTRACT

Tuberculosis (TB) is one of the oldest and most-deadly human diseases. The main etiological agent, *Mycobacterium tuberculosis*, caused approximately 10.4 million new infections and 1.6 million deaths in 2016. The World Health Organization estimates that 1/3 of the world population harbors a latent TB infection. This pathogen can survive asymptomatically in the host for decades, but the extent of its metabolic activity during such latent infections is unclear. To respire and metabolize in host cells, *M. tuberculosis* must acquire essential metals and acquire or synthesize enzyme cofactors. Herein we explore control of the copper-acquisition sigma factor, SigC, by copper. We also interrogate genes predicted to function in the synthesis of co-enzyme B_{12} (Co-B_{12}) in *M. tuberculosis*.

Copper is a cofactor of electron-transfer enzymes, including a Zn/Cu-dependent superoxide dismutase, and a type a/a3 respiratory complex in *M. tuberculosis*. Intracellular free copper levels are nearly undetectable; therefore, pathogenic bacteria have evolved mechanisms to scavenge this essential metal. The *sigC* gene enables growth in copper-starved medium and upregulates expression of *ctpB* and the *PPE1-nrp* operon.

Here, we demonstrate *sigC* is absolutely required for growth in copper-chelated medium and that copper destabilizes SigC in *M. tuberculosis*. This supports a model in which SigC is post-translationally regulated by copper levels.

In *M. tuberculosis*, Co-B_{12} functions in methionine synthesis, fatty-acid metabolism, and ribonucleotide reduction. To understand the role of Co-B_{12} in *M. tuberculosis*, we assessed predicted Co-B_{12} biosynthetic genes from *M. tuberculosis* in *Salmonella* Typhimurium Co-B_{12} synthesis pathway mutants. Results indicate that 16 genes functionally complement late-cobalt insertion specific Co-B_{12} biosynthetic genes from *S.* Typhimurium. These data suggest that *M. tuberculosis* may synthesize Co-B_{12} in low oxygen environments in its host. Hypoxic *in vitro* cultivation of *M. tuberculosis* did not result in detectable Co-B_{12} synthesis, suggesting that other signals or factors may be required. This body of work expands the knowledge base of mechanisms for survival and metabolism by *M. tuberculosis*, and informs future research to target critical components in the development of effective antibiotics and vaccines.

INDEX WORDS: *Mycobacterium tuberculosis*, Sigma Factor, SigC, Copper, Metal Acquisition, Chelator, Coenzyme B_{12}, Metabolism, Gene Regulation

INVESTIGATIONS INTO SIGMA FACTOR C REGULATION AND COENZYME B_{12} SYNTHESIS IN MYCOBACTERIUM TUBERCULOSIS

by

SAMANTHA LYNN TUCKER

B.S., Allegheny College, 2012

A Dissertation Submitted to the Graduate Faculty of The University of Georgia in Partial Fulfillment of the Requirements for the Degree

DOCTOR OF PHILOSOPHY

ATHENS, GEORGIA

2018

INVESTIGATIONS INTO SIGMA FACTOR C REGULATION AND COENZYME B_{12} SYNTHESIS IN MYCOBACTERIUM TUBERCULOSIS

by

SAMANTHA LYNN TUCKER

Major Professor:	Russell Karls
Committee:	Frederick Quinn
	Anna Karls
	Jorge Escalante-Semerena
	Vincent Starai

Electronic Version Approved:

Suzanne Barbour
Dean of the Graduate School
The University of Georgia
May 2018

DEDICATION

This work is dedicated to my family and friends, past and present.

ACKNOWLEDGEMENTS

There are so many people to acknowledge and thank for helping me on this journey. First, my advisor, Dr. Russell Karls has been an excellent mentor and source of guidance. His attention to detail and dedication to his students is beyond comparison. Dr. Karls' willingness to discuss ideas and plans has shaped my investigative skills and has allowed me to develop into the type of scientist that I wanted to become. I would also like to thank my committee members for their incredible insight, kindness, and willingness to collaborate with me; offering so much advice, reagents, and equipment to help me achieve my goals. Next, Shelly Helms has been a voice of guidance in the lab, and an outstanding friend everywhere else. Her advice and friendship, our office dinosaurs, get-away lunches, and cookie parties have made this experience so bright.

I also acknowledge my amazing family members and friends, who have supported me and are always available when I need them. I thank my father for always talking me through my most difficult decisions over a gin, my mother for all of her love and support, and my sister for always looking out for me. Next, I would like to acknowledge my fiancé, Keith who is always a voice of love and reason, and is a feeling of home. Lastly, I have some of the greatest friends, and I thank them for their support, love, and sticking by me even with my crazy schedule. Especially Robin for always being there to listen and help, and for staying close and Adrian for always pushing through challenges and finding the positives in life, and helping me to do the same.

TABLE OF CONTENTS

Page

LIST OF TABLES

Page

LIST OF FIGURES

Page

CHAPTER 1

INTRODUCTION

Despite the long history of tuberculosis disease (TB) in humans and efforts to eradicate it, *Mycobacterium tuberculosis* remains a leading cause of morbidity and mortality by a single etiological agent (1). According to the 2017 World Health Organizations (WHO) Tuberculosis World Report, 10.4 million people developed TB disease and 1.6 million deaths from the disease occurred in 2016 (1). Among new infections, 3.5% of cases were multidrug-resistant TB (MDR-TB), with 9% of these being extensively drug-resistant (XDR-TB) (1). The widely-used TB vaccine, bacille Calmette-Guérin (BCG), is a live-attenuated strain of *Mycobacterium bovis* developed post World War I by Albert Calmette and Camille Guérin (2). While this vaccine provides protection against disseminating forms of TB, such as meningitis, in young children, its efficacy in adults is low (2). Given the global health threat of TB and the rise in MDR-TB incidence, continued study of this pathogen is imperative. A better understanding of *M. tuberculosis* physiology and metabolism within the human host will lead to more rational and hypothesis-driven drug and vaccine design.

Sigma factor C (SigC) is one of 13 identified sigma factors in *M. tuberculosis*. This transcription initiation factor is necessary for *M. tuberculosis* virulence in both murine and guinea pig infection models (3, 4). SigC promoter binding sites were identified upstream of *ctpB*, which encodes a putative metal-binding P-type ATPase, as well as upstream of the *PPE1-nrp* operon (5, 6). The *Mycobacterium marinum* homolog

of this operon is predicted to encode proteins that produce a metal chelator (7). There is no identified anti-sigma factor for SigC (8). Two promoter regions have been located upstream of *sigC*, which is transcribed at high levels; however, *sigC* is not auto-regulated (9, 10). Understanding the mechanism of regulation for SigC in relation to metal availability is the first focus of this dissertation.

Many eukaryotic and prokaryotic organisms, including *M. tuberculosis*, utilize cobalamin, also known as Co-enzyme B_{12} or Co-B_{12}, as a cofactor for three main types of enzymes: corrinoid dehalogenases, methyltransferases, and isomerases (11). In *M. tuberculosis*, there are three Co-B_{12}-dependent enzymes: a methionine synthase (MetH), methylmalonyl-CoA mutase (MutAB), and a class II ribonucleotide reductase (NrdZ). Additionally, the *M. tuberculosis* genome encodes homologs to many of the Co-B_{12} biosynthetic enzymes characterized in other organisms. Despite this, there is limited evidence suggesting that *M. tuberculosis* and other TB-causing mycobacteria synthesize Co-B_{12} *in vitro* (12–14). Examining the function of predicted Co-B_{12} biosynthetic genes and the production of Co-B_{12} in *M. tuberculosis* is the second focus of this dissertation.

CHAPTER 2

LITERATURE REVIEW

2.1. *MYCOBACTERIUM TUBERCULOSIS*

History and Taxonomy

Mycobacterium tuberculosis is an intracellular human pathogen and the main causative agent of tuberculosis (TB) disease in humans. It is in the family of Mycobacteriaceae and the order Actinobacteria. Phylogenetic analysis supports origination of *M. tuberculosis* in East Africa about 70,000 years ago and co-evolution of this pathogen with humans (15). Written accounts of TB disease in ancient Egyptian, Indian, and Chinese date back about 5,000 years. Evidence of TB disease has been found in mummified human remains from ancient Egypt and from ancient Peru (2, 16). In the 1800s, the high prevalence of TB in Europe led to glamorization of the outward appearances caused by the disease such as red lips, glassy eyes, and thin bodies (2).

It was not until 1865 that TB was shown to be caused by infection. Jean-Antione Villemin transferred fluid from a TB victim to a rabbit, and showed evidence of disease transmission (2). Nearly 20 years later, in 1882, Robert Koch was the first to culture *M. tuberculosis* on solid medium. Subsequently, in 1890, he reported the potential of the protein mixture tuberculin derived from the bacteria for prevention and diagnosis of TB disease (17). Work on tuberculin by Clemens Freiherr von Pirquet and Charles Mantoux

established a test for infection based on the immune response to the *M. tuberculosis* antigens (2). In the 1930s, Florence Seibert developed the purified protein derivative (PPD) skin test for *M. tuberculosis* diagnosis. This diagnostic test is nearly identical to the PPD diagnostic used today (2).

Epidemiology

Tuberculosis is the leading cause of death in humans from a single infectious agent world-wide and approximately 1/3 of the human population is latently infected with the etiological agent. About 20 countries, mainly in Sub-Saharan Africa and Asia account for 90% of the global TB burden (1). For 2016, 4.1% of new cases and 19% of previously-treated TB cases were rifampicin-resistant TB (RR-TB) or rifampicin and isoniazid-resistant TB (MDR-TB). Of these, 6.2% were considered extensively drug resistant (XDR-TB) meaning that the *M. tuberculosis* isolate was resistant to rifampicin, isoniazid, fluoroqinolones, and at least one second-line injectable, such as kanamycin, capreomycin, or amikacin (1).

While the majority of human TB cases are caused by *M. tuberculosis*, there are 9 mycobacterial species that currently make up the *M. tuberculosis* complex (MTC). These bacteria cause TB, or TB-like disease in mammals. The MTC includes human pathogens: *M. tuberculosis, M. africanum, and M. canettii*; the Bovidae family pathogens: *M. bovis, M. caprae*, *M. mungi, and M. orygis*; the rodent pathogen *M. microti*; and the pinniped pathogen *M. pinnipedii* (18). The most-common zoonotic source of human TB is from cattle infected with *M. bovis*; Approximately 1-2% of TB cases annually in the US result from *M. bovis* infection (19). Globally there were 147,000 reported cases and 12,500

deaths related to zoonotic TB in 2016. Unfortunately, with limitations of diagnostic and reporting methods the actual burden of zoonotic TB is thought to be much higher (20).

Cell Wall

The rod-like *M. tuberculosis* bacilli are identified clinically by Ziehl-Neelsen acid-fast staining of the thick lipid-rich cell wall. The cell wall of *M. tuberculosis* consists of lipid/glycolipid/peptidoglycan matrices featuring an outer membrane which includes 70-90 carbon-length mycolic acids covalently anchored to the arabinogalactan matrix that is attached to the peptidoglycan layer, which is bound to the cytoplasmic membrane (21). The surface lipids of *M. tuberculosis* provide a hydrophobic barrier that protects against polar antibiotics, antimicrobial peptides, reactive oxygen and nitrogen radicals generated by innate and adaptive host immune systems, other toxic molecules, and mechanical damage. The outer leaflet of the outer membrane includes multiple types of glycolipids including trehalose-glycolipids, phenolic-glycolipids, lipomannan and lipoarabinomannan (22). Also present are virulence-associated lipids, phthiocerol dimycocerosates (PDIMs), that consist of 28 carbon-length fatty acids derived from branched methylmalonyl units (22). Within the *M. tuberculosis* genome, a 50-kb region encompassing 13 genes has been shown to be required for PDIM synthesis (23). It has also been shown that PDIM lipids aid in protection against reactive nitrogen intermediates and are major contributors to virulence (24–26). Synthesis of PDIM lipids also function as a means for dissipating build-up of propionyl-CoA. When *M. tuberculosis* utilizes odd carbon-length fatty acids, such as those derived from cholesterol as a carbon source, propionyl-CoA is generated (27). Build-up of propionyl-CoA can lead

to blockage of gluconeogenesis and depletion of TCA-cycle intermediates (28, 29). One way *M. tuberculosis* assimilates excess propionyl-CoA is through conversion into methylmalonyl-CoA by the Co-B_{12}-dependent methylmalonyl-CoA mutase. The molecule can then be used as a precursor for cell wall lipid synthesis (30).

Growth Requirements

The *M. tuberculosis* bacilli are non-motile and non-sporulating (31, 32). The doubling time of *M. tuberculosis* ranges from 12-48 hours depending on growth conditions and carbon source availability. Studies have shown that during infection, *M. tuberculosis* utilizes glycerol, fatty acids, and cholesterol as carbon sources (30, 33, 34). This dynamic range allows *M. tuberculosis* to survive in multiple niches within the host including inside of the macrophages, granulomas, and adipose tissue (35). During initial infection, these bacteria respire aerobically; however, the bacilli will respire and persist in microaerophilic/hypoxic environments, such as within tubercles (aka granulomas) generated by host immune responses to wall in infection centers (36, 37). The Wayne culture method is an established model for inducing *M. tuberculosis* dormancy by allowing the bacteria to grow and deplete the oxygen in a sealed vessel with a fixed head-space to culture-volume ratio (36). When cultured using the Wayne method, *M. tuberculosis* will reach a state of non-replicating persistence, which is proposed to model aspects of latent *M. tuberculosis* infection. The DosRST regulatory system controls gene expression leading to non-replicating persistence. As the bacteria sense a reduction in oxygen levels, the DosRST system upregulates genes involved in nitrate reduction, fatty-acid metabolism, and DNA repair (38, 39). This system also helps the bacteria emerge

from a dormant state and re-establish growth upon sensing an oxygenated environment (38, 40). The DosRST regulon has also been shown to be required for *M. tuberculosis* survival in mouse and guinea pig infection models (41). Another culture method to produce a microaerophilic environment is static culture of *M. tuberculosis* in minimal media to form a pellicle of growth at the aerobic/liquid interface (42–44). When grown as a pellicle, *M. tuberculosis* is physiologically distinct from *M. tuberculosis* grown in shaking cultures; pellicle cultures produce more mycolic acids and express more immunogenic surface antigens (44, 45). Both Wayne cultures and pellicle cultures of *M. tuberculosis* exhibit phenotypic antibiotic tolerance that is not evident in shaking cultures (36, 44, 46). This antibiotic tolerance is a characteristic of *M. tuberculosis* infection and has been demonstrated in a humanized mouse model (46).

Infection and Immunology

Most *M. tuberculosis* infections are thought to begin when aerosolized bacilli are inhaled into the lungs. In humans, active respiratory infection is characterized by symptoms including fever, coughing, sneezing, hemoptysis, atrophy, and fatigue (47). After the bacilli are phagocytosed by alveolar macrophages, they enter a phagosome. Bacteria-containing phagosomes typically fuse with lysozomes which contain caustic molecules to degrade the foreign bodies within the fused organelles. *M. tuberculosis* can inhibit phago-lysosomal fusion to minimize exposure to damaging molecules (48). The *M. tuberculosis* bacilli encode a protein tyrosine phosphatase (PtpA) which exclude the vesicular proton ATPase from the phagosomal membrane, thereby blocking acidification within the phagosome (49, 50). There are five type VII secretion systems encoded by *M.*

tuberculosis, named ESX-1 through ESX-5 (51). The action of the ESX-1 secretion system allows *M. tuberculosis* to release virulence factors and bacterial products from the phagosome into the cytosol (52, 53). The secreted effector proteins of the ESX-3 secretion system are involved in *M. tuberculosis* virulence and iron acquisition (54).

Through secretion of effector proteins, *M. tuberculosis* can alter cytokine activation and other signaling pathways more favorable for the bacilli. These bacteria exploit anti-apoptotic pathways to promote necrotic cell death and facilitate bacilli spreading (55, 56). Positive-disease outcome is reliant on immune activation through IL-12 and IFN-γ, and the $CD4^+$ T-cell response (56). The *M. tuberculosis* infection spreads to the lung parenchyma through migration of infected macrophages or by direct infection of epithelial cells. Infected macrophages and dendritic cells migrate to the lymph nodes for T-cell priming (57, 58). The *M. tuberculosis* bacilli are capable of infection and survival in a variety of tissue types including alveolar epithelial cells and adipose tissues (35, 59). Approximately 15-20% of TB cases are extra-pulmonary, which includes infection in the brain, meninges, spinal cord, urogenital tract and others tissues. In many cases, extra-pulmonary infection presents with no apparent lung pathology (60, 61).

In 90% of cases, the innate and/or adaptive immune responses are capable of controlling *M. tuberculosis* infections through killing the bacteria or halting the infection through granuloma formation resulting latent tuberculosis infection (LTBI) (56). Dynamic immune cell aggregates, known as granulomas, and possibly adipose cells may serve as reservoirs for *M. tuberculosis* bacilli during LTBI (35). Once LTBI is established, an infected person is not contagious and no longer manifests disease symptoms. It is estimated that 2 billion people have established LTBI (1). Individuals

with LTBI are at risk for reactivation of active TB disease. This return to active infection typically coincides with a weakening of the host immune system that can result from outside factors such as infections with HIV, development of autoimmune diseases, or administration of corticosteroids (62, 63).

Granulomas are hallmarks of both active and latent TB infection in humans. There are three broad categories of granulomas (64, 65). Solid granulomas are intact bodies encased in fibrous tissues containing central macrophages, with surrounding dendritic cells, and T and B lymphocytes. Necrotic granulomas are also intact, but have diffuse and hypoxic centers (64). Finally, caseous granulomas have liquefied centers and higher oxygen content, but with decomposition of central structures. The amount and type of granulomas present during active and latent infections vary and will change throughout the course of infection (65).

Diagnosis

For patients presenting with symptoms of active TB disease, the WHO recommends a series of diagnostic assays. These include smear microscopy with acid-fast staining, sputum culturing, growth-based drug susceptibility tests, and the Xpert® MTB/RIF detection and drug-susceptibility assay (Cepheid Inc., Sunnyvale, CA) (1). The Xpert® and the recently-developed Xpert® Ultra tests are nucleic acid amplification-based point-of-care (POC) diagnostics that use Real-Time PCR technology in a cartridge system to detect *M. tuberculosis* DNA in un-processed sputum samples in approximately 2 hours. These assays use multiple probes to amplify the core region of the *M. tuberculosis* RNA polymerase gene *rpoB*. The *rpoB* gene is associated with >95% of

rifampicin-resistant strains and because the majority of rifampicin-resistant strains are also resistant to isoniazid, this diagnostic can be used as an indicator for MDR-TB (1). Mutations in *rpoB* will inhibit DNA hybridization to one or more probes; thus allowing for POC detection of *M. tuberculosis* DNA and allowing health-care workers to choose appropriate antibiotic therapy. The Xpert® and Xpert® Ultra tests have between 81 and 88% sensitivity for detection of *M. tuberculosis* and resistance (66, 67). Although Xpert® and Xpert® Ultra provide a POC diagnostic, the lack of 100% sensitivity and specificity mean that accurate diagnosis still requires the long-term growth-based detection assays. There are currently many molecular and non-molecular diagnostic tools being developed and evaluated to bypass wait time of culture-based diagnostic techniques (1).

The tuberculin skin test (TST) and interferon gamma release assays (IGRAs) are the standard tests for *M. tuberculosis* exposure and LTBI; however, there are major drawbacks to both due to the non-specific nature of the tests. The TST developed in the 1930s relies on a delayed hypersensitivity response to complex mixture of mycobacterial antigens. In general, a bolus of antigens is injected intradermally and the induration caused by an immune response to the antigens is measured after 48-72 hours. Due to the non-specific nature of the TST antigens, exposure to non-tuberculous mycobacteria, as well as vaccination with BCG, can result in false-positive test results (47). Additionally, some people who have been exposed to *M. tuberculosis* will remain TST negative. Interferon-gamma-release assays (IGRAs) are more sensitive for detecting *M. tuberculosis* exposure because they rely on stimulation of immune cells by the *M. tuberculosis*-specific antigens ESAT-6, CFP-10, and TB7.7 (68). These assays also have greater specificity than TST because they include internal controls for measuring positive

and negative responses to the antigens not present in the BCG vaccine strain. Some of the drawbacks to IGRAs are the need for whole blood samples to run the test, specialized equipment, and high costs.

Treatment and Vaccination

Due to the ability of *M. tuberculosis* to persist within the host and present phenotypic drug resistance, even treatment for drug-susceptible strains of *M. tuberculosis* requires long-term use of multiple antibiotics. The CDC/WHO-recommended treatment regimen for *M. tuberculosis* infection is 2 months of daily or 2-3 times per week doses of rifampicin (RIF), isoniazid (INH), pyrazinamide (PZA), ethambutol (EMB) therapy, followed by a 4 month continuation phase of daily or 2-3 times weekly administration of RIF and INH (69). For individuals with RR-TB or MDR-TB, the current WHO-recommended treatment program consists of 4-6 months of combination therapy with kanamycin, moxifloxacin, prothionamide, clofazimine, INH, PZA, and EMB; followed by 5 months of treatment with moxifloxacin, clofazimine, PZA, and EMB (70). In cases of XDR-TB, other antibiotics including linezolid, streptomycin, and cycloserine will be incorporated into the treatment regimen (70).

There are 17 drugs in various stages of clinical trials for use as anti-TB therapy. These include some repurposed drugs and some novel compounds. Of note are two antibiotics, Bedaquiline and Delamanid, which have received accelerated approval and are currently in use in many countries for treatment of MDR/XDR-TB (1). Unfortunately, as is the case with many antibiotics, resistance to both of these antibiotics have already been identified (71).

Many factors can alter and/or extend the treatment of TB including HIV co-infection and other health conditions, such as reduced liver and renal function which limit drug processing (69). Additionally, because the majority of infected individuals are in low-income socioeconomic situations, lack of access to proper healthcare creates roadblocks to successful treatment. These blocks include reduced access to antibiotics, lack of transportation to clinics, and lack of patient compliance.

The only vaccine against *M. tuberculosis* infection approved globally is bacille Calmette-Guérin (BCG), a live-attenuated strain of *Mycobacterium bovis* (1). This vaccine is protective against disseminated TB in infants, but has limited efficacy in protecting against pulmonary TB disease in adolescents and adults (72–74). There are currently 12 vaccine candidates in the pipeline at various phases of clinical trials; these candidate vaccines represent a wide range of platforms, including adenoviral vectors, live-attenuated strains, non-tuberculous mycobacteria, and subunit vaccines (1)**.** It will cost an estimated $52 billion dollars over the next five years to implement the TB treatment and prevention strategies currently available (1). With a global financial burden of this magnitude, it is imperative to continue research on this pathogen to develop better diagnostics, treatments, and preventatives.

2.2 SIGMA FACTOR C

The Sigma Factor Subunit

Bacteria possess a multi-subunit RNA polymerase (RNAP) for transcription. Core RNAP must associate with a subunit known as a sigma factor to form a RNAP

holoenzyme capable of sequence-specific DNA recognition and transcription initiation (75). Bacteria produce multiple sigma factors. Each forms a unique RNAP holoenzyme which recognizes a different DNA sequence (promoter) to direct transcription of the unique set of genes that comprise the regulon of the sigma factor. After transcription initiates, the sigma factor dissociates from the core RNAP. There are two categories of sigma factors: the sigma-70 family which phylogenetically cluster with sigma-70 (RpoD) from *Escherichia coli* and the sigma-54 family which cluster with *E. coli* sigma-54 (RpoN) (75). In *M. tuberculosis* strain H37Rv, 13 sigma-70 family members have been annotated (76). The sigma-54 family is not found in Actinomycetes (77, 78).

Members of the sigma-70 family contain one to four conserved regions connected by flexible linkers. At the amino terminus is region 1 which can be further divided into sub-regions 1.1 and 1.2. Region 1.1 often functions to block DNA binding by free sigma factors (79, 80). Region 2 contains four sub-regions. Of these, region 2.2 is involved in RNAP binding. Region 2.3 functions in melting the DNA strands to form a transcription bubble for transcription initiation, while region 2.4 functions in recognition of the -10 promoter element located approximately 10 bp upstream from the transcription start site (79, 81). Region 3 is made up of sub-regions 3.0, 3.1, and 3.2. Region 3.1 is thought to help with recognition of the extended -10 promoter element (82). Region 4 has a major RNAP-binding determinant and is divided into sub-regions 4.1 and 4.2. Region 4.2 has been implicated in -35 promoter element recognition and in binding transcriptional activators (75, 83).

The sigma-70 family has also been subdivided into four groups based on structure and purpose. Group 1 includes the primary sigma factors responsible for transcription of

essential genes. Group 1 sigma factors contain all four regions. In *M. tuberculosis*, group 1 is represented by SigA, which is responsible for transcribing housekeeping genes under low-stress conditions (84). Group 2 sigma factors are primary-like sigma factors that play a role in stress responses. Group 2 sigma factors are only present in some bacteria. In *M. tuberculosis*, group 2 is represented by SigB which is a general stress response sigma factor that is controlled from multiple promoters specific to SigF, SigE, SigH, or SigL (9, 85, 86). Group 3 consists of alternative sigma factors. These sigma factors lack region 1 and may be required for heat-shock response or motility (75). No mode of motility has been defined for *M. tuberculosis* (87–89). In *M. tuberculosis*, SigF is considered a group 3 sigma factor that functions in stress response (10, 87–89). Group 4 is the largest group and may control production of proteins with extra-cytoplasmic function (ECF). Members of group 4 sigma factors only have conserved regions 2 and 4. The stress responses defined for ECF sigma factors vary widely. These include: oxidative stress, heat shock, surface stress, metal concentrations, and virulence (3, 4, 90–92). In *M. tuberculosis*, group 4 sigma factors are represented by the following: SigC, SigD, SigE, SigG, SigH, SigI, SigJ, SigK, SigL, and SigM (78).

The ECF Sigma Factors of *M. tuberculosis*

With 10 ECF sigma factors, *M. tuberculosis* has one of the highest alternative sigma factor to mega-base pair ratios of any obligate pathogen (78). Using a sigma factor inducible-expression system in BCG, chromatin immunoprecipitation assays were performed to identify promoters for the *M. tuberculosis* ECF sigma factors (5). Additionally, many studies have attempted to characterize the role in survival and

pathogenesis for these ECF sigma factors. The complexity of gene regulatory networks and the wide range of possible growth conditions leave many unanswered questions about the roles for each ECF sigma factor in *M. tuberculosis*.

Sigma Factor D

Sigma factor D is important in virulence and is upregulated during starvation (93). It has also been shown to regulate genes involved in heat shock, oxygen-sensing, and INH response (93). Mouse infection models demonstrate slight attenuation of an *M. tuberculosis* strain lacking an intact *sigD* gene (93).

Sigma Factor E

Sigma factor E is known to be important for *M. tuberculosis* survival in macrophages, as well as for full virulence in a BALB/c mouse infection model (85, 94) . It is also one of only two ECF sigma factors to be conserved in the degenerate genome of *Mycobacterium leprae*. Expression of *sigE* is increased due to stresses such as heat-shock, sodium dodecyl sulfate- or vancomycin-induced surface damage, and oxidative stress**.** There are multiple promoters for *sigE*; one of which is Sig^{H}-dependent and is induced in response to heat-shock and oxidative stress (85, 89, 94, 95).

Sigma Factor G

The sigma factor G gene, *sigG*, is transcribed from two promoters, and is part of a methylglyoxal detoxification regulon (96). Deletion of *sigG* from *M. tuberculosis* strain

CDC1551 impairs ability to infect macrophages; however, there is no reduction in infectivity when *sigG* is deleted from *M. tuberculosis* strain H37Rv (96, 97).

Sigma Factor H

Sigma Factor H is part of a stress response network that also includes SigE and SigB. Additionally, SigH regulates genes involved in DNA repair, stress response and thiol metabolism (9, 98). Deletion of *sigH* does not inhibit bacterial burdens in the lungs of C57BL/6 mice, but it does result in reduced lung pathology and increased mouse survival (98).

Sigma Factors I and J

Genes encoding sigma factors SigI and SigJ are both highly expressed during stationary phase, and it has been shown that SigJ regulates expression of SigI (99, 100). Sigma factor J is involved in H_2O_2 stress response and SigI is involved in cold-shock response (99, 101).

Sigma Factor K

The ECF sigma factor SigK is conserved in MTC mycobacteria, but absent in nontuberculous mycobacteria. It is known that SigK controls expression of *sigK*, the SigK anti-sigma factor gene *rskA*, and the genes encoding antigenic proteins Mpt70, Mpt80, and DipZ (5, 84, 102). The role for SigK in *M. tuberculosis* pathogenesis has not been established.

Sigma Factor L

Sigma Factor L is known to transcribe genes involved in polyketide synthesis as well as secreted and membrane proteins (103). There is increased survival in mice infected with *M. tuberculosis* lacking *sigL*; however, bacterial loads in the lungs and spleen are comparable to wild-type (95, 103).

Sigma Factor M

The sigma factor SigM has been shown to positively regulate expression of the Esx-secreted proteins EsxU, EsxT, EsxE, and EsxF (104, 105). Additionally, it is a negative regulator of many virulence-associated polyketide synthesis genes (105). In both mouse and guinea pig infection models, deletion of *sigM* does not result in a loss of virulence for *M. tuberculosis* (4, 92). This may be due to down-regulation of known virulence determinants.

Sigma Factor C

Sigma factor C is present in all tuberculous mycobacteria, and is one of only two group 4 sigma factors encoded in the pathogen *Mycobacterium leprae* (106). Non-pathogenic mycobacteria, such as *M. smegmatis,* do not have a SigC homolog (107). In *M. tuberculosis,* transcription of *sigC* was elevated relative to *sigA* during exponential growth and reduced during stationary phase and after exposure to different stressors, such as heat shock or oxidative stress (89). In *M. tuberculosis, sigC* is not required for growth in complex media; however, there is a significant growth defect of *M. tuberculosis* strain Erdman∆*sigC* relative to parent strain Erdman when grown in chemically-defined Sauton

medium after serial passaging (6)**.** *In vivo, sigC* is required for *M. tuberculosis* lethality in DBA/2 mice and in SCID mice (3, 6). Deletion of *sigC* from *M. tuberculosis* also results in attenuation of virulence and reduced numbers of lung and spleen granulomas in infected guinea pigs (4).

Chromosome-immunoprecipitation assays identified a SigC-RNAP binding site in the *Rv95-PPE1* intergenic region and another upstream of the *ctpB* in BCG (5). The *sigC* gene in BCG is identical to *M. tuberculosis sigC*. Microarray studies with *M. tuberculosis* demonstrate that short-term (4-hour) artificial induction of *sigC* expressed from a tetracycline-inducible promoter in complex media result in elevated transcription of genes in the *PPE1-nrp* operon and *ctpB*; each of these genes has been proposed to function in copper uptake (6). After 48-hour *sigC* induction, these same genes were transcribed at higher levels, but copper-toxicity response genes were also elevated (6). Microarray studies in Sauton medium indicated elevated transcription of the *PPE1-nrp* operon in *M. tuberculosis* strain Erdman relative to *M. tuberculosis* Erdman∆*sigC* (6). A growth defect of the *M. tuberculosis* Erdman∆*sigC* strain in Sauton medium is reversed by copper sulfate supplementation (6). Restoration of growth is not detected in the mutant when supplemented with either zinc sulfate or calcium chloride (6). These data suggest that SigC may play a role in the regulation of copper uptake.

The mechanism for SigC regulation is currently poorly understood. While many sigma factors are controlled post-transcriptionally by a cognate anti-sigma factor encoded in the same operon, no anti-sigma factor gene is co-transcribed in an operon with *sigC*. In fact, *sigC* is monocistronic and located within a cluster of predicted coenzyme Co-B_{12} synthesis genes. However, *in silico* analysis identified two potential anti-sigma factor

genes not located in operons encoding a sigma factor. The first, *Rv0093*, located in a possible operon divergently-transcribed from the *PPE1-nrp* operon contains a Zn-finger binding motif characteristic of anti-sigma factors that function in response to redox stress (8, 108). The second candidate is SirR, which is similar to the anti-SigE factor RseA from *E.coli* (8). *In vitro* co-expression and immunoprecipitation of the predicted anti-sigma factor binding region of SigC with the predicted sigma-binding region of Rv0093 or SirR failed to show an interaction between SigC and either protein (8). Three amino acid residues (R178, I181, and V185) in region 4.2 of *E. coli* SigE have been found to be required for binding of RseA; substitution of any of these amino acids to glycine or alanine resulted in no interaction of SigE and RseA (109). Amino acid sequence alignment indicates that *M. tuberculosis* SigC has arginine, leucine and alanine at these respective positions (8). Additional studies have shown at least two promoters upstream of *sigC*, one of which is recognized by SigA (10). Deletion of *sigC* does not affect transcription from these promoters indicating that *sigC* transcription is not autoregulated (10). Additional studies examining post-translational SigC stability may lead to understanding of the mechanism of SigC regulation.

2.3 COPPER IN *M. TUBERCULOSIS*

Copper Toxicity Response

During phagosome activation, metal ion pumps increase intraphagosomal metal concentrations; free copper ion concentration inside of the macrophage phagosome can be as high as 400 μM during initial *M. tuberculosis* infection (110). In *M. tuberculosis*, there are multiple systems to overcome copper toxicity. The RicR regulon is controlled

by the regulated-in-copper protein RicR that de-represses transcription of metallothionein (*mymT*), multi-copper oxidase (*Rv0846*), and membrane lipoprotein (*lpqS*) genes in the presence of copper (111). The copper-sensitive-operon repressor CsoR de-represses transcription of copper-efflux P-type ATPase gene *ctpV* in response to elevated copper levels in *M. tuberculosis* (112). This system works in conjunction with the outer membrane channel protein MctB; loss of either *ctpV* or *mctB* in *M. tuberculosis* results in increased copper sensitivity and reduced virulence in guinea pigs (112–114).

Copper-Dependent Enzymes in *M. tuberculosis*

Although *M. tuberculosis* and other bacteria are susceptible to copper toxicity, *M. tuberculosis* encodes Cu-dependent enzymes, including: Zn/Cu superoxide dismutase (SodC) and cytochrome C oxidase (CtaD) of the aa_3 –type respiration complex. SodC is localized to the periplasm and functions during initial infection to protect against reactive oxygen radicals (115, 116). The aa_3 –type super complex provides the most energy-efficient terminal oxidase in the presence of oxygen. During chronic infection, the high-affinity, low-efficiency ubiquinol oxidase is upregulated in *M. tuberculosis* (37). The need for alternate respiration mechanisms in chronic infections may be due to a lack of oxygen or copper ions to support respiration by the aa_3-type complex. The estimated concentration of free copper ions in the blood and blood plasma is 1 μg/g; however, in normal human cells not primed against infectious agents, intracellular free copper is nearly undetectable (117, 118). In the cell, copper is bound within chaperone proteins, storage molecules, and copper-cofactored enzymes (119). During LTBI, *M. tuberculosis* must compete with the host for this limited supply to meet its copper needs.

2.4 COBALAMIN

History and Structure

Interest in adenosylcobalamin or coenzyme B_{12} (Co-B_{12}) began in the 1920s when Murphy and Minot discovered that crude liver extracts worked as a cure for pernicious anemia (120). Twenty years later, Co-B_{12} was isolated from the extracts and assigned the name vitamin B_{12}. In 1948, Dorothy Hodgkins used X-ray crystallography to determine the structure of vitamin B_{12} (cyanocobalamin), which has a cyano group replacing the upper adenosyl ligand to the central cobalt atom (121). In nature, cobalamins are highly-complex molecules derived from the macrocyclic intermediate uroporphyrinogen III (122). Coenzyme B_{12} has a corrin ring which chelates a central cobalt atom. Linked to the cobalt atom is a variable upper axial ligand. Upper axial ligands reported include an adenosyl (AdoCbl), methyl (MeCbl), hydroxyl (OHCbl), or glutathionyl (GSCbl) group (123, 124). Commercially prepared vitamin B_{12} has a cyano group as the upper axial ligand. The coenzymatic forms include adenosylcobalamin and co(I)balamin, which has no upper ligand (11, 125). The final cobamide molecule has a lower ligand that can form a coordination bond with the cobalt ion of the corrin ring and is attached to the corrin macrocycle via a structure known as the nucleotide loop. The structure of coenzyme B_{12} contains the lower axial ligand 5, 6 dimethylbenzimidazole (DMB); however, organisms can also incorporate other bases like adenine and phenolics (126).

Co-B_{12} Dependent Enzymes

Co-B_{12} functions as an enzyme cofactor for a variety of cellular processes. The three main categories of Co-B_{12}-dependent enzymes are corrinoid dehalogenases, methyltransferases, and isomerases. In *M. tuberculosis*, the Co-B_{12}-dependent enzymes identified are methionine synthase (MetH), methylmalonyl CoA mutase (MutAB), and ribonucleotide reductase (NrdZ) (127). The Co-B_{12}-dependent methionine synthase, MetH, is a methyltransferase that uses Co-B_{12} to facilitate the transfer a methyl group from 5-methyltetrahydrofolate to homocysteine to generate methionine (128). The genome of *M. tuberculosis* strain H37Rv encodes the genes for a functional MetH protein, as well as a Co-B_{12}-independent methionine synthase MetE, which catalyzes direct transfer of a methyl group from a triglutamate derivative of 5-methyltetrahydrofolate (129). In *M. tuberculosis* strain CDC1551, the gene encoding MetH has a loss-of-function C-terminal deletion and is a methionine auxotroph in the presence of Co-B_{12} due to a Co-B_{12} riboswitch regulating *M. tuberculosis metE* translation (13). In *M. tuberculosis, metE* is one of two genes under control of a Co-B_{12} riboswitch. The other gene is *PPE2*, which may play a role in cobalt transport (13, 130).

Methylmalonyl-CoA mutase (MutAB) is a Co-B_{12}-dependent enzyme involved in the methylmalonyl pathway for propionyl-CoA assimilation. MutAB uses AdoCbl as cofactor to interconvert (R)-methylmalonyl-CoA and succinyl-CoA (11, 131). In *M. tuberculosis*, MutAB is a heterodimer encoded by two genes, *mutA* (*Rv1492*) and *mutB* (*Rv1493*). When these genes are deleted from *M. tuberculosis*, the organism is incapable of surviving *in vitro* on odd-carbon length fatty acids when the 2-methylcitric acid cycle is chemically blocked with 3-nitropropionate (14, 29).

Ribonucleotide reductases (RNR) function in DNA synthesis to reduce ribonucleotides to 2-deoxyribonucleotides. There are four classes of RNRs. The class II enzymes use Co-B_{12} as a cofactor for reducing activity (132). *M. tuberculosis* encodes two RNRs: a class I oxygen-dependent enzyme, made of the subunits NrdE and NrdF2, and a class II enzyme (NrdZ) which uses AdoCbl in conjunction with a protein thiyl radical to reduce ribonucleotides to deoxyribonucleotides (133). The presence of *nrdZ* in mycobacteria is not consistent with the typical phylogenetic distribution, indicating that *nrdZ* was likely inherited through horizontal gene transfer (127).

Defined Co-B_{12} Biosynthetic Pathways

Although a large number of organisms use Co-B_{12}-dependent enzymes, synthesis of the cobamides is exclusive to bacteria and archaea (134). *De novo* generation of cobamides requires approximately 30 enzymes. The Co-B_{12} biosynthetic pathway has been well characterized for some species such as *Salmonella enterica* subsp *enterica* serovar Typhimurium (*S.* Typhimurium) and *Pseudomonas denitrificans* (134). Various organisms are also capable of transporting cobamides and incomplete corrinoids into the cell for use (135–137). Many bacteria and archaea encode systems for removing and remodeling the lower ligand base of cobamides (138–140).

Pathways for Co-B_{12} synthesis in *S.* Typhimurium and *P. denitrificans* differ in the timing of the central cobalt atom insertion into the corrin ring. The assembly of the corrin ring structure is sometimes referred to as the anaerobic or aerobic synthesis route and correlates with early or late cobalt insertion by *S.* Typhimurium or *P. denitrificans*, respectively (122, 141). Typically, genes annotated as aerobic cobyric acid synthesis

genes have the prefix *cob*, and genes annotated as anaerobic synthesis genes have the prefix *cbi* (141). Genes involved in nucleotide loop assembly and attachment are also typically annotated with *cob* prefixes (122). In the early-insertion pathway, cobalt is inserted into the tetrapyrrole ring in the second step of synthesis following the conversion from the precursor uroporphyrinogen III to precorrin 2. In *S. Typhimurium*, cobalt insertion is catalyzed by the sirohydrochlorin cobaltochelatase CbiK or by the multifunctional siroheme synthase CysG (142). Another cobaltochelatase is used by some anaerobic Co-B_{12} producers including *Bacillus megaterium* and *Mycobacterium avium* subsp. *paratuberculosis* is CbiX (141, 143). The *M. tuberculosis* genome encodes the *cbiX* homolog *Rv0259c*. During aerobic Co-B_{12} synthesis, cobalt is added to the ring structure as one of the last steps of adenosyl-cobinamide-phosphate (AdoCbl-P) synthesis. Aerobic cobalt insertion commonly occurs through the trimeric cobaltochelatase enzyme encoded by *cobN*, *cobS*, and *cobT* (144). The *M. tuberculosis* genome encodes a *cobN* (*Rv2062*) homolog and *Rv2850*, which is annotated to encode a magnesium chelatase that may function as a cobalt chelatase for late cobalt insertion similar to other aerobic producers (76, 130). Genome sequencing of 200 *M. tuberculosis* clinical isolates showed 17 with functional mutations in *cobN* (15). Given the presence of both early-cobalt and late-cobalt insertion pathway gene homologs, it is still unclear which mechanism is used by *M. tuberculosis* to produce Co-B_{12}. In the late stages of Co-B_{12} synthesis, the lower ligand base is joined with adenosylcobamide (AdoCbl-P) to yield adenosylcobalamin (Co-B_{12}) , or another complete cobamide such as pseudocobalamin, containing an adenosine in both the upper and lower ligand positions.

Biosynthesis and Transport of Co-B_{12} in *M. tuberculosis*

Despite appearing to have a complete set of genes for Co-B_{12} synthesis, *M. tuberculosis* fails to produce Co-B_{12} under most conditions assayed (6, 13, 14, 29). One study from the 1970s reported results of a *Lactobacillus leichmannii*-feeding assay that showed *Mycobacterium smegmatis*, *Mycobacterium phei* and *Mycobacterium bovis* BCG (BCG) each produced detectable Co-B_{12} when cultured in stationary Roux bottles in Sauton medium supplemented with $CoCl_2$ and KCN (12). This specific growth technique and bioassay has never been replicated for *M. tuberculosis*. Other studies examining synthesis of Co-B_{12} in *M. tuberculosis* using shaking cultures in the complex medium Middlebrook 7H9 or in minimal Sauton medium supplemented with varying carbon sources have repeatedly demonstrated that *M. tuberculosis* does not produce Co-B_{12} under such conditions (6, 14, 29).

It has been demonstrated that deleting *metE* from *M. tuberculosis* H37Rv is only possible if the bacteria are supplied exogenous Co-B_{12} (13). A study assessing the function the Co-B_{12}-dependent methylmalonyl pathway showed that *M. tuberculosis* H37Rv is a Co-B_{12} auxotroph when the Co-B_{12}-independent pathway for propionyl-CoA assimilation through the 2-methylcitric acid cycle pathway is blocked by addition of 3-nitropropionate (3NP) (14). This finding implies that under standard *in vitro* shaking conditions, *M. tuberculosis* does not synthesize Co-B_{12}. Additional work identified Rv1819c as the probable Co-B_{12}/corrinoid transporter for *M. tuberculosis* (137). That study demonstrated that *M. tuberculosis* was incapable of surviving *in vitro* after *Rv1819c* was deleted and the Co-B_{12}-independent pathway for propionyl-CoA utilization was blocked by 3NP, even when exogenous Co-B_{12} was provided (137). Taken together,

these studies demonstrate that under *in vitro* aerobic conditions *M. tuberculosis* bacilli are unable to generate Co-B_{12}. Regardless of *in vitro* growth studies, the presence of predicted homologs for all steps of the Co-B_{12} synthesis pathway in the *M. tuberculosis* genome implies that it is capable of producing the molecule under as-yet unidentified environmental conditions. Characterization of Co-B_{12} synthesis in mycobacteria, as well as assessment of predicted *M. tuberculosis* Co-B_{12} synthesis genes should help to elucidate the environmental conditions and host niches in which *M. tuberculosis* bacilli produce functional Co-B_{12}.

CHAPTER 3

REGULATION OF MYCOBACTERIUM TUBERCULOSIS SIGMA FACTOR C BY COPPER[1]

[1] Samantha L. Tucker, Frederick D. Quinn, Russell K. Karls. To be submitted to *Journal of Bacteriology*.

ABSTRACT

One of the most successful pathogens, *Mycobacterium tuberculosis* is capable of persisting as a latent infection in humans for decades or actively replicating and causing tuberculosis (TB) disease. As an obligate pathogen, the species must acquire nutrients and minerals from various environments in its host. While too much copper is toxic to bacteria, this metal functions in key processes that include superoxide radical detoxification and aerobic respiration in *M. tuberculosis*. Sigma factor C (SigC) functions in copper acquisition by this pathogen through directing transcription of *ctpB* and the 6-gene *PPE1-nrp* operon that are predicted to encode a cytoplasmic copper import pump and enzymes that synthesize a copper chelator, respectively. While the *sigC* gene is transcribed at high levels under multiple conditions, it is not auto-regulated. SigC function is only required when copper is scarce.

In the present study, we demonstrate that *sigC* enables *M. tuberculosis* to effectively compete with the copper-specific chelator tetrathiomolybdate (TTM) for trace amounts of copper. Next, post-transcriptional *sigC* levels were monitored by quantitative immunoblot analyses. Induced expression of *sigC* controlled from a tetracycline-inducible promoter in *M. tuberculosis* resulted in greater detection of the protein in copper-chelated versus copper-supplemented medium. Following 24-hour *sigC* induction in copper-chelated medium, addition of copper ions and chloramphenicol resulted in a greater reduction of SigC levels than with either copper or the protein synthesis inhibitor alone after 4 hour incubation, which suggests that copper leads to degradation of SigC rather than a reduction in new synthesis of the protein. As cysteine residues can function in copper-binding, mutants of *M. tuberculosis* with alanine substitutions in the Cys-Gly-

Cys sequence located in the turn portion of the helix-turn-helix DNA-binding region 4.2 of SigC reduced growth in copper-chelated media, implicating this domain in SigC function. The data support a model in which SigC functions in a low-copper environment to direct transcription of copper-uptake genes; when ample copper is acquired and aerobic respiration is restored, SigC is unfolded, possibly due to direct binding of copper ions, and degraded.

INTRODUCTION

Mycobacterium tuberculosis is the etiological agent of tuberculosis (TB), which results in 1-2 million deaths annually (1). The live-attenuated *Mycobacterium bovis* strain bacille Calmette-Guérin (BCG) administered at birth is effective in preventing disseminated disease in young children, but has variable efficacy against pulmonary TB disease in adults (73). Incidence of multi-drug resistant TB is increasing, which is making this disease more difficult and expensive to treat. An estimated one third of all humans harbor latent *M. tuberculosis* infection and are at risk for developing active TB disease (1). The threat of re-activated disease increases with immune-compromising events such as HIV co-infection or immunosuppressive drug therapy. To develop better vaccines and to identify antibiotic targets against *M. tuberculosis*, it is imperative to understand the adaptive physiology of this pathogen.

Metal ion overloading in phagocytic cells is a host defense mechanism against microbes (110, 145). In response to *M. tuberculosis* infection, the concentrations of free copper inside of macrophage phagosomes can reach 400 μM (110). Multiple systems exist in *M. tuberculosis* to respond to toxic copper levels. The repressor protein RicR

controls multiple genes in response to elevated amounts of copper. These loci include *mymT* encoding a cysteine-rich copper-storage protein metallothionein, *Rv0846* which encodes a putative multi-copper oxidase, and *lpqS* encoding a membrane lipoprotein predicted to function in copper efflux (111). A second copper-responsive repressor, CsoR, de-represses transcription of its own operon which includes *ctpV* encoding a copper-exporting P-type ATPase (112, 146). This system works in conjunction with the outer membrane channel protein MctB. Loss of either *ctpV* or *mctB* in *M. tuberculosis* results in increased copper sensitivity and reduced virulence in guinea pigs (114).

Although protection from copper toxicity is essential for survival of *M. tuberculosis*, this metal is required by various enzymes including Zn/Cu superoxide dismutase (SodC) and cytochrome C oxidase (CtaD) as part of the aa_3 –type respiratory complex. SodC functions during initial infection to help mitigate oxidative damage from superoxide radicals (115, 116). The aa_3 –type complex provides the most energy-efficient terminal oxidase for aerobic respiration (37). During chronic lung infection, the high-affinity/low-energy ubiquinol oxidase is induced in *M. tuberculosis* (37). The upregulation of this alternative respiratory system may be due to hypoxia or a lack of available copper ions during latent infection. The estimated normal concentration of free copper ions in the human body is 1.6 μM; however, intracellular free copper is virtually undetectable (117, 118). During infection, *M. tuberculosis* must compete with the host to meet its copper needs.

A copper-specific uptake system has yet to be proven in bacterial pathogens including *M. tuberculosis*; however, this species encodes a predicted P-type ATPase, CtpB, that has a Cu^{+}-binding signature (113). Reduced transcription of *ctpB* in response to a high level

(0.5 mM) of copper chloride in *M. tuberculosis* is the opposite of what would be expected for a copper-efflux pump (113). In vivo chromosome-immunoprecipitation/DNA microarray studies in BCG revealed primary binding sites for SigC upstream of *ctpB* and the *PPE1-nrp* operon (5). Transcription of *ctpB in vitro* was only detected when RNA polymerase (RNAP) holoenzyme was reconstituted from core RNAP and sigma factor C (SigC), but not with any of the other *M. tuberculosis* sigma factors (5). Transcriptional studies demonstrated that forced expression of *sigC* in either *M. tuberculosis* or BCG resulted in increased transcription of *ctpB* and genes in the *PPE1-nrp* operon in complex medium (Middlebrook 7H9 broth) (6). In chemically-defined Sauton medium, transcription of this operon was upregulated in a wild-type *M. tuberculosis* strain relative to a mutant deleted for *sigC* (6). Components of the homologous *Mycobacterium marinum nrp* operon have been proposed to function in the synthesis of a zinc chelator (7). Serial passage of a *M. tuberculosis sigC* mutant resulted in growth impairment relative to its parent strain in Sauton medium, but no growth defect was evident when the mutant was cultured in 7H9 broth (6). Addition of copper sulfate to Sauton medium reversed the growth defect of the mutant to near wild-type levels (6). In contrast, addition of zinc sulfate, another metal not part of Sauton medium, did not improve growth of the *sigC* mutant (6).

SigC has been shown to be important for virulence in both murine and guinea pig *M. tuberculosis* infection models; however, this protein was not required for replication in macrophages (3, 4). Regulation of SigC is unclear. An anti-sigma factor for SigC has not been identified and SigC does not transcribe its own gene (8, 10). Under standard *in vitro*

culture conditions, *sigC* is transcribed at high levels and not induced *in vitro* by heat shock, surfactants, cold shock, or low aeration (89).

The relationship between copper availability and growth of a *sigC* deletion mutant, as well as SigC-directed transcription of the metal-transport gene *ctpB* and the predicted metal chelator-synthesis operon *PPE1-nrp* demonstrate SigC function in copper acquisition. The lack of a known regulatory mechanism for SigC, led us to hypothesize that SigC is regulated by copper. This work investigates the effects of copper on SigC protein stability and function. The results indicate a need for SigC under copper-chelated conditions. The protein is degraded in *M. tuberculosis* if ample copper is available. A Cys-Gly-Cys motif in region 4.2 of SigC is required for full function of the protein in copper-starved conditions.

METHODS

Bacterial Strains

All strains and plasmids used in these studies are listed in Table 3.1. Mycobacterial strains examined include: *Mycobacterium tuberculosis* strain Erdman, a *sigC* internal deletion mutant of strain Erdman (Δ*sigC*), the mutant complemented with *sigC* on a chromosome-integrating plasmid (Δ*sigC::sigC*), derivatives of Erdman or Δ*sigC* carrying replicating plasmid pSR173 encoding myc-tagged SigC expressed from a tetracycline-inducible promoter or those transformed with pSR173 derivatives encoding site-directed alanine-replacement mutations in SigC are indicated (Table 3.1). For mutagenesis to encode alanine residues in SigC at positions 156, 157, and/or 158, a

region of *sigC* incorporating the mutations was obtained by PCR of pSR173 template using forward primer P1502 (encodes an *Nsi*I restriction site) paired separately with different 5′ phosphorylated reverse primers (P1498, P1499, P1500, or P1501). Each PCR product was digested with *Nsi*I and ligated with *Nsi*I/*Pvu*II-digested pSR173 vector. Competent *E. coli* TAM1 cells (Active Motif) were transformed with the ligated DNA selecting for resistance to hygromycin [0.1 mg/ml]. Plasmids were screened by restriction analysis and *sigC* regions confirmed by DNA sequencing (Genewiz). An empty vector control plasmid, pSLT37, was created by digesting pSR173 with *Pac*I and *Nsi*I, blunting the DNA ends and self-ligating the vector band to remove *sigC*. Each *sigC*-mutated plasmid was electroporated into the *M. tuberculosis* strain Δ*sigC*.

For growth studies, strains were cultured at 37°C in Sauton medium supplemented with 0.025% Tylaxopol (SMT) (147). When required for plasmid maintenance, hygromycin or kanamycin was added to a final concentration of 50 μg/ml or 20 μg/ml, respectively. For studies monitoring growth by optical densities, bacteria were cultured with shaking (70 rpm) at 37°C and sub-cultured to OD_{600} =0.01. Chemicals used in growth experiments included the following: Ammonium tetrathiomolybdate (TTM) was used at concentrations of 5 or 10 μM, as indicated. Copper sulfate was added at a final concentration of 10 or 40 μM, as indicated. Chloramphenicol was used at 50 μg/ml. Anhydrous tetracycline (aTc) was used at 1 μg/ml. Assays were performed in triplicate and three independent experiments were performed. Two-way ANOVA was used to determine statistical significance.

AlamarBlue® Cell Viability Assay

AlamarBlue® (Invitrogen) assay was used to monitor metabolic activity of *M. tuberculosis* strains cultured in the presence or absence of copper chelator (TTM or bathocuprionedisulfonic acid, BCS) copper sulfate, and/or sodium ascorbate. For each assay, bacteria were grown until turbid in SMT and subcultured to OD_{600} = 0.02, and then diluted 5-fold with SMT. For each condition, 0.1 ml aliquots of diluted bacteria were seeded in triplicate wells of 96-well plates containing 0.1 ml of SMT with varying concentrations of additives. The final concentrations of TTM or BCS ranged from 0 to 500 μM. The final concentrations of copper sulfate ranged from 0 to 250 μM. The final concentration of aTc was 10 ng/ml. For sodium ascorbate, final concentrations ranged from 0 to 1 mM. Zinc sulfate was used at a final concentration of 10 μM. Plates were incubated stationary for 7 days at 37°C. Following incubation, 20 μl AlamarBlue reagent and 20 μl 2.5% Tyloxapol were added to a set of positive control wells seeded with *M. tuberculosis* Erdman in SMT. Plates were incubated at 37°C until color conversion of the positive control wells from blue to pink/purple, typically 24 hours. Then, the same volumes of AlamarBlue and 2.5% Tyloxapol were added to the remaining wells and plates were incubated at 37°C up to 96 hours for color conversion. These assays were also performed as described above in the absence of bacteria.

Preparation of Protein Lysates and Immunoblots

To monitor levels of myc-SigC in *M. tuberculosis* Erdman/pSR173 (Table 3.1), bacteria were cultured in SMT as described above. Cultures were induced at an OD_{600} = 0.6 with 1 μg/ml anhydrous tetracycline and supplemented with 5 μM TTM, 10 μM

copper sulfate, or both, and then incubated an additional 24 hours. For measuring myc-SigC stability, cultures were grown to OD_{600} = 0.6 prior to addition of 1 μg/ml aTc and 10 μM TTM. After 24-hour incubation, 40 μM copper sulfate and/or 50 μg/ml chloramphenicol was added and cultures incubated 4 hours. Cells were harvested by centrifugation (1200 x g, 5 minutes, at 4°C). Pellets were washed once with sterile PBS and re-suspended in 1 ml PBS containing 2 mM EDTA, 1 mM PMSF, and 10% of a mini cOmplete™ protease inhibitor (Roche). Cells were disrupted with 0.1-mm diameter zirconia/silica beads in a BeadBeater (BioSpec Products) for two 40-second cycles at 4800 rpm with chilling on ice ≥ 2 minutes between cycles. Cell debris was removed by centrifugation (8,000 x g, 10 minutes) and supernatants filtered through 0.22 μM PVDF membranes and stored at -80°C. Prior to analysis, thawed lysates (~0.2 ml) were concentrated to ~75 μl by vacuum centrifugation in a SpeedVac (Savant). Protein concentrations were determined by Pierce BCA Protein Assay (Thermo Scientific). Equal amounts of protein (30 mg) were heated (99°C, 10 minutes) in 1X SDS loading buffer (60 mM Tris-HCl--pH 6.85, 10% glycerol; 2% SDS, 0.05 bromophenol blue, 1.25 % β-mercaptoethanol) and resolved on NuPAGE 4-12% Bis/Tris gels (Invitrogen). Proteins were transferred to nitrocellulose membranes (Bio-Rad). Membranes were blocked with Blocking Reagent (BioRad) at 3% (w/v) in 1X TBS with 0.001%Tween 20 (TBST) for 1 hour at room temperature with rocking. For immunoblot analyses, primary antibodies used were either 1:4000 dilution of mouse clone 9E10 monoclonal antibody against c-myc (Sigma-Aldrich) or 1:20,000 dilution of mouse monoclonal antibody against the β-subunit of *E. coli* RNA polymerase (Neoclone); the diluent used was 1% Blocking Reagent in 1X TBST. Membranes were incubated with primary antibody overnight with

rocking at 4°C. Membranes were washed 3 times in 1X TBST and incubated with rocking for 2 hours at room temperature with secondary goat anti-mouse-HRP antibody (Jackson Laboratory) at 1:10,000 dilution in 1% Blocking Reagent in 1X TBST. Membranes were then washed 3 times with 1X TBST and secondary antibodies were detected with Luminata Classico HRP substrate (Millipore) and imaged on a ChemiDoc^{TM} XRS+ Molecular Imager® (BioRad). For densitometry analysis, pixel intensities of myc-SigC bands were determined with BioRad ImageLab software (BioRad). Pixel intensities of myc-SigC bands were normalized to those measured for RNAP-β in the same sample. Each condition was tested in triplicate, and each experiment was performed independently three times. Statistical significance between groups was determined using a one-way ANOVA.

RESULTS

Chelation of Cu(I) or Cu(II) Inhibits Growth of a *M. tuberculosis sigC* Mutant.

To examine the effects of copper starvation on a *M. tuberculosis* mutant containing an internal deletion in *sigC*, growth of the mutant (*M.tb*Δ*sigC*), parent *M. tuberculosis* Erdman, and complemented mutant (*M.tb*Δ*sigC*::*sigC*) strains were examined. Strains were cultured in Sauton medium (SMT) containing 5 μM of the copper chelator ammonium tetrathiomolybdate (TTM). Additionally, growth of the mutant was examined in SMT containing both 5 μM TTM and 10 μM copper sulfate. Results show that the parent and complemented *sigC* mutant grew in the presence of TTM; however, the *sigC* mutant failed to grow when the chelator was present unless copper sulfate was

also added (Figure 3.1). The *sigC* mutant was also able to grow in SMT medium without additional copper if the chelator was absent (Figure 3.7). Note that although the SMT recipe lacks any copper-containing ingredients, trace amounts are likely present. Together, these data indicate *M. tuberculosis* SigC function is likely only needed under conditions in which copper levels are extremely low.

AlamarBlue assays were performed to further explore conditions in which *sigC* is required for copper acquisition by *M. tuberculosis.* The *sigC* mutant and parent strain were seeded into wells of 96-well plates containing SMT and increasing amounts of either TTM or a Cu(I)-specific chelator bathocuprionedisulfonic acid (BCS) and incubated for 7 days at 37°C before addition of AlamarBlue and further incubation to allow time for the indicator dye to be converted from blue to pink by metabolic activity of the bacteria. Results indicate that in this timeframe, strain Erdman grew well in the presence of up to 8 μM TTM, but the *sigC* mutant did not grow at the lowest level of TTM tested, 2 μM, or at any higher concentration (Figure 4.2A). In the presence of BCS, the *sigC* mutant grew at levels up to 8 μM, while the parent strain was uninhibited even at 500 μM (Figure 3.2B). We next examined whether the growth inhibition of the *sigC* mutant was reversible by copper supplementation. The mutant was cultured in SMT medium containing chelator (10 μM TTM or 15 μM BCS) and copper sulfate ranging from 2 to 250 μM (Figure 3.2C). Addition of 2 to 31 μM copper sulfate restored growth in the presence of TTM, but at higher concentrations growth inhibition was observed, suggesting the metal may be reaching toxic levels (Figure 3.2C). Addition of 2-250 μM of copper sulfate reversed the growth inhibition by BCS (Figure 3.2C). As the *sigC* mutant grew well in the presence of 2-4 μM BCS (Figure 3.2B), we examined whether

addition of a reductant would increase the inhibitory effect of BCS. The reductant sodium ascorbate was added in a range from 4 μM to 1 mM to wells containing the *sigC* mutant in SMT with either 1 or 2 μM BCS. Addition of the reductant at any of the tested concentrations blocked growth of the *sigC* mutant (Figure 3.2D). There was no effect of the various additives in SMT on the Alamar Blue reagent, except for slight color conversion at 1 mM sodium ascorbate (Figure 3.8). Together, these data indicate that in SMT medium Cu(II) is better utilized for growth by the *sigC* mutant than is Cu(I).

Copper Availability Alters Detectable myc-SigC Levels.

To determine if copper effects the levels of SigC in *M. tuberculosis*, plasmid pSR173 encoding myc-tagged SigC under control of a tetracycline-inducible promoter was used (5). Strain Erdman carrying plasmid pSR173 was subcultured into SMT medium alone and with either 5 μM TTM or 10 μM copper sulfate, or both chemicals. Production of myc-SigC was induced in all cultures for 24 hours by addition of 1 μg/ml aTc. Cell lysates of *M. tuberculosis* were prepared and equal protein loads resolved by SDS-PAGE. Quantitative immunoblot analysis was used to compare myc-SigC levels under each condition. Levels of the protein were normalized to a cytoplasmic control protein, the beta subunit of RNA polymerase (RNAP-β). Results indicated no significant difference in detectable myc-SigC from cultures containing 10 μM copper sulfate relative to that detected in SMT alone (Figure 3.3). Addition of 5 μM TTM significantly increased myc-SigC levels 1.7-fold compared to the SMT cultures and 2.7-fold relative to cultures containing copper sulfate (Figure 3.3). Addition of both TTM and copper sulfate

resulted in a 2.3-fold decrease in the amount of detectable myc-SigC relative to the amount of myc-SigC detected in the SMT control. (Figure 3.3).

To assess whether copper impacts production or stability of SigC, expression of myc-SigC in Erdman/pSR173 was induced with 1 μg/ml aTc for 24 hours in the presence of 10 μM TTM and then incubated for 4 hours following addition of nothing or 40 μM copper sulfate alone or with 50 μg/ml protein synthesis inhibitor chloramphenicol. Addition of copper sulfate alone or in conjunction with chloramphenicol resulted in significant reduction of detectable myc-SigC (Figure 3.4). For copper sulfate, there was a 1.3-fold decrease in detectable myc-SigC, and a greater decline of 2.7 fold occurred in the presence of both copper sulfate and chloramphenicol (Figure 3. 4). There was no significant difference in detectable myc-SigC levels in cultures containing TTM or TTM with chloramphenicol (Figure 3.4). This suggests that the addition of copper leads to degradation of myc-SigC rather than inhibition of protein new synthesis.

The Cys-Gly-Cys Motif of SigC Contributes to Function

As it was reported that a cysteine-rich domain with C-X-C motifs functions in sensing of copper by sigma factor CorE in *Myxococcus xanthas* (148, 149), we examined the *M. tuberculosis* SigC sequence and identified a Cys-Gly-Cys motif (amino acids 156-158) in the turn of the helix-turn-helix DNA binding motif found in sigma factor region 4.2 (Figure 3.5A). To determine if this motif contributes to SigC function, derivatives of plasmid pSR173 were created to encode myc-SigC with alanine mutations at individual positions of the C-G-C motif or replacing both cysteine residues to create these four motif lesions: A-G-C, C-A-C, C-G-A, and A-G-A. Each of these plasmids, pSR173, and a

control plasmid lacking *sigC* were separately introduced into *M.tb*Δ*sigC* and growth assessed by AlamarBlue assay in SMT cultures. As expected, all strains grew in SMT lacking chelator (Figure 3.5B, Row 1). In the presence of 5 μM TTM, the strain encoding wild-type SigC (C-G-C) grew, but none of the strains with SigC mutations converted the indicator dye from blue to pink (Figure 3.5B, Row 2). In TTM-containing cultures in which SigC was induced with 10 ng/ml aTc, each of the C-G-C motif mutants showed some metabolic conversion of the indicator dye, but not to the same extent as wild-type, indicative of partial SigC function (Figure 3.5B, Row 3). Supplementation of SMT + 5 μM TTM cultures with 10 μM copper sulfate resulted in comparable growth (similar color conversion) as wildtype for all SigC mutants, including the empty vector control (Figure 3.5B, Row 4). This was consistent with earlier results in which the growth defect of *M.tb*Δ*sigC* in SMT + TTM was reversible by copper sulfate addition (Figure 3.2A). To determine if TTM is specific for copper, the strains were assayed in SMT + 5 μM TTM + 10 μM zinc sulfate. While the strain encoding wild-type SigC grew under this condition, all strains lacking SigC or with C-G-C mutations failed to grow (Figure 3.5B, Row 5). These data indicate that zinc cannot reverse the growth defect of a *sigC* mutant caused by copper chelation (compare to Figure 3.6B, Row 2). Taken together, these results indicate that each of the residues in the C-G-C motif are required for full function of SigC in copper acquisition by *M. tuberculosis*.

DISCUSSION

SigC is a known virulence determinant of *M. tuberculosis* involved in copper acquisition in low-copper conditions (4, 6). SigC promoter sites have been identified in

the regions upstream of *ctpB* and the *PPE1-nrp* operon (5). A growth defect develops in the *sigC* deletion mutant *M.tb*Δ*sigC* after multiple passages in the chemically-defined SMT medium prepared without copper contamination (6). Chelation of copper with TTM in SMT medium consistently results in a complete absence of growth of *M.tb*Δ*sigC* (Figure 3.1). The same defect does not occur in the parental strain or the complemented mutant. Addition of 10 μM copper sulfate reversed the growth defect caused by the presence of 5 μM TTM for *M.tb*Δ*sigC* in SMT medium (Figure 3.1). These results confirm the role for *sigC* in copper acquisition by *M. tuberculosis* when levels of the metal are extremely low.

For *M. tuberculosis* to survive inside a host, it must effectively compete with host storage systems to acquire copper. We observed that strain Erdman grew in SMT containing up to 8 μM TTM or up to 500 μM BCS, but the *sigC* mutant did not grow in the presence of 2 μM TTM or 16 μM BCS (Figure 3.2). Addition of 2 μM copper sulfate to cultures of the *sigC* mutant containing 10 μM TTM or 15 μM BCS restored growth. This result combined with the observation that addition of sodium ascorbate to SMT cultures with only 1 μM BCS blocked *M.tb*Δ*sigC* growth (Figure 3.2), suggests that the mutant is unable to effectively compete for Cu(I). Taken together, these data support a role for SigC in acquiring Cu(I).

Regulation of SigC at the protein levels was unclear. A common mechanism for control of secondary sigma factors is by an anti-sigma factor encoded in the same operon; however, *sigC* is monocistronic and an anti-sigma factor for SigC has not been confirmed. The *sigC* gene has been reported to be transcribed at high levels under multiple *in vitro* growth conditions (89). Transcript mapping identified at least two

promoters upstream of *sigC*, but neither required SigC, suggesting that this gene is not autoregulated (8, 10). Crystallographic analysis of intact SigC protein was not reported due to difficulties with protein solubility (8, 150). Structural analysis of sigma factor regions 2 and 4 of SigC purified separately, led investigators to conclude that these regions likely interact in the absence of core RNA polymerase (8). Immunoblot assays showed a significant decrease in the amount of detectable myc-SigC from induced *M. tuberculosis* cultures containing 10 μM copper sulfate compared to cultures containing 5 μM TTM (Figure 3.3). These results indicate that SigC protein levels are reduced when ample copper is present. When copper sulfate and the protein synthesis inhibitor chloramphenicol were added to cultures containing high levels of myc-SigC, there was a significant 2.7-fold decrease in the amount of detectable myc-SigC within 4 hours (Figure 3.4); however there was no decrease in the amount of detectable SigC following a 4 hour incubation with only chloramphenicol (Figure 3.4). Taken together, these results suggest that the presence of free copper ions lead to degradation of SigC protein, rather than prevention of new protein synthesis. The instability of SigC in the presence of Cu(II) ions would also explain the difficulties of SigC purification. When expressed in *E. coli*, the protein must be purified from inclusion bodies under denaturing conditions and refolded in buffer containing EDTA, reducing agent, and zinc sulfate (8, 150, 151).

The CorE protein of *Myxococcus xanthus* was identified as a sigma factor that is activated by binding Cu(II) and inhibited by Cu(I). In response to Cu(II), CorE functions to upregulate copper toxicity-response genes including *cuoB* encoding a multicopper oxidase as well as *copA* and *copB* encoding P-type ATPases (149). The activity of CorE-dependent genes is reduced if Cu(II) is chelated by TTM, but addition of Cu(I) chelators

BCA or BCS increase activity of the sigma factor (149). *In vitro* EMSA indicate that CorE requires Cu(II) and BCS to stably bind to the *copB* promoter (149). Sequence alignments of myxobacteria CorE-like sigma factors showed multiple cysteine residues including C-X-C motifs required for activity (148).

Within the turn of the helix-turn-helix motif in region 4.2 of *M. tuberculosis* SigC is a C-G-C sequence (8). As SigC functions in copper acquisition, we hypothesized that the C-G-C region might function in copper sensing. Site-directed mutagenesis of this motif impaired the ability of SigC to effectively compete with TTM for copper unless protein levels were artificially induced (Figure 3.5). While this data indicates that the C-G-C motif is required for SigC function, it remains to be determined if this is due to reduced SigC stability, reduced binding to core RNAP, or reduced binding of SigC-RNAP to the *PPE1* promoter.

These data along with results of previous studies of SigC-mediated transcription support a model for SigC regulation (Figure 3.6). In an environment with ample free copper, the metal ions enter the periplasm through outer membrane porins and *M. tuberculosis* maintains redox balance through efficient respiration by a copper-dependent aa3-type super-complex. Under this condition, SigC function is not necessary, and the ample copper levels lead to protein degradation. However, in an environment with extremely-low available free copper, the bacteria are unable to acquire sufficient amounts of the metal by diffusion to efficiently respire, which creates more reduced conditions within the cell. The bacteria respond by increasing surface lipids, such as phthiocerol dimycocerosates (PDIMs), to dump electrons and partially restore redox balance to the TCA cycle (152). This increase in surface lipids may cover the porins and further limit

copper acquisition. The lack of available copper allows SigC to stabilize and direct transcription of the *PPE1-nrp* operon and *ctpB* gene to produce a copper chelator and a copper-importing ATPase. This would enable the bacteria to efficiently acquire copper from its surroundings and transport it into the cytoplasm, where the metal replenishes the cofactor need of the aa3-type super complex, which regains function to efficiently transfers electrons to oxygen and restore redox balance, resulting in oxidation of Cu(I) ions to Cu(II). Increased copper concentrations will again lead to degradation of SigC to prevent additional copper import. Additional studies to elucidate the interaction between SigC and copper to further support this model are in progress.

Table 3.1 Plasmids and strains used in this study

Plasmid	**Key Features**	**Source/Reference**
pGS1551sigC	L5*att/int*, *aph*, *oriE*, *M. tuberculosis sigC* with native promoter	(6)
pSR173	*hyg*, $P_{smyc\text{-}tetO}$:myc-*sigC*, *oriE*, *oriM*, *tetR*	(153)
pSLT37	pSR173 without *sigC*	This study
pRK140	pSR173 with *sigC* (C156A)	This study
pRK141	pSR173 with *sigC* (G157A)	This study
pRK142	pSR173 with *sigC* (C158A)	This study
pRK143	pSR173 with *sigC* (C156A/C158A)	This study
Strain	**Key features**	**Source/Reference**
M.tb	*M. tuberculosis tuberculosis* Erdman-CDC	Tuberculosis/Myco-bacteriology Branch, CDC
*M.tb*Δ*sigC*	*M. tuberculosis* Erdman Δ*sigC*	(6)
*M.tb*Δ*sigC::sigC*	Δ*sigC*/pGS1551sigC	(6)
M.tb/pSR173	Erdman/pSR173	(6)
*M.tb*Δ*sigC*/pSR173	*M.tb*Δ*sigC*/pSR173	This study
*M.tb*Δ*sigC*/pSLT37	*M.tb*Δ*sigC*/pSLT37	This study
*M.tb*Δ*sigC*/pRK140	*M.tb*Δ*sigC*/pRK140	This study
*M.tb*Δ*sigC*/pRK141	*M.tb*Δ*sigC*/pRK141	This study
*M.tb*Δ*sigC*/pRK142	*M.tb*Δ*sigC*/pRK142	This study
*M.tb*Δ*sigC*/pRK143	*M.tb*Δ*sigC*/pRK143	This study

Table 3.2 Primers used in this study

Primer	Sequence
P1498	5′-TGCTCGGGCTGTCCTATGCGGACGCCGCGGCGGTGGCAGGCTGC CCGGTGGGCACCATCCGA-3′
P1499	5′-CTGCTCGGGCTGTCCTATGCGGACGCCGCGGCGGTGTGCGCATGC CCGGTGGGCACCATCCGA-3′
P1500	5′-CTGCTCGGGCTGTCCTATGCGGACGCCGCGGCGGTGTGCGGCG CACCGGTGGGCACCATCCGA-3′
P1501	5′-TGCTCGGGCTGTCCTATGCGGACGCCGCGGCGGTGGCAGGCGCA CCGGTGGGCACCATCCGA-3′
P1502	5′-ACCATGCATCTAGCCGGTGAGGTCGTCGGGCTCCGCGTCGGCAAGCA GCGCATCGCGCGCTCGAGCGACACGGGATCGGATGGTGCCCACCGG-3′

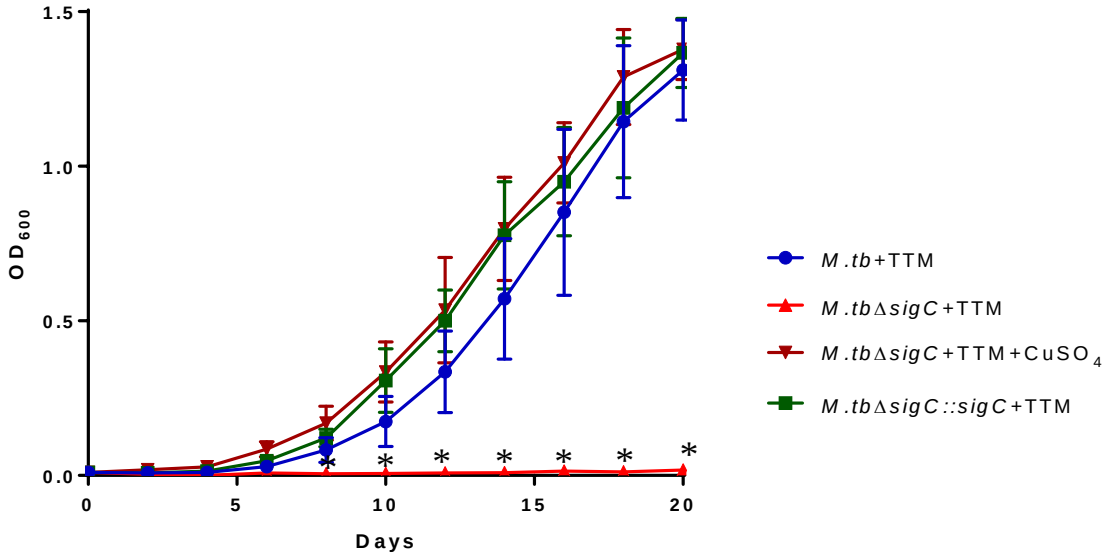

Figure 3.1 Examination of the growth requirement for *sigC* by *M. tuberculosis* in copper-depleted medium. Growth of *M. tuberculosis* strain Erdman (*M.tb*), the *sigC* deletion mutant (*M.tb*Δ*sigC*), and the complemented strain *M.tb*Δ*sigC*::*sigC* cultured in SMT with 5 μM TTM +/-10 μM copper sulfate was monitored by absorbance. Results shown are the average of three experiments, each with three biological replicates per condition. (*) The statistical significance between *M.tb*Δ*sigC* cultured in 5 μM TTM alone versus all other tested strains and conditions was determined using a two-way ANOVA, ($p < 0.0001$).

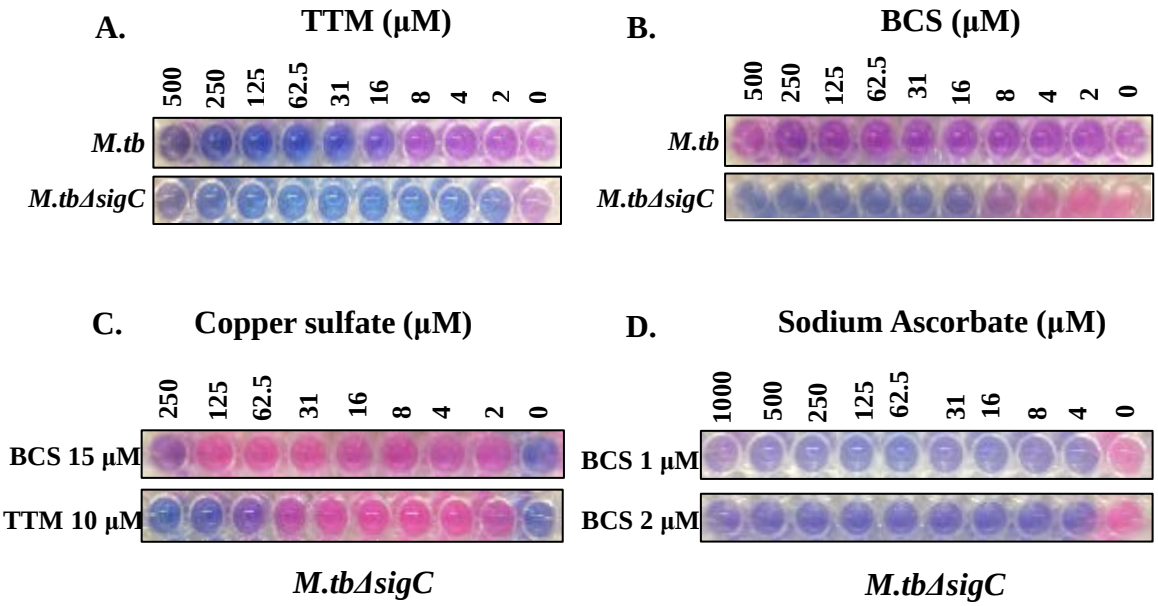

Figure 3.2 Examination of the effects of copper chelators, copper ions, and reductant on growth of *M. tuberculosis* strains. AlamarBlue assays were performed for both *M.tb* and *M.tb*Δ*sigC* grown in SMT with copper chelator alone or in conjunction with copper sulfate or sodium ascorbate. Bacteria were seeded at a 1:5 dilution from cultures diluted to an OD_{600} =0.02 in 96-well plates and incubated at 37°C for 7 days prior to AlamarBlue addition. The plate photos shown were taken 96 hours after addition of the indicator dye. Growth of *M.tb* and *M.tb*Δ*sigC* was examined over a range of concentrations of copper-chelator TTM (A) or BCS (B). Growth of *M.tb*Δ*sigC* was examined in medium with varying concentrations of copper sulfate in the presence of either 15 µM BCS or 10 µM TTM (C). Growth of *M.tb*Δ*sigC* with varying concentrations of sodium ascorbate and either 1 or 2 µM BCS (D).

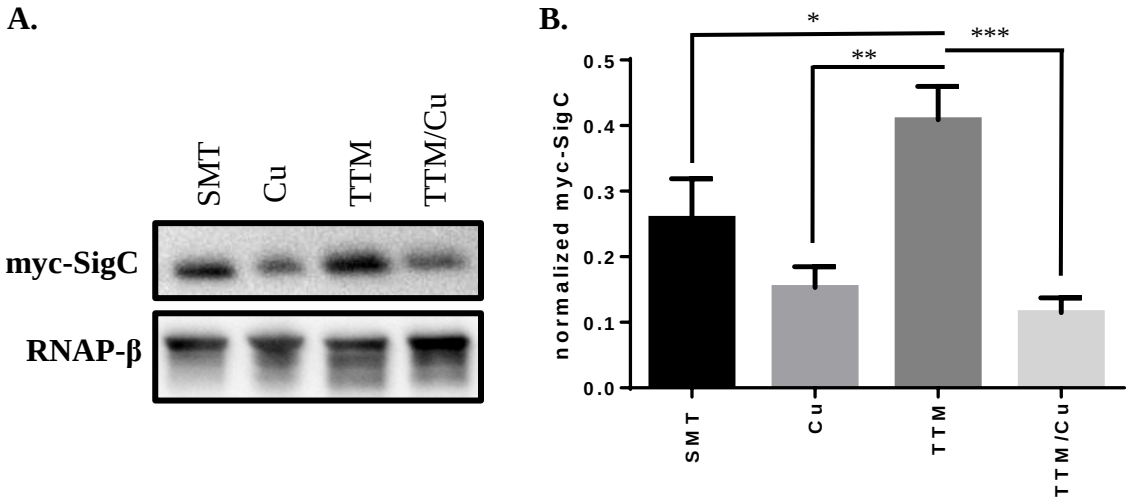

Figure 3.3 Examination of the effects of copper on myc-SigC stability. Strain *M.tb*/pSR173 was grown at 37°C to OD_{600} ≈0.6 in SMT with hygromycin [50 μg/ml]. Expression of myc-SigC was induced by addition of aTc [1 μg/ml]. At the time of induction, 5 μM TTM and/or 10 μM copper sulfate was added to replicate cultures. After 24-hour incubation at 37°C, cells were harvested and lysed. Proteins were resolved by SDS-PAGE and transferred to nitrocellulose membranes. Immunoblotting and densitometry were performed to quantify amounts of detectable myc-SigC relative to RNA polymerase β subunit (RNAP-β) using antibodies to each protein. Representative immunoblots for both proteins are shown for the indicated growth condition (A). Densitometry analysis of myc-SigC normalized to RNAP-β. Results shown represent the mean of three independent experiments with each condition assessed with 3 biological replicates (n=9) (B). One-way ANOVA was used to determine statistical significance (*p=.0082, **p =0.0018, ***p<0.0001).

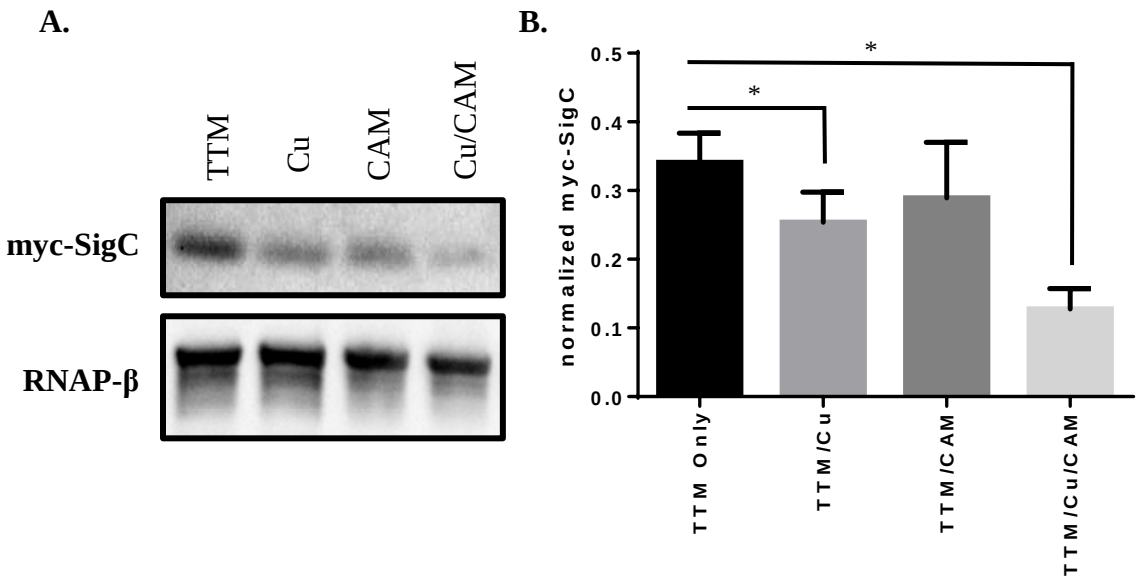

Figure 3.4 Quantification of the effects of copper on *in vivo* myc-SigC levels. Strain *M.tb*/pSR173 was grown at 37°C to OD_{600} ≈0.6 in SMT with hygromycin [50 μg/ml]. Expression of myc-SigC was induced by addition of aTc [1 μg/ml]. At the time of induction, 10 μM TTM was added to the cultures. After 24-hour incubation at 37°C, 10 μM copper sulfate (Cu) and/or 50 μg/ml chloramphenicol (CAM) was added and cultures incubated 4 hours. Cells were harvested and lysates separated by SDS-PAGE. Immunoblotting and densitometry were performed to quantify myc-SigC and RNAP-β (A). Levels of myc-SigC were normalized to RNAP-β. Results shown represent the mean of three independent experiments with each condition assayed with 3 biological replicates (n=9) (B). One-way ANOVA was used to determine statistical significance (*p≤ 0.006).

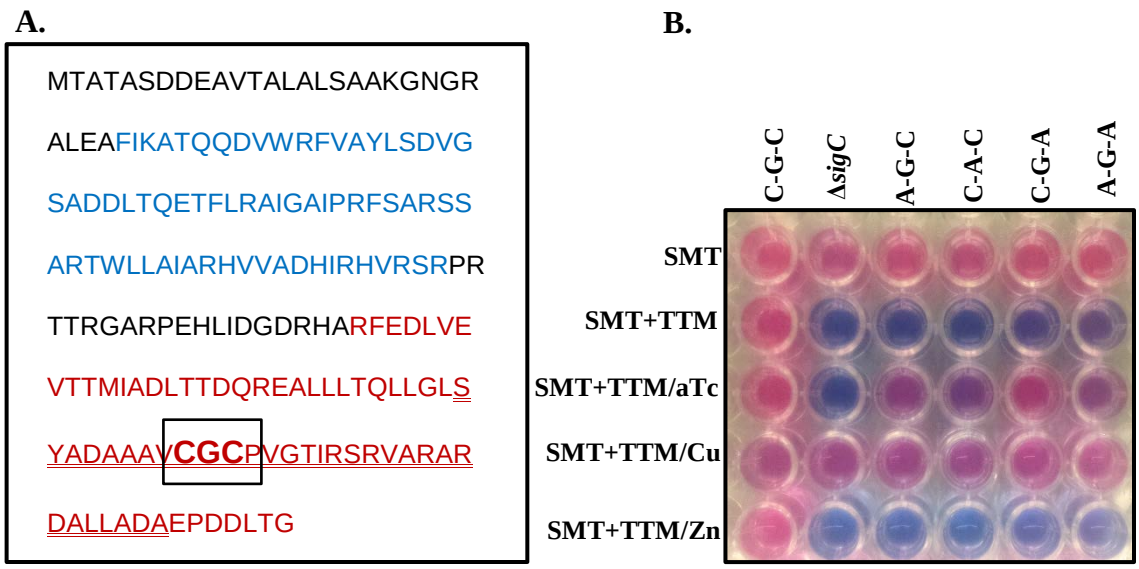

Figure 3.5 Examination of the C-G-C motif in SigC for function in copper acquisition. Depicted in panel A is the amino acid sequence of *M. tuberculosis* SigC, with sigma factor region 2 shown in blue, and region 4 in red. Region 4.2 (underlined) contains a helix-turn-helix motif (the turn portion of the motif is boxed) for DNA recognition of the -35 element of a promoter (8, 90). A C-G-C sequence (emboldened) is located within this motif. Panel B: The importance of the C-G-C motif for SigC activity was evaluated by Alamar Blue cell viability assay with *M.tbΔsigC* strains carrying plasmids encoding myc-tagged SigC with the wildtype motif (C-G-C) or with individual residues changed to alanine or a plasmid deleted for *sigC* (Δ*sigC*) downstream from an anhydrotetracyline (aTc)-inducible promoter. Bacteria were seeded at a 1:5 dilution from cultures diluted to an OD_{600} =0.02 in SMT medium alone or with 5 μM TTM, 10 ng/ml aTc, 10 μM copper sulfate, 10 μM zinc sulfate in 96-well plates and incubated at 37°C for 7 days prior to addition of AlamarBlue and incubation 4 more days to allow metabolic activity to reduce the indicator dye from blue to pink. Results are representative of assays performed on a minimum of 3 biological replicates assayed twice.

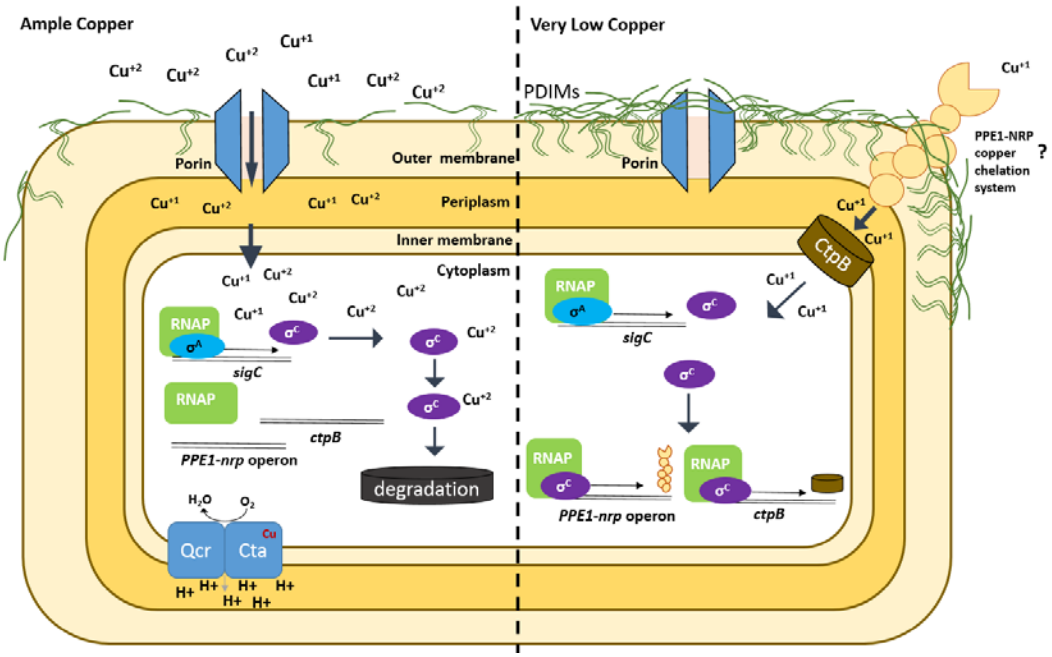

Figure 3.6 Model for SigC regulation in *M. tuberculosis*. Depicted is the proposed regulatory mechanism for SigC in *M. tuberculosis*. The *sigC* gene is transcribed by SigA (σ^A) under multiple conditions at a high level. Under conditions where ample free copper is available, Cu(II) enters the bacteria by diffusion through outer membrane porins, enters the cytoplasm by an unknown copper transporter. Under this condition, the bacteria are able to support aerobic respiration through the copper-dependent CtaCDE type aa3-oxidase. The Cu(II) levels build and lead to degradation of SigC (σ^C). However, under very low copper conditions, respiration is reduced, leading to synthesis of long outer membrane lipids (such a PDIMs) to help utilize electrons generated by metabolic activity of the TCA cycle. These lipids likely block the porins and limit passive copper uptake. The cytoplasm becomes more reduced and the lack of Cu(II) allows SigC to stabilize and direct transcription of the *PPE1-nrp* operon and *ctpB* to chelate and transport captured copper into the cells. As copper levels increase, respiration is restored and the redox level becomes more oxidizing, causing Cu(I) to oxidize to Cu(II) which destabilizes SigC to stop expression of the copper-uptake genes.

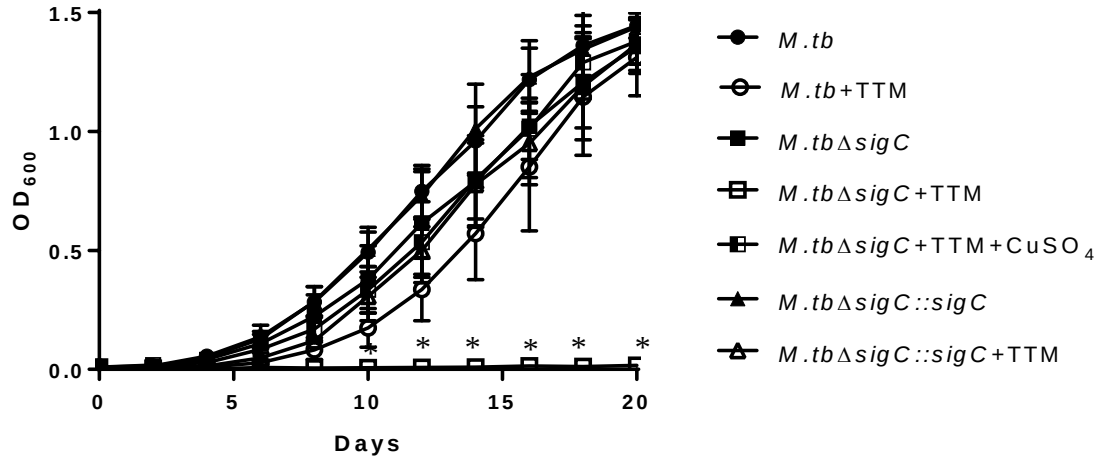

Figure 3.7 Growth of *M. tuberculosis* strains in the presence or absence of copper and copper chelator. *M. tuberculosis* strain Erdman (*M.tb*), the *sigC* deletion mutant (*M.tb*Δ*sigC*), and complemented mutant (*M.tb*Δ*sigC*::*sigC*) were cultured in SMT with or without 5 μM TTM with 10 μM $CuSO_4$, as indicated. The optical density (OD_{600}) results shown are the average of three experiments, each with three biological replicates per condition. (*) The statistical significance between *M.tb*Δ*sigC* cultures containing 5 μM TTM and all other strains and conditions was determined using a two-way ANOVA, ($p < 0.0001$).

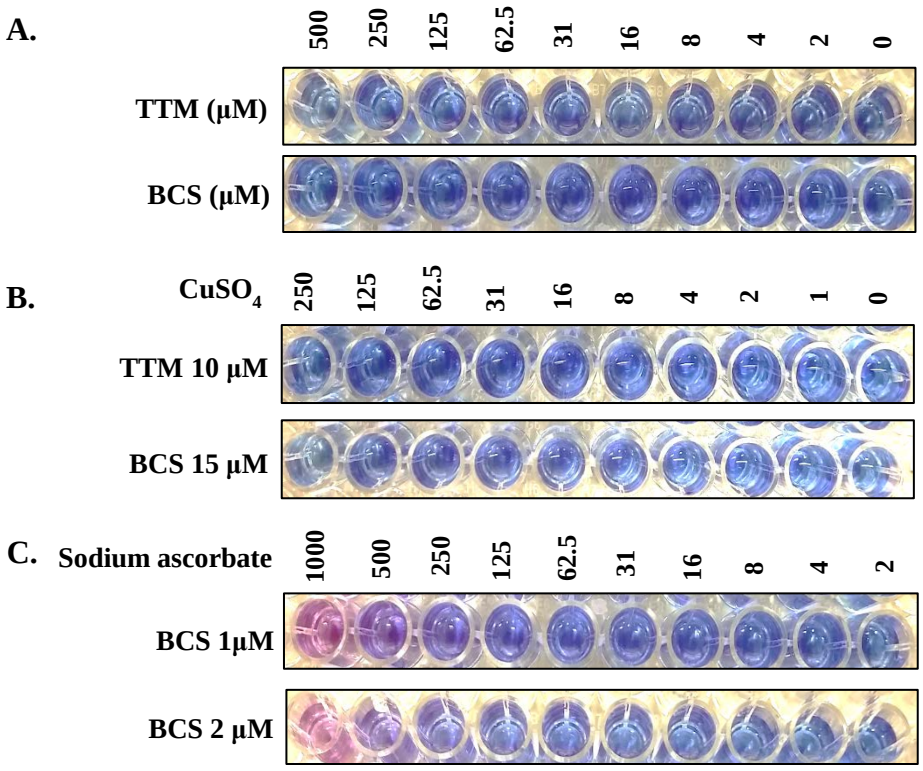

Figure 3.8 The effects of various media supplementation on Alamar Blue reagent color conversion. AlamarBlue assays were performed for SMT containing copper chelator alone or in conjunction with copper sulfate or sodium ascorbate. Media with additives were incubated for 7 days at 37°C prior to AlamarBlue addition. The plate photos shown were taken 96 hours after addition of the indicator dye. (A) SMT containing a range of concentrations of copper-chelator TTM or BCS. (B) Medium with varying concentrations of copper sulfate in the presence of either 15 μM BCS or 10 μM TTM. (C) Medium with varying concentrations of sodium ascorbate and either 1 μM or 2 μM BCS.

CHAPTER 4

MYCOBACTERIUM TUBERCULOSIS ENCODES GENES WITH FUNCTIONS IN COENZYME B_{12} SYNTHESIS[1]

[1] Samantha L. Tucker, Stacey Crockett, Ashitha Rajeurs, Frederick Quinn, Russell Karls. To be submitted to *Journal of Bacteriology*.

ABSTRACT

The obligate human pathogen *Mycobacterium tuberculosis* is found in diverse host niches. Over the course of active, latent, and reactive infections, the bacilli experience environments that vary in acidity, toxicity, oxygen content, and nutrient availability. For adaptive survival, *M. tuberculosis* has evolved mechanisms to tailor its metabolism to maximize persistence within the host. Coenzyme B_{12} (Co-B_{12}) represents an important cofactor for fatty acid metabolism, methionine synthesis, and DNA synthesis in *M. tuberculosis*. While the *M. tuberculosis* genome encodes homologs of many identified Co-B_{12} biosynthetic genes, *in vitro* production of the coenzyme has not been reported in over 40 years. However, transcriptional and proteomic data indicate the expression of some Co-B_{12} biosynthetic genes during human infection and under specific *in vitro* culture conditions. To assess the capacity of *M. tuberculosis* to synthesize Co-B_{12}, predicted Co-B_{12} biosynthetic genes from this pathogen were expressed in *Salmonella Typhimurium* Co-B_{12} auxotrophs containing specific blocks in the pathway. Results indicate that *M. tuberculosis* gene *Rv0259c* restores Co-B_{12} synthesis to a *S.* Typhimurium *cbiK* mutant defective in the early-cobalt insertion step of the pathway conserved in microbes that produce Co-B_{12} anaerobically. This result suggested that *M. tuberculosis* may synthesizes Co-B_{12} under hypoxic conditions. However, growth of the bacteria by the Wayne hypoxic method or in stationary pellicle cultures did not result in lysates that supported growth of a *S.* Typhimurium B_{12} auxotroph. Importantly, 16 of the 19 *M. tuberculosis* genes introduced into *S.* Typhimurium mutants with blocks at different steps of the Co-B_{12} pathway restored production of the coenzyme. Taken together, the conservation of such a large number of genes functional in anaerobic Co-B_{12}

synthesis strongly supports the hypothesis that *M. tuberculosis* produces this co-enzyme in hypoxic niches within its human host.

INTRODUCTION

Mycobacterium tuberculosis is the leading cause of death by a single infectious agent world-wide (1). There were an estimated 10.4 million new cases of tuberculosis disease (TB) and 1.6 million deaths in 2016 (1). Of the reported cases in 2016, 3.5% were multi-drug resistant strains of *M. tuberculosis* (1). The live, attenuated *M. bovis* bacille Calmette-Guérin vaccine is largely ineffective at preventing pulmonary TB in adults (1). A better understanding of *M. tuberculosis* physiology, metabolism, and replication within the host will aid the development of new vaccines and antibiotics.

Adenosylcobalamin, also known as co-enzyme B_{12} (Co-B_{12}, B_{12}), is a complex tetrapyrrole with a cobalt center that functions as a cofactor for multiple enzymes. Co-enzymatic forms include adenosylcobalamin, which contain an adenosyl group as the upper axial ligand to cobalt (Figure 4.1), and cob(I)alamin, which lacks an upper cobalt ligand (11). Other cobalamins have an upper methyl, hydroxyl, or glutathionyl moiety (134, 154). Commonly-known vitamin B_{12} contains a cyano-group as the upper axial ligand. Co-enzyme B_{12} molecules have a lower ligand that can coordinate with the cobalt ion and is linked to the corrin macrocycle via a nucleotide loop. Cobalamins have 5, 6 - dimethylbenzimidazole (DMB) as the lower ligand (Figure 4.1). Only bacteria and archaea are known to synthesize Co-B_{12}; however, many organisms, including humans synthesize enzymes requiring cobalamins as cofactor (11).

The *M. tuberculosis* genome encodes three Co-B_{12}-dependent enzymes: methionine synthase (MetH), methylmalonyl-CoA mutase (MutAB), and a class II ribonucleotide reductase (NrdZ). Two B_{12}-responsive riboswitches were identified in the *M. tuberculosis* genome (141, 155). One was shown to control production of the Co-B_{12}-independent methionine synthase MetE, and the other is located upstream of the *PPE2-cobQ1-cobU* operon, which encodes two Co-B_{12} biosynthetic gene homologs (155, 156). Recent reports have indicated that *M. tuberculosis* does not produce Co-B_{12} under standard *in vitro* growth conditions or during macrophage infection (14, 29, 156, 157). However, it has been demonstrated that this pathogen is able to convert and utilize cobalamin and other cobamides imported by a B_{12} transporter, Rv1819c (137).

Homologs to many Co-B_{12} biosynthetic pathway genes are predicted in *M. tuberculosis*, but function of these genes has not been confirmed (158). Transcription studies showed increased expression of a predicted Co-B_{12} synthesis *cobI* homolog in the distal lung of a human with TB relative to *in vitro* culture of the bacteria (159). Proteomic analyses revealed that when *M. tuberculosis* is cultured stationary as a pellicles in minimal medium, two predicted Co-B_{12} biosynthetic pathway proteins, CobD and CobB, were detected in culture filtrates (160). Wayne and Hayes reported that slow depletion of available oxygen by growth of *M. tuberculosis* in sealed cultures induces a state of non-replicating persistence (NRP) (36). Transcriptional analyses of bacteria in this model revealed many genes altered in response to oxygen depletion (38). One of the genes upregulated by hypoxia is *nrdZ* , which encodes a class II Co-B_{12}-dependent ribonucleotide reductase, NrdZ (38, 161). Together, these examples support the

possibility that *M. tuberculosis* may require and produce Co-B_{12} in hypoxic environments within the host.

Biosynthesis of Co-B_{12} can require up to 30 enzymes, and variations exist across species (141). Of the organisms studied in detail, Co-B_{12} synthesis follows one of two general pathways (141). These pathways differ in the timing of cobalt atom insertion, mechanism for ring contraction, and the presence of oxygen-instable intermediates (134, 162, 163). An organism which typifies the early-cobalt insertion pathway is the anaerobically producing *Salmonella enterica* ssp. *enterica* serovar Typhimurium (*S.* Typhimurium) (142). The functions of many *S.* Typhimurium Co-B_{12} synthesis enzymes have been defined genetically, biochemically, or both (134, 164, 165). Deletions of individual Co-B_{12} biosynthetic genes in *S.* Typhimurium have also been used for assessment of genes from other prokaryotes for function in Co-B_{12} synthesis (166, 167)**.**

In the present study, we utilize *S.* Typhimurium Co-B_{12} auxotrophic strains with mutations in specific Co-B_{12} biosynthetic pathway genes to assess *M. tuberculosis* genes predicted to function in different steps of the pathway. We also directly assay for Co-B_{12} production by *M. tuberculosis* grown as pellicle cultures and in the Wayne hypoxic model. Results indicate that 16 *M. tuberculosis* genes restored Co-B_{12} biosynthesis to *S.* Typhimurium mutants blocked at different steps in the pathway. While Co-B_{12} was not detected in extracts from *M. tuberculosis* cultures, the observation that numerous intact *M. tuberculosis* genes are functional in Co-B_{12} biosynthesis supports the hypothesis that this pathogen synthesizes the cofactor in host environments that have not yet been suitably replicated *in vitro*.

METHODS

Bacterial Strains

Strains used in this study are indicated in Table 4.1. All *E. coli* and *S.* Typhimurium strains were maintained in Luria Bertani (LB) broth, or on LB agar grown aerobically at 37°C. Cultures were supplemented with carbenicillin [50 μg/ml] when required. Unless otherwise indicated, the *S.* Typhimurium strains used in this study were previously created in the laboratory of Dr. Jorge Escalante using the methods of Datsenko and Wanner (Table 4.2) (168).

For *M. tuberculosis* strains grown as pellicles, bacteria were first cultured on solid Lowenstein-Jensen Media (BD BBL^{TM}) and incubated at 37°C for 21-28 days. Colonies were then suspended in 1 ml Sauton medium (147). To inoculate pellicle cultures, 0.1 ml of the suspended bacteria was added to each non-vented T-175 flask containing 75-100 ml of Sauton medium supplemented with 5 μM cobalt chloride, 3.5 μM zinc sulfate, and 10 μM potassium cyanide. Cultures were incubated at 37°C stationary until a solid bacterial layer covered the surface or maintained for as long as 12 months. For Wayne cultures, *M. tuberculosis* bacteria were inoculated to an OD_{600} = 0.02 into 20 ml of Dubos broth base (42) supplemented with 5 μM cobalt chloride and 1 μg/ml methylene blue (redox indicator) in 30 ml rubber-stoppered crimp-top vials containing a flea magnet, sealed, and incubated at 37°C with slow stirring.

Construction of Plasmids

Plasmid derivatives of pBAD-TOPO (Invitrogen) encoding predicted *M. tuberculosis* Co-B_{12} biosynthesis pathway genes under the control of an arabinose-inducible promoter are listed in Table 4.2. To construct these plasmids, genes were PCR amplified from *M. tuberculosis* strain H37Rv genomic DNA with *Pfu*-Ultra II Hotstart Master Mix (Agilent) using the primers listed in Table 4.4. After adding phosphates to the 5′ ends with T4 polynucleotide kinase (New England Biolabs), the PCR products were ligated into pBAD-TOPO vector that had been digested with *Nco*I and *Pme*I and DNA ends blunted with T4 DNA polymerase and dNTPs (New England Biolabs). Ligated DNAs were introduced into chemically-competent *E. coli* TAM1 cells (Active Motif) selecting for resistance to carbenicillin [50 μg/ml]. Plasmids were confirmed by PCR and DNA sequencing.

Transformation of *S.* Typhimurium Mutants

Each *S.* Typhimurium strain was grown to an OD_{600} = 0.4-0.6 in LB broth. For each electroporation, 1 ml of culture was collected by centrifugation (10,000 x g, 2 min.) Supernatant was decanted and the pellet was washed with 1 ml cold, sterile dH_20 twice. Following the second wash, the cells were suspended in 0.1 ml of cold sterile dH_20 and transferred to a pre-chilled 2-mm electroporation cuvette (Bio-Rad). Approximately 20-50 ng of plasmid DNA was added to the cells. The samples were pulsed at 2.5 kV, 200 Ω, and 25 μF using a GenePulser Xcell^{TM} electroporator (Bio-Rad). Cells were recovered in

1 ml of LB broth at 37°C for 1 hour with shaking and then plated onto LB agar plates containing carbenicillin [50 μg/ml].

Assay for *M. tuberculosis* Co-B_{12} Gene Function

Salmonella Typhimurium strains with specific Co-B_{12} biosynthetic gene mutations, and the corresponding strain encoding a predicted *M. tuberculosis* Co-B_{12} gene on a pBAD-TOPO plasmid were grown overnight shaking at 37°C in LB broth. When required, carbenicillin [50 μg/ml] was added. Bacteria were pelleted (10,000 x g, 2 min.) and washed twice with 0.9% NaCl. Following the second wash, the supernatant was discarded and cells streaked on modified Vogel-Bonner agar plates (169) containing trace metal solution (170), 0.2% arabinose (v/v), and +/- 1 μg/ml cyanocobalamin. When required, 1 mM of L-glutamine (Gibco^{TM}), and 100 μM of 5, 6 dimethylbenzimidazole (DMB) were also added. Galactose at 0.2% (v/v) served as a carbon source. Cultures were grown in GasPak^{TM} containers with a fresh GasPak^{TM} EZ Anaerobe Container System pouch (BD) at 37°C for 72 hours, followed by aerobic incubation at 37°C for 24 hours. All strains were assayed a minimum of three times in duplicate.

Preparation of Cell Extracts from *M. tuberculosis* Cultures

The pellicles of *M. tuberculosis* bacteria from static cultures were drained of liquid and washed with 0.1 M sodium phosphate buffer (pH 7.0). Cells were lysed in extraction buffer (0.1 M Na_2HPO_4, pH adjusted to 4.5 with acetic acid; 0.005% KCN) with a tissue

homogenizer. The lysates were transferred into glass screw-capped tubes and incubated for 30 minutes at 90°C in a water bath prior to removal from the biolevel-3 laboratory. With the caps tightened, the lysates were autoclaved for 30 min, cooled to room temperature, and transferred into 1.5 ml tubes and clarified by centrifugation (10,000 x g, 5 min). The supernatants were filtered through 0.22 µM PVDF membranes, concentrated to approximately 50 µl in a SpeedVac (ThermoSavant), and stored at -20°C until assayed.

From Wayne cultures (36), the mycobacterial cells were harvested by centrifugation (3000 x g, 5 min), washed once with an equal volume 0.1 M sodium phosphate buffer (pH 7.0), re-suspended in extraction buffer (0.1 M Na_2HPO_4, pH adjusted to 4.5 with acetic acid; 0.005% KCN) and disrupted with 0.1 mm diameter zirconia/silica beads in a Bead Beater (BioSpec Products) with three 40-second cycles at 4800 rpm. The lysates were transferred into glass screw-capped tubes and incubated for 30 minutes at 90°C in a water. With the caps tightened, the lysates were then autoclaved for 30 min, cooled to room temperature, and transferred into 1.5 ml tubes and clarified by centrifugation (10,000 x g, 5 min). The supernatants were filtered through 0.22 µM PVDF membranes, concentrated to approximately 50 µl in a SpeedVac and stored at -20°C until assayed.

Assay for Detection of B_{12}

Salmonella Typhimurium strain JE212 was cultured overnight in LB medium at 37°C with shaking (180 rpm). Culture aliquots (1 ml ea.) were transferred into 1.5 ml tubes and collected by centrifugation (10,000 x g, 5 min). Pellets were washed twice with

1 ml 0.9% NaCl and cells suspended in 1 ml of 0.9% NaCl. For each assay plate, 0.2 ml cells were mixed with 3 ml molten (56°C) 0.6% noble agar, and poured onto Vogel-Bonner minimal medium agar plates (169) supplemented with 11 mM glucose and 0.1 mM histidine. After agar solidification, 5 µl of each mycobacterial lysate and 2 µl cyanocobalamin (100 µg/ml) were spotted on the plates. Plates were incubated at room temperature for approximately 15 min (to allow the liquid to be absorbed) and then incubated inverted 12-18 hours at 37°C. Growth of *S.* Typhimurium JE212 in spotted areas indicates the presence of B_{12}.

RESULTS AND DISCUSSION

We recently reported that under aerobic culture conditions in Middlebrook 7H9 media only nontuberculous mycobacteria synthesize Co-B_{12} (6). That study also demonstrated that *cobK* and *cobU* from *M. tuberculosis* can restore Co-B_{12} synthesis to *Mycobacterium smegmatis* mutants lacking the respective homolog. Here we explore the hypothesis that *M. tuberculosis* produces the coenzyme by a process comparable to anaerobic producers exemplified by *S.* Typhimurium. The genome of *M. tuberculosis* encodes homologs to many genes that function in the *S.* Typhimurium Co-B_{12} synthesis pathway (Figure 4.1; Table 4.3, Columns 1-3). To ascertain whether these *M. tuberculosis* genes function in Co-B_{12} synthesis, each gene was PCR-amplified from *M. tuberculosis* genomic DNA with the indicated primers (Table 4.4) and cloned in plasmid pBAD-TOPO for arabinose-inducible expression in *S.* Typhimurium strains. Relevant features of the plasmids generated are indicated in Table 4.2. Strains generated after introduction of the plasmids into auxotrophic *S.* Typhimurium Co-B_{12} biosynthetic

pathway mutants are listed in Table 4.1. The parent, auxotrophic *S.* Typhimurium B_{12} pathway mutants, and the mutants after genetic complementation with *M. tuberculosis* genes were assayed for growth on Vogel-Bonner minimal medium agar supplemented with 0.2% arabinose. Results of functional complementation at individual steps in the biosynthetic pathway are detailed below and a summary of the results is provided in Table 4.3 and Figure 4.3.

Functional Complementation of *S.* Typhimurium Co-B_{12} Pathway Mutants with *M. tuberculosis* Genes

Rv2847 / *S.* Typhimurium *cysG*

The first part of the Co-B_{12} synthesis pathway converts uroporphyrinogen III to cob(II)yrinic acid a,c-diamide (Figure 4.1). In this stage, methylation of various porphyrin ring carbon atoms facilitate ring reduction/loss of C-20 and the insertion of the central cobalt atom. The first committed step in Co-B_{12} synthesis is the conversion of uroporphyrinogen III to precorrin-2 (sirohydrochlorin) (Figure 4.1). For this step, many aerobic Co-B_{12} producers use a homolog to the SAM-dependent methyltransferase encoded by *cobA* in *P. denitrificans* (171). However, *S.* Typhimurium utilizes the siroheme synthase encoded by *cysG* (172). The encoded CysG protein is a fusion of uroporphyrinogen-III methyltransferase and precorrin-2 dehydrogenase/ferrochelatase (134). In the *M. tuberculosis* H37Rv Mycobrowser database (158), two potential siroheme synthase/uroporphyrin III C-methyltransferases are encoded by *Rv0511*

(annotated as *hemD*) and *Rv2847* (annotated as *cysG*). The predicted sizes of Rv0511 (565 AA) and Rv2847 (405 AA) are more similar to *S.* Typhimurium CysG (457 AA) than to *P. denitrificans* CobA (280 AA). The encoded amino acid sequence of Rv2847 has 32% identity and 48% similarity spanning 95% of *S.* Typhimurium CysG (Table 4.3). In *M. tuberculosis*, *Rv2847* is located in an operon with other predicted Co-B_{12} biosynthetic genes; therefore, *Rv2847* was examined to determine if it could substitute for *S.* Typhimurium *cysG* to enable conversion of uroporphyrinogen III to sirohydrochlorin. Arabinose-induced expression of *M. tuberculosis Rv2847* in *S.* Typhimurium *cysG* mutant strain JE9734 resulted in growth on Vogel-Bonner plates (Figure 4.2, Table 4.3). This complementation result, combined with the homology between Rv2847 and *S.* Typhimurium CysG supports *M. tuberculosis Rv2847* encoding a C-2 and C-7 uroporphyrinogen-III methyltransferase and its annotation as *cysG*.

Rv0259c / S. Typhimurium *cbiK*

Timing of cobalt insertion into the tetrapyrrole ring is one of the major differences between aerobic and anaerobic Co-B_{12} production. In aerobic synthesis, cobalt is inserted into a nearly complete precorrin ring, whereas in the anaerobic pathway, cobalt insertion occurs immediately after the action of CysG (142). In *S.* Typhimurium, the sirohydrochlorin cobaltochelatase encoded by *cbiK* inserts cobalt as the second step in Co-B_{12} ring synthesis to produce cobalt-sirohydrochlorin (Figure 4.1). While the *M. tuberculosis* genome does not encode a CbiK homolog, it has *Rv0259c* which encodes a protein with 23% identity/41% similarity to CbiX, a sirohydrochlorin cobaltochelatase from *Bacillus megaterium* which synthesizes Co-B_{12} anaerobically (173, 174). To

determine if *Rv0259c* functions in early cobalt insertion, it was expressed from an arabinose-inducible promoter in the *S.* Typhimurium *cbiK* mutant JE13809. Arabinose-induced expression of *Rv0259c* resulted in growth of the strain when cultured anaerobically on Vogel-Bonner agar (Figure 4.2). This suggests that *M. tuberculosis* may follow an early-cobalt insertion pathway. The non-tuberculous mycobacterial species *Mycobacterium avium subsp. paratuberculosis* also encodes a CbiX homolog. We have previously reported that this species synthesizes Co-B_{12} aerobically (6). Interestingly, Cossu and colleagues reported that *cbiX* and other anoxically-induced metabolic genes are upregulated in this bovine intestinal pathogen when exposed to acid-nitrosative multi-stress which suggests *M. avium subsp. paratuberculosis* may also have capacity for anaerobic Co-B_{12} synthesis (175). Together, these data support the annotation of Rv0259c as CbiX.

Rv2066 / S. Typhimurium *cbiL/cbiH*

C-20 methylation of cobalt-sirohydrochlorin to cobalt-factor III in *S.* Typhimurium is catalyzed by CbiL (Figure 4.1). The N-terminus of *M. tuberculosis* Rv2066 has 48% similarity to *S.* Typhimurium CbiL (Table 4.3). The C-terminal Rv2066 region has 53% similarity to *S.* Typhimurium CbiH (Table 4.3), which catalyzes the methylation of cobalt factor III to cobalt-precorrin-4 (Figure 4.1). Both *S.* Typhimurium strains JE8238 (Δ*cbiL*32) and JE8239 (Δ*cbiH*29) were transformed with plasmid pSC3 encoding *M. tuberculosis Rv2066*. In both cases, arabinose-induced expression of *M. tuberculosis Rv2066* resulted in growth of the complemented *cbiL* and *cbiH* mutants (Figure 4.2). Interestingly, *cobI* from the aerobic Co-B_{12} producer *P. denitrificans* was

reported not to functionally complement a *S.* Typhimurium *cbiL* mutant despite having 20-40% AA identity (176). Thus, our data further supports the hypothesis that *M. tuberculosis* utilizes an early-cobalt insertion pathway for Co-B_{12} synthesis and indicates that *Rv2066* encodes a bi-functional enzyme with both CbiL and CbiH activities.

Rv2071c / *S.* Typhimurium *cbiF*

The next step in early-cobalt Co-B_{12} synthesis is C-11 methylation. This process is catalyzed by either the precorrin-4 C-11 methyltransferase CobM in aerobic Co-B_{12} producers to yield precorrin-5 or by the cobalt-precorrin-4 C-11 methyltransferase CbiF in *S.* Typhimurium resulting in cobalt-precorrin-5A (134). The *M. tuberculosis* Rv2071c (annotated as CobM) protein has 65% similarity/45% identity to *S.* Typhimurium CbiF (Table 4.3). Expression of *Rv2071c* in the *S.* Typhimurium *cbiF*-defective strain JE8235 resulted in restoration of growth of the mutant in the absence of Co-B_{12} (Figure 4.2). Thus, *M. tuberculosis* is capable of completing the first 5 steps in anaerobic-type early-cobalt Co-B_{12} synthesis.

Rv2068c / *S.* Typhimurium *cbiG* and *Rv2067c* / *S.* Typhimurium *cbiD*

The next two steps in Co-B_{12} synthesis are catalyzed by enzymes CbiG and CbiD in *S.* Typhimurium (Figure 4.1). Conversion of cobalt-precorrin-5A to cobalt-precorrin-5B in *S.* Typhimurium utilizes CbiG to open a 6-membered delta-lactone ring and eliminate acetaldehyde to yield cobalt-precorrin-5B (163, 177). Methylation of cobalt-precorrin-5B at C-1 is catalyzed by SAM-dependent methyltransferase CbiD to produce cobalt-precorrin-6A (163). In the aerobic late-cobalt insertion pathway, C-1 methylation

is catalyzed by CobF which facilitates removal of the extruded methylated C-20 group as acetic acid prior to C-1 methylation (163). Although non-tuberculous mycobacteria produce Co-B_{12} and encode a *cobF* homolog, *M. tuberculosis* lacks homologs of either *cobF* or *cbiD*. It has been hypothesized that the lack of a *cobF* or *cbiD* homolog underlies the inability of *M. tuberculosis* to produce Co-B_{12} (178); however we have shown previously that expression of *cobF* from *M. smegmatis* or *M. marinum* in *M. tuberculosis* does not result in aerobic Co-B_{12} synthesis. Downstream and divergently-transcribed from *M. tuberculosis Rv2066/cobI* is *Rv2067c*, predicted to encode a SAM-dependent methyltransferase that could serve as a nonorthologous replacement for c*obF* (179). Transcription of *Rv2067c* was upregulated in human clinical lung granulomas relative to *in vitro* cultured *M. tuberculosis* bacteria (159). Upstream of *Rv2067c* is *blaC*, which encodes a beta-lactamase (158). The genomic proximity of genes encoding both a putative methyltransferase and a known ring-breaking enzyme (albeit, not a delta-lactonase) to *Rv2066* led us to entertain the possibility that *M. tuberculosis* may have evolved a novel process to convert cobalt-precorrin-5A to cobalt-precorrin-6A. We first assessed whether *S.* Typhimurium strain JE7859 lacking *cbiD* could be functionally complemented with *M. tuberculosis Rv2067c*. Unfortunately, an answer could not be obtained due to JE7859 continuing to grow in the absence of Co-B_{12} (Figure 4.2). This indicates that in *S.* Typhimurium another enzyme can provide the function of CbiD. Conditions in which JE7859 fails to grow in the absence of B_{12} must first be identified before assessment of *Rv2067* in the Co-B_{12} synthesis can be determined (Figure 4.2). We next co-expressed *blaC* and *Rv2067c* in the *cbiG*-deficient *S.* Typhimurium strain JE8236. Expression of *blaC* and *Rv2067c* from an arabinose-inducible promoter was not

sufficient to support growth of JE8236 on minimal medium, indicating that these genes do not complement function of *cbiG* (Figure 4.2). Even in known Co-B_{12} producing organisms, not all mechanisms have been fully established (134, 141). Thus, it is possible that *M. tuberculosis* may use an undefined gene to provide this function.

Rv2070c / *S.* Typhimurium *cbiJ*

Cobalt-precorrin-6X reductase, CbiJ, in *S.* Typhimurium requires NADPH for reduction to cobalt-precorrin-6B (162). Organisms following the late-cobalt insertion pathway use a homolog, CobK to perform a similar reduction of precorrin-6A to precorrin-6B (176). Expression of *M. tuberculosis Rv2070c* (annotated as *cobK*) in the *cbiJ*-deficient Co-B_{12} auxotrophic *S.* Typhimurium strain JE8237 restored growth of the mutant on Vogel-Bonner agar (Figure 4.2). We have previously reported that this gene can also substitute for *M. smegmatis cobK* in aerobic Co-B_{12} synthesis.

Rv2072c / *S.* Typhimurium *cbiE/T*

In *S.* Typhimurium, conversion from cobalt-precorrin-6B to cobalt-precorrin-8 is catalyzed by two enzymes: a cobalt-precorrin-6B C-5 methyltransferase, CbiE, and a cobalt-precorrin-6B-decarboxylating C-15 methyltransferase, CbiT. However, another early-cobalt inserting organism, *Bacillus megaterium*, uses the fusion enzyme CbiET for this conversion (163). Late-cobalt inserters also utilize a fusion enzyme, CobL, for precorrin C-5 and C-15 methylation and decarboxylation of the acetate attached to C-12 (180). The *M. tuberculosis* genome encodes a *cobL* homolog, *Rv2072c*. The C-terminus of Rv2072c shares 43% similarity and 28% identity with *S.* Typhimurium CbiE (Table

4.3). The N-terminus shares 44% similarity and 28% identity with *S.* Typhimurium CbiT (Table 4.3). Co-B_{12} auxotrophic *S.* Typhimurium strains lacking either *cbiE* or *cbiT* grew on Vogel-Bonner agar in the absence of Co-B_{12} when *M. tuberculosis Rv2072c* was introduced and expressed from an arabinose-inducible promoter (Figure 4.2). This suggests that *M. tuberculosis* Rv2072c functions as a CbiET fusion enzyme.

Rv2065c / *S.* Typhimurium *cbiC*

Conversion of cobalt-precorrin-8 to cobyrinic acid is catalyzed by the cobalt-precorrin methylmutase CbiC in *S.* Typhimurium (163). Efforts to assess if the *cbiC* homolog *Rv2065* (annotated as *cobH*) can substitute for a *S.* Typhimurium *cbiC* mutant were initiated; however, multiple attempts to create a pBAD-TOPO derivate encoding *M. tuberculosis Rv2065* resulted in plasmids with deletions. This suggests that leaky expression of *M. tuberculosis Rv2065* in the pBAD-TOPO vector is toxic to *E. coli*. For this reason, it was not possible to test if *Rv2065* can substitute for *S.* Typhimurium *cbiC* in B_{12} synthesis.

Rv2848c / *S.* Typhimurium *cbiA*

Conversion of cobyrinic acid to cob(II)yrinic acid a,c-diamide is catalyzed by the cobyrinic acid a,c-diamide synthase CbiA in *S.* Typhimurium (181). This enzyme functions to add glutamine-derived amides to the cobyrinic acid molecule (134, 182). Expression of the *cbiA* homolog *Rv2848c* (annotated as *cobB*) in the *S.* Typhimurium *cbiA* mutant JE21352 restored Co-B_{12} synthesis to the mutant when both 0.2% arabinose and 1 mM glutamine was added to the Vogel-Bonner plates (Figure 4.2).

Rv2062c (*cobN*)-*Rv2850c* / no *S.* Typhimurium homolog

In aerobic, late-cobalt, Co-B_{12} synthesis, hydrogenobyrinic acid a,c-diamide would be converted to cob(II)byrinic acid a,c-diamide by insertion of the cobalt atom by cobaltochelatase complex CobNST complex (183). Analysis of over 200 clinical isolates from *M. tuberculosis* revealed polymorphisms in the *cobN* homolog (*Rv2062c*), many of which may alter protein function (15, 127). In *M. tuberculosis*, no CobST complex has been identified; however, a predicted magnesium chelatase, Rv2850c has been suggested to function with Rv2062c (179). These enzymes are characteristic of the late-cobalt insertion pathway; therefore, it was not possible to test *Rv2062c* and *Rv2850c* function in *S.* Typhimurium B_{12} pathway mutants. The presence of clinical isolates with functional mutations in *cobN*, coupled with evidence presented above that *Rv0259c* encodes sirohydrochlorin cobaltochelatase function suggests that *M. tuberculosis* may only synthesize Co-B_{12} by an early-cobalt insertion pathway.

Rv0306 / *S.* Typhimurium *fldA*

Once cobalt is inserted into the corrin ring structure, the pathways in early-cobalt and late-cobalt inserting organisms follow a similar mechanisms for ligand attachment (Figure 4.1). In *S.* Typhimurium, *fldA* encodes flavodoxin I, which reduces cob(II)yrinic acid a,c-diamide to cob(I)yrinic acid a,c-diamide (184). Other organisms, such as *Sinorhizobium meloti*, and *Rhodobacter capsulatus* utilize the NAD(P)H –flavin oxidoreductase BluB for this function (185, 186). *M. tuberculosis Rv0306* encodes a homolog with 45% similarity and 33% identity to *bluB* from *R. capsulatus*. As *fldA* is an

essential gene in *S.* Typhimurium, it was not possible to assess whether a *M. tuberculosis* homolog, *Rv0306*, could restore Co-B_{12} synthesis to an *fldA* mutant.

Rv2849c / *S.* Typhimurium *cobA*

In both early- and late-cobalt insertion pathways, attachment of the nucleotide loop will not occur without adenosylation at the upper axial position of the cobalt atom in the planar corrin ring of cob(I)yrinic acid *a,c*-diamide to produce adenosylcobyrinic acid *a,c*-diamide (187, 188). This reaction is catalyzed by the ATP-dependent adenosyltransferase CobA in *S.* Typhimurium (189), which is annotated in late-cobalt cobalamin producers as CobO. The *M. tuberculosis cobA* homolog *Rv2849c* (annotated as *cobO*) is predicted to encode a protein with 39% identity and >50% similarity to *S.* Typhimurium CobA and to CobO from *P. denitrifcans* (Table 4.3). Expression of *Rv2849c* in *S.* Typhimurium *cobA* deletion mutant JE1293 restored growth on Vogel-Bonner medium, which supports Rv2849c as an adenosyl transferase functioning in Co-B_{12} synthesis (Figure 4.2).

Rv0255c / *S.* Typhimurium *cbiP*

Amidation of the *b, d, e,* and *g* side chains of adenosylcobyrinic acid *a,c*-diamide to generate adenosylcobyric acid is catalyzed by the cobyric acid synthase CbiP in *S.* Typhimurium or CobQ in late-cobalt Co-B_{12} producers (181, 182, 190). The *Rv0255c* (annotated as *cobQ1*) gene in *M. tuberculosis* encodes a homolog with 56% similarity/43% identity (Table 4.3). An *S.* Typhimurium *cbiP* -defective mutant**,** JE588,

regained the ability to grow on B_{12}-deficient medium after transformation with a plasmid expressing *Rv0255c* from an arabinose-inducible promoter (Figure 4.2).

Rv2231c / *S.* Typhimurium *cobD*

The L-threonine-*O*-3-phosphate decarboxylase, CobD, in *S.* Typhimurium is responsible for generating (R)-1-amino-2-propanol-*O*-2 phosphate (191). This product is then attached to the *f* side chain of adenosylcobyric acid. In *M. tuberculosis*, the *Rv2231c* gene (annotated as *cobC*) encodes a homolog with 31% identity and 44% similarity to *S.* Typhimurium CobD (Table 4.3). Growth of a *S.* Typhimurium *cobD* mutant in Vogel-Bonner medium occurred after complementation with a plasmid encoding *Rv2231*c in the presence of arabinose (Figure 4.2).

Rv2236c / *S.* Typhimurium *cbiB*

Attachment of (R)-1-amino-2-propanol-*O*-2 phosphate to adenosylcobyric acid to generate adenosylcobinamide-phosphate is catalyzed in *S.* Typhimurium by the synthatase CbiB (192). The *M. tuberculosis* gene *Rv2236c* (annotated as *cobD*) is predicted to encode a homolog with 36% identity and 50% similarity to CbiB (Table 4.3). Expression of *Rv2236c* from an arabinose inducible promoter restored growth of an *S.* Typhimurium *cbiB* mutant on Vogel-Bonner agar (Figure 4.2).

Rv0254c / *S.* Typhimurium *cobU*

Conversion of adenosylcobinamide-phosphate to adenosyl-GDP-cobinamide is catalyzed by a multifunctional adenosylcobinamide kinase/adenosylcobinamide-

phosphate guanylyltransferase labeled CobU in early-cobalt or CobP in late-cobalt Co-B_{12} producers (134, 193). Our previous studies have shown that *M. tuberculosis Rv0254c* can restore Co-B_{12} synthesis to a *cobU* mutant of the soil saprophyte *M. smegmatis* (6). The Rv0254c sequence from *M. tuberculosis* has 54% similarity with its *S.* Typhimurium CobU homolog (Table 4.3). Arabinose-induced expression of *M. tuberculosis Rv0254c* in a *S.* Typhimurium *cobU* mutant restored growth of the mutant on Vogel-Bonner medium (Figure 4.2).

Rv2207 / *S.* Typhimurium *cobT*

In *S.* Typhimurium, a nicotinate mononucleotide (NaMN):5,6-dimethylbenzimidazole phosphoribosyltransferase, CobT, adds a 5′-phosphoribosyl group onto aromatic ring structures in preparation for attachment of the lower ligand to the corrin ring (194). The lower ligand, 5, 6-dimethylbenzimidazole, is attached to adenosyl-GDP-cobinamide to produce adenosylcobalamin; however, CobT from other organisms is capable of phosphoribosylating adenine and other aromatic ring structures such as phenol and *p*-cresol, which can also be attached to the adenosyl-GDP-cobinamide (195, 196). CobT from *M. tuberculosis* shares 50% similarity and 35% identity with CobT of *S.* Typhimurium. When *M. tuberculosis cobT homolog Rv2207* was expressed from an arabinose-inducible promoter in *S.* Typhimurium *cobT* mutant JE2423, the mutant regained the ability to grow on Vogel-Bonner agar indicating that *Rv2207* functions in Co-B_{12} synthesis (Figure 4.2).

Rv2208 / *S.* Typhimurium *cobS*

Condensation of α-DMB-ribose-5´-phosphate with adenosyl-GDP-cobinamide is catalyzed by the adenosylcobalamin-5´ synthase CobS in *S.* Typhimurium (197). The product of this reaction is adenosylcobalamin-phosphate. CobS from *M. tuberculosis* shares 45% similarity and 30% identity with CobS from *S.* Typhimurium. Expression of the *M. tuberculosis cobS* homolog *Rv2208* in an *S.* Typhimurium *cobS* mutant restored growth of the mutant on Vogel-Bonner medium supplemented with 100 μM DMB and 0.2% arainose; this supports that *M. tuberculosis Rv2208* encodes an adenosylcobalamin-5´ synthase that functions in Co-B_{12} synthesis (Figure 4.2).

Rv2228 / *S.* Typhimurium *cobC*

In *S.* Typhimurium, the *cobC* gene encodes a phosphatase that functions in the final step of Co-B_{12} synthesis to cleave the phosphate from adenosylcobalamin-phosphate creating adenosylcobalamin (197). In *M. tuberculosis*, this function is carried out by the bi-functional enzyme Rv2228, which possesses a C-terminal RNAse HI domain and an N-terminal ribazole-phosphatase domain (198). The N-terminal ribazole-phosphatase domain of Rv2228 shares 43% similarity and 27% identity with CobC of *S.* Typhimurium. We attempted to confirm this result by genetic complementation of a *S.* Typhimurium *cobC* mutant with *Rv2228*, but were unable to create culture conditions that prevented growth of the *cobC* mutant (Figure 4.2).

Assessment of Co-B_{12} Synthesis by *M. tuberculosis*

Transcriptional analysis and proteomic studies reported that some predicted Co-B_{12} biosynthetic pathway genes or proteins from *M. tuberculosis* were upregulated in pellicle cultures and in human distal lung infections (159, 160). To test the hypothesis that *M. tuberculosis* synthesizes Co-B_{12} under hypoxic or microaerophilic environments, the presence of Co-B_{12} in cell lysates from *M. tuberculosis* cultured as stationary pellicles or in the Wayne hypoxic model was evaluated using the *S.* Typhimurium B_{12} auxotrophic strain JE212 (199, 200). As detailed in the Methods, lysates prepared from *M. tuberculosis* cultures were spotted onto Vogel-Bonner agar plates previously overlaid with JE212 in top agar (6). As a positive control, cyanocobalamin was spotted on each plate. After overnight incubation, growth of JE212 in spotted areas indicates the presence of B_{12}. Using this method, growth was detected where cyanocobalamin was spotted, but not in areas spotted with lysates from the *M. tuberculosis* pellicle cultures or from the Wayne cultures (Figure 4.3). These negative results indicate that the bacteria are not producing Co-B_{12} under these growth conditions. As these growth conditions are crude approximations for complex microenvironments that *M. tuberculosis* bacilli encounter inside the host, additional nutritional factors or signals required to induce Co-B_{12} synthesis are likely lacking. It remains unclear where in the host these bacteria require B_{12}. Now that we have defined several *M. tuberculosis* genes with roles in Co-B_{12} synthesis, infection studies with pathway mutants should aid in identifying host niches where the mutants fail to persist compared to wild type.

Concluding Remarks

The results of the studies presented show that multiple *M. tuberculosis* genes can substitute for known genes in the *S.* Typhimurium Co-B_{12} biosynthetic pathway. Of most importance, *cysG* and *Rv0259c* from *M. tuberculosis* encode functions more characteristic of anaerobic corrin ring synthesis; both function in early-cobalt insertion (Figure 4.2 and Table 4.3). The gut pathogen and Co-B_{12} producing species *M. avium* subsp. p*aratuberculosis* encodes an *Rv0259c* homolog, *cbiX*, which is upregulated along with homologs to *cbiA* and *cobT* under anaerobic stress (175). This suggests that *M. tuberculosis* may also be capable of Co-B_{12} synthesis under some type of hypoxic condition. In a laboratory setting, *M. tuberculosis* can be gradually depleted of oxygen using the Wayne culture method (36); however, this creates non-replicating persistent cultures with very low metabolic requirements (36). Transcriptome analysis of *M. tuberculosis* Wayne cultures showed upregulation of the Co-B_{12}-dependent ribonucleotide reductase gene *nrdZ*, but did not show upregulation of any predicted Co-B_{12} biosynthetic genes (38). Direct assessment of Wayne-cultured *M. tuberculosis* did not yield Co-B_{12} detectable via an *S.* Typhimurium B_{12} auxotroph feeding assay (Figure 4.3). This suggests that *M. tuberculosis* does not require Co-B_{12} under these *in vitro* specific culture conditions. Although proteomic data from *M. tuberculosis* pellicle cultures show CobB and CobD (38), we were unable to detect Co-B_{12} in cell lysates from pellicle-grown *M. tuberculosis*.

In conclusion, we interrogated predicted Co-B_{12} genes from *M. tuberculosis* using a library of *S.* Typhimurium Co-B_{12} biosynthetic pathway mutants and identified 16 *M. tuberculosis* genes that can overcome different Co-B_{12} pathway blocks. Importantly, the

results indicate that *M. tuberculosis* has the potential to perform early-cobalt insertion which is more characteristic of anaerobic Co-B_{12}-producing organisms. Additional investigation to identify niches in the host that induce *M. tuberculosis* Co-B_{12} synthesis is ongoing and will help determine if this pathogen is indeed capable of complete *de novo* synthesis of the co-enzyme.

Table 4.1 Strains used in this study

Strain	**Genotype/relevant characteristics**	**Source**
***S.* Typhimurium**		
TR6583	*metE205, ara-9*	J. Escalante Laboratory Collection (201)
Derivatives of TR6583		
JE212	*metE205, ara-9,* Δ299(*hisG-cob*)	J. Escalante Laboratory Collection (200)
JE9734	*metE205, ara-9, cysG*::*cat*	J. Escalante Laboratory Collection
JE13809	*metE205, ara-9,* Δ*cbiK*31	J. Escalante Laboratory Collection
JE8238	*metE205, ara-9,* Δ*cbiL*32	J. Escalante Laboratory Collection
JE8239	*metE205, ara-9,* Δ*cbiH*29	J. Escalante Laboratory Collection
JE8235	*metE205, ara-9,* Δ*cbiF*27	J. Escalante Laboratory Collection
JE7859	*metE205, ara-9,* Δ*cbiD*24	J. Escalante Laboratory Collection
JE8237	*metE205, ara-9,* Δ*cbiJ*30	J. Escalante Laboratory Collection
JE8241	*metE205, ara-9,* Δ*cbiE*25	J. Escalante Laboratory Collection
JE8242	*metE205, ara-9,* Δ*cbiT*26	J. Escalante Laboratory Collection
JE8240	*metE205, ara-9,* Δ*cbiC*23	J. Escalante Laboratory Collection
JE21352	*metE205, ara-9,* Δ*cbiA*7::*cat*+	J. Escalante Laboratory Collection
JE8236	*metE205, ara-9,* Δ*cbiG*28	J. Escalante Laboratory Collection
JE1293	*metE205, ara-9, cobA*366::Tn10d(*cat*+)	J. Escalante Laboratory Collection (189)
JE588	*metE205, ara-9,* Δ*cbiP*236::Tn10d(Tc)	J. Escalante Laboratory Collection (200, 202)

JE2216	*metE205, ara-9, cobD*1302::Tn10d(Cm)	J. Escalante Laboratory Collection (203, 204)
JE8185	*metE205, ara-9,* Δ*cbiB*1309	J. Escalante Laboratory Collection (192)
JE4732	*metE205 ara-9* Δ*cob*272 (Δ*cobUST*/pJO30 *cobST* + *cat*)	J. Escalante Laboratory Collection (205)
JE2423	*metE205 ara-9 cobT*109::MudJ *recA1*	J. Escalante Laboratory Collection (194)
JE2848	*metE205 ara-9* Δ*cobS*1313	J. Escalante Laboratory Collection (197)
JE2718	*metE205 ara-9* Δ*cobC*1151	J. Escalante Laboratory Collection (197)
KQ900	JE9734 + pSC1 (*Rv2487c*)	This study
KQ901	JE13809 + pSC2 (*Rv0259*)	This study
KQ902	JE8238 + pSC3 (*Rv2066*)	This study
KQ903	JE8239 + pSC3 (*Rv2066*)	This study
KQ904	JE8235 + pSC4 (*Rv2071cc*)	This study
KQ905	JE7859 + pSC5 (*Rv2067c*)	This study
KQ907	JE8237 + pSC7 (*Rv2070c*)	This study
KQ908	JE8241 + pSC8 (*Rv2072c*)	This study
KQ909	JE8242 + pSC8 (*Rv2072c*)	This study
KQ911	JE21352 + pSC10 (*Rv2848c*)	This study
KQ913	JE1293 + pAR21 (*Rv2849c*)	This study
KQ914	JE588 + pAR30 (*Rv0255c*)	This study
KQ915	JE2216 + pAR20 (*Rv2236c*)	This study
KQ916	JE8185 + pAR23 (*Rv2231c*)	This study

KQ917	JE4732 + pAR32 (*Rv0254c*)	This study
KQ918	JE2423 + pAR24 (*Rv2207*)	This study
KQ919	JE2848 + pAR26 (*Rv2208*)	This study
KQ920	JE2718 + pAR29 (*Rv2228*)	This study
M. tuberculosis		
Erdman	*M. tuberculosis* strain Erdman	Tuberculosis/Mycobacteriology Branch, CDC

Table 4.2 Plasmids used in this Study

Plasmid	**Key features**	**Source**
pBAD-TOPO	Arabinose-inducible expression vector, *araC*, *bla*, pBR322 *ori*	Invitrogen
pSC1	pBAD-TOPO + *Rv2847c*	This study
pSC2	pBAD-TOPO + *Rv0259*	This study
pSC3	pBAD-TOPO + *Rv2066*	This study
pSC4	pBAD-TOPO + *Rv2071c*	This study
pSLT36	pBAD-TOPO+ *Rv2068c+Rv2067c*	This study
pSC5	pBAD-TOPO + *Rv2067c*	This study
pSC7	pBAD-TOPO + *Rv2070c*	This study
pSC8	pBAD-TOPO + *Rv2072c*	This study
pSC10	pBAD-TOPO + *Rv2848c*	This study
pAR21	pBAD-TOPO + *Rv2849c*	This study
pAR30	pBAD-TOPO + *Rv0255c*	This study
pAR20	pBAD-TOPO + *Rv2331c*	This study
pAR23	pBAD-TOPO + *Rv2236c*	This study
pAR32	pBAD-TOPO + *Rv0254c*	This study
pAR24	pBAD-TOPO + *Rv2207*	This study
pAR26	pBAD-TOPO + *Rv2208*	This study
pAR29	pBAD-TOPO + *Rv2228*	This study

Table 4.3 Comparison of Co-B_{12} biosynthetic enzymes of *S.* Typhimurium and predicted homologs or non-orthologous replacements from *M. tuberculosis*

***S.* Typhimurium enzyme**	***M. tuberculosis* enzyme**	**Percent Similarity/Identity**	**Functional Complement**
CysG	Rv2847c/CysG	48/32	yes
CbiK	Rv0259/CbiX	Non-orthologous	yes
CbiL	Rv2066/CobI	48/28	yes
CbiH	Rv2066/CobI	53/38	yes
CbiF	Rv2071c/CobM	65/45	yes
CbiG	Rv2068c/BlaC	Non-orthologous	no
CbiD	Rv2067c	Non-orthologous	unable to inhibit mutant growth
CbiJ	Rv2070c/CobK	44/27	yes
CbiE	Rv2072c/CobL	43/28	yes
CbiT	Rv2072c/CobL	44/28	yes
CbiC	Rv2065/CobH	49/33	unable to generate plasmid
CbiA	Rv2848c/CobB	51/35	no
FldA	Rv0306/BluB	Non-orthologous	
CobA (btuR)	Rv2849c/CobO	56/39	yes
CbiP	Rv0255c/CobQ1	56/43	yes
CobD	Rv2231c/CobC	44/31	yes
CbiB	Rv2236c/CobD	50/36	yes
CobU	Rv0254c/CobU	54/39	yes
CobT	Rv2207/CobT	50/35	yes
CobS	Rv2208/CobS	45/30	yes
CobC	Rv2228	43/27	Previously characterized(198)

Table 4.4 Primers used in this study

P2071	5′-GTGACCGAGAACCCCTATCTGGTCG-3′
P2072	5′-TTACGAATTGTTTAAACCCCGAACGCCGCT-3’
P2073	5′-ATGAACCTGATCTTGACGGCCCAC-3’
P2074	5′-TCAAAGATCAAGCGTTACTGGTGTCGGCGTGCCATG-3’
P2075	5′-ATGTCAGCTCGGGGCACGCTG-3’
P2076	5′-TCAGTCAGAGTGGCGGCTCGACTTTGTC-3’
P2077	5′-GTGGCCGGGACCCGTGAC-3’
P2078	5′-CTAAGGCCGCAATCGCCGGTATCC-3’
P2079	5′-ATGACGGTCTATTTCATCGGAGCGGGC-3’
P2080	5′-TCACTGTGCATACCGACCGTGCCG-3’
P2081	5′-GTGACCGACGATCATCCGCGC-3’
P2082	5′-CTATCAGAGGCGGGCAGAGCTACC-3’
P2083	5′-GTGACACGGGTGTTGTTGCTCGGC-3’
P2084	5′-TCACCGGCTAGGCAGACCG-3’
P2328	5′-ATGATAATCGTTGTCGGGATCGGCGC-3’
P2086	5′-TCATCGCTTGGTCACCGACCACTG-3’
P2087	5′-GTGCTGGACTACCTACGCGACGCC-3’
P2088	5′-TCATTCTCGGTCGCTGGCTATCGCATTGAC-3’
P2327	5′-ATGCGAGTATCTGCGGTGGCCGTCGC-3’
P1833	5′-TTACGCTCGTGGAGTATTGCAGGC-3’
P1828	5′-CTCTGGATTCTTGGCCCGCAC-3’
P1829	5′-TCATCGGCGTCCTCCACG-3’
P1830	5′-CCGCAGGGCAATCCGCTC-3’

P1831	5′-TCACCACTCGATGCCCTTCTG-3’
P1832	5′-CGAGTATCCGCAGTGGCCG-3’
P1833	5′-TTACGCTCGTGGAGTATTGCAGGC-3’
P1834	5′-TTTGCATGCACTTGGCAGACCAGGGCC-3’
P1835	5′-CTACGGACGACGGCGGTAAACCAACATCACGG-3’
P1836	5′-ATCGGATTCGCGCCGGTGTCGAC-3’
P1837	5′-TCACGGTGAGACTGCCGG-3’
P1838	5′-ATGCGTTCTCTTGCAACAGCTTTCGCATTCGC-3’
P1839	5′-CTAAAGCCGGGCCAAGCC-3’
P1927	5′-AAAGTTGTCATCGAAGCCGACGGC-3’
P1921	5′-CTATAGATAGCCTGTCTGATTCACCAATCGCACC-3’
P1922	5′-ATGAGATCACTAGCAACAGCTTTCGCATTCGCAACG-3’
P1925	5′-CTAAAGCCAGGACAAGCCCGCAAGCGTCACG-3’
P1926	5′-GTGATAGGATTCGCGCCGGTGTCGAC-3’
P1935	5′-ATGTCGGGTCTGCTGGTCGC-3’
P1936	5′-TCATGGAGCACCCGGAGCGAGAAAGGGC-3’
P1937	5′-GTGCGGATCGGGCTCGTGC-3’
P1938	5′-CTAACGAGCAGATAGACGTTCGCGGCGCAG-3’
P1939	5′-CGGATACTGGTCACTGGCGGC-3’
P1940	5′-TCACAGCTTGAGCACACGTCCG-3’
P1843	5′-GCAACTCTCTACTGTTTCTCCATACCCG-3’
P1844	5′-CTGCGTTCTGATTTAATCTGTATCAGGCTG-3’
P2357	5’-TTATAAGCGACCGTCAACCTGCTGC-3’

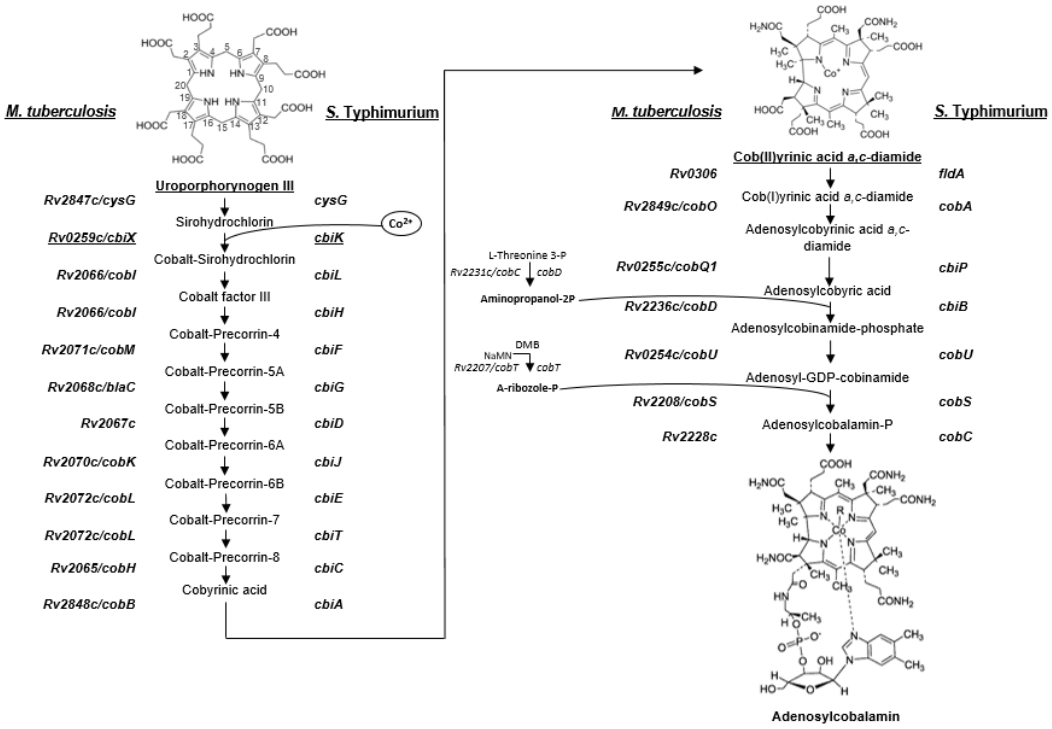

Figure 4.1: The *S.* Typhimurium Co-enzyme B_{12} pathway and *M. tuberculosis* genes with potential to function at different steps. Depicted is the Co-B_{12} biosynthetic pathway of *S.* Typhimurium indicating the genes encoding enzyme that function at each step. Also shown are predicted homologs or nonorthologous replacements in *M. tuberculosis* strain H37Rv as annotated in Mycobrowser[29] that may function at each step. Genes from *M. tuberculosis* that do not have *S.* Typhimurium homologs are underlined. The pathway begins with uroporphyrinogen III, the last precursor shared with the heme and siroheme biosynthetic pathways; the carbon atoms of the macrocycle are numbered 1-20. Methylation of various carbon atoms is required for the insertion of the central cobalt atom and removal of C-20 and reduction of the macrocycle ring. Pathway steps after intermediate cob(II)yrinic acid a,c-diamide function to add an adenosyl group as the upper axial cobalt ligand and 5, 6-dimethylbenzimidazole as the lower axial ligand which is also attached to the macrocycle by a ribonucleotide loop to produce adenosylcobalamin. The upper ligand (R) can be removed or replaced to the form required for specific Co-B_{12}-dependent enzymes.

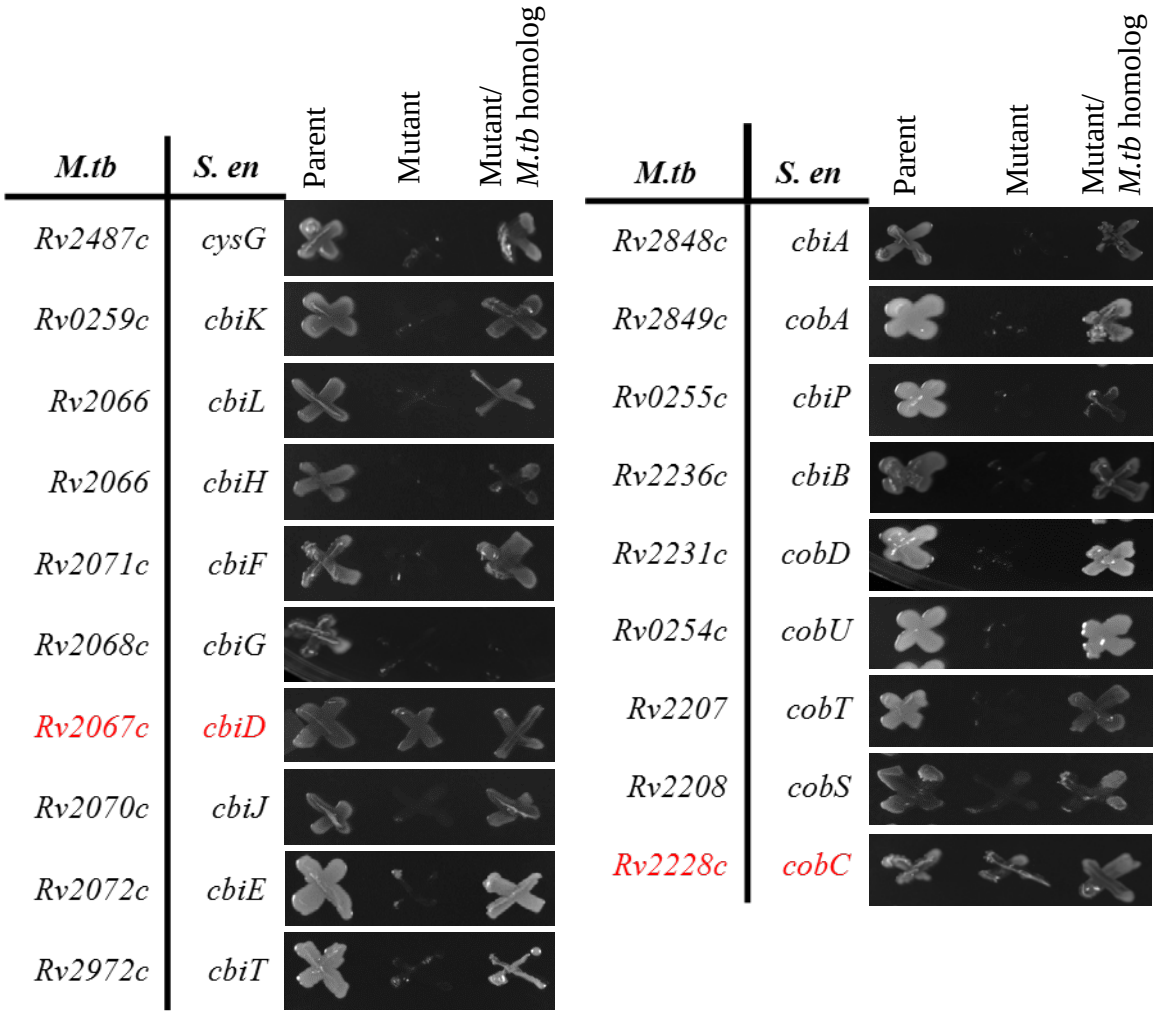

Figure 4.2: Functional complementation assays of *S.* Typhimurium Co-B_{12} synthesis pathway mutants with *M. tuberculosis* gene homologs or nonorthologous replacements. Predicted Co-B_{12} synthesis genes from *M. tuberculosis* (*M.tb*) were expressed on plasmids from an arabinose-inducible promoter in *S.* Typhimurium (*S.en*) Co-B_{12} auxotrophic mutants with deletions in specific Co-B_{12} biosynthetic genes. For each assay, the *S.* Typhimurium parent strain (JE6583), the mutant strain lacking the indicated gene, and the mutant strain expressing the indicated *M. tuberculosis* gene were patched on Vogel-Bonner agar plates supplemented with 0.2% arabinose and incubated anaerobically at 37°C for 48 hours. For *S.* Typhimurium *cbiD* and *cobC* mutants (highlighted in red), no condition resulted in loss of mutant growth; therefore, complementation conclusions could not be made.

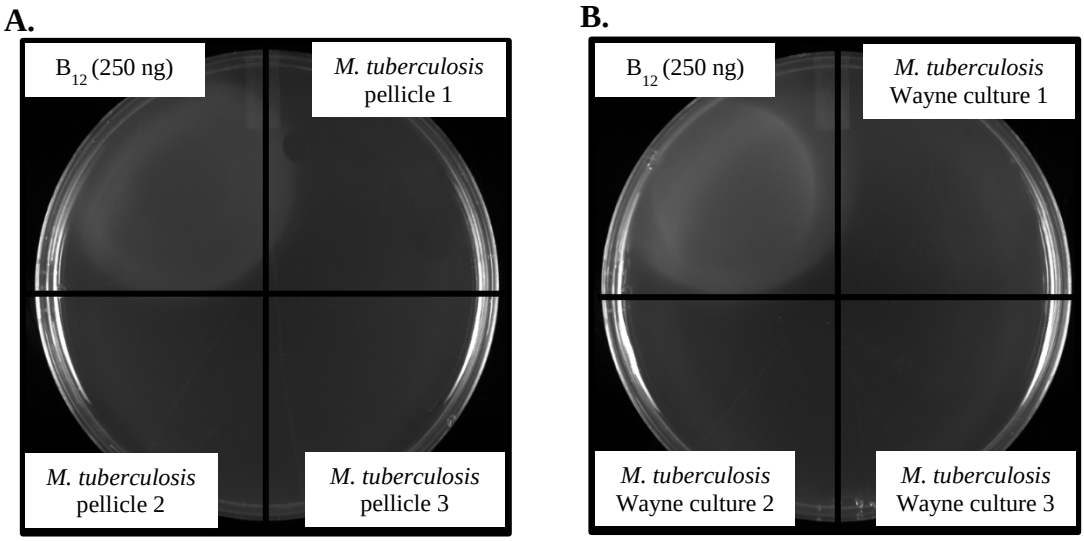

Figure 4.3: Assay for Co-B_{12} production by *M. tuberculosis* harvested from long-term pellicle or Wayne cultures. The *S.* Typhimurium B_{12} auxotrophic strain JE212 was overlaid onto Vogel-Bonner minimal medium agar and spotted with 250 ng cyanocobalamin (B_{12}) or 5 µl of cell lysate from *M. tuberculosis* cultures grown as stationary pellicles or as hypoxic Wayne cultures. Zones with JE212 growth indicate the presence of B_{12}. A: Assays from *M. tuberculosis* harvested approximately 1 year after inoculation of stationary pellicle cultures in Sauton medium supplemented with 5 µM cobalt chloride and 10 µM potassium cyanide. B: Assay of *M. tuberculosis* cells harvested from 1 year old Wayne cultures previously inoculated and sealed within stoppered vials with a 1:2 air headspace-to-liquid ratio containing Dubos medium supplemented with 5 µM cobalt chloride. Images are representative of three independent assays, each performed in duplicate.

CHAPTER 5

CONCLUSIONS

Currently tuberculous (TB) results in more human deaths annually than any other disease caused by a single infectious agent (1). The success of *M. tuberculosis* is largely attributable to its ability to adapt to different environments in the host. This pathogen can survive in a number of host niches including within macrophages, granulomas, and adipose tissues. In response to changing environments, *M. tuberculosis* alters its metal transport systems, cellular respiration, carbon source utilization, and other metabolic processes. This work examined two systems, copper homeostasis and Co-B_{12} synthesis, which are likely important for *M. tuberculosis* survival within specific host niches.

Beginning with copper homeostasis, *M. tuberculosis* utilizes two copper-sensing repressor proteins in response to copper toxicity; CsoR, which controls production of the copper-efflux pump *ctpV*, and RicR that regulates synthesis of a multicopper oxidase and a metallothionein (112, 111). While high amounts of copper are toxic to the bacilli, *M. tuberculosis* encodes at least two copper-dependent enzymes, the Zn/Cu superoxide dismutase SodC, and cytochrome C oxidase CtaD of the aa3-type respiration complex (115, 37). SodC functions alongside other superoxide dismutases, like the iron-cofactored SodA, and functions early in infection to protect the bacilli against extracellular and periplasmic superoxides (115, 206)**.** The aa3-type respiration complex is the most energy efficient mechanism for cellular respiration for *M. tuberculosis*, but an alternative, yet less efficient copper-independent b/d ubiquinol oxidase system also exists in *M.*

tuberculosis (37). Transcription of *ctaD* is downregulated during chronic infection in a mouse model (37). This downregulation is coupled with increased b/d ubiquinol oxidase transcription; however, *in vitro* exposure to nitric oxide or hypoxia in complex medium does not result in transcriptional changes to *ctaD* (37). This suggests that host-specific conditions, such as the possible lack of copper ions result in changes to respiratory mechanisms in *M. tuberculosis*.

Previous research has demonstrated that RNA transcription sigma factor C (SigC) is necessary for full virulence of *M. tuberculosis* in both mice and guinea pig infection models (4, 3). Our laboratory has also shown that SigC is required for growth of *M. tuberculosis* in media lacking copper (6). Additionally, forced over-production of SigC results in transcription of *ctpB,* encoding a P1B-type ATPase with a copper-binding motif, and the *PPE1-nrp* operon, which is predicted to function in synthesis of a metal chelation system (6). Lastly, in a defined Sauton medium lacking copper ions, loss of *sigC* results in increased transcription of the copper-independent cytochrome b/d ubiquinol oxidase system (6). These data lead to the hypothesis that SigC may be functioning in copper homeostasis in *M. tuberculosis*.

Chapter 3 of this dissertation investigated the role of copper on SigC regulation in *M. tuberculosis*. We first confirmed the necessity of SigC for growth of *M. tuberculosis* strain Erdman in chemically-defined Sauton medium (SMT) in the presence of the copper-specific chelator ammonium tetrathiomolybdate (TTM). An *M. tuberculosis* derivative lacking functional SigC (*M. tb*Δ*sigC*) did not grow when 5 μM TTM was added to SMT. Growth of this mutant was restored when 10 μM copper sulfate was added in conjunction with TTM. This result confirmed the previous observation that SigC

is necessary for copper import under copper-limited conditions. Next, Alamar Blue assays showed that copper chelation by either TTM or the copper(I) chelator bathocuproinedisulfonic acid (BCS) reduced the viability of *M. tb*Δ*sigC* compared to strain Erdman. The defect of the mutant was absent when copper sulfate was added in conjunction with either chelator. Lastly, addition of a reductant, sodium ascorbate, rendered the mutant more sensitive to BCS. These data support that SigC function is required for copper acquisition when the levels of the free metal are extremely low.

While the hallmark of latent infection is the granuloma, and bacilli reside there (207, 159), *M. tuberculosis* can also infect other cell types and will persist in phenotypically healthy tissue within the host (208–210). Extra-pulmonary reactive disease can occur in regions such as the brain, skin, and internal organs (210, 35, 69). PCR of normal-appearing tissues have been shown to be positive for *M. tuberculosis* DNA (210). One identified non-pulmonary reservoir for the bacilli is adipose tissue (35). Copper overloading in the phagolysosome is a known host defense mechanism (145) and *M. tuberculosis* has multiple systems to combat copper toxicity (112, 111); however, in a resting eukaryotic cell, free copper ions are nearly undetectable (118). During a latent infection, where *M. tuberculosis* persists within resting cells such as adipose tissue, it may need to scavenge copper from the host to meet its needs. In this setting, *M. tuberculosis* may utilize the metal-chelator predicted to be encoded by the *PPE1-nrp* operon (7), as well as the metal-binding CtpB (113) to scavenge copper from the host. Transcription of these genomic targets is regulated by SigC in relationship to copper availability, and SigC is required for full virulence in both mouse and guinea pig

infection models (4, 6). These findings add support to the hypothesis that SigC is required to maintain a low level of available copper in *M. tuberculosis.*

To further characterize the relationship between SigC and copper homeostasis, the post-transcriptional effects of copper ions on myc-tagged SigC were analyzed. Immunoblot analysis of an *M. tuberculosis* strain encoding myc-tagged SigC expressed from a tetracycline-inducible promoter was used to examine stability of the protein under different copper conditions. Detectable myc-SigC was significantly decreased by 2.7-fold when the bacteria were cultured in SMT in the presence of 10 μM copper sulfate versus 5 μM TTM. This suggests that chelation of copper ions from the medium results in more available SigC protein. The detrimental effects of copper ions on SigC were then shown using the protein synthesis inhibitor chloramphenicol, which allowed for measurement of total protein loss. To cultures in which myc-tagged SigC expression was induced with tetracycline for 24 hours in the presence of TTM, copper sulfate with or without chloramphenicol was added. After 4 hours, a significant reduction in myc-SigC was measured in cultures containing copper sulfate, and an even greater reduction in myc-SigC was measured in cultures containing both copper sulfate and chloramphenicol. No significant change in myc-SigC detection occurred due to chloramphenicol alone, which suggests that the reduction in myc-SigC abundance was due to copper ions increasing degradation of the protein in *M. tuberculosis*, rather than blocking transcription or translation of new myc-SigC protein.

These experiments provide insight into a possible regulatory mechanism for SigC. The promoter upstream of *sigC* is recognized by the *M. tuberculosis* primary sigma factor, SigA; therefore, *sigC* is transcribed at high levels when SigA is active (89), and no

anti-sigma factor system has been identified for SigC (8). It is also known that tetracycline-induced myc-tagged SigC expression leads to upregulation of copper-toxicity response genes after 48 hours in a complex medium (6). Given the toxic effects of copper-overloading, an alternative system for SigC regulation must exist. The data presented here suggests that SigC protein degradation may be regulated by copper concentration. SigC produced in the presence of a chelator remains detectable after incubation with the protein synthesis inhibitor chloramphenicol, but is lost when incubated with copper ions and chloramphenicol. This leads to a model where in copper-limited conditions, SigC is present and able to initiate transcription of the target sequences; however, once copper concentrations are sufficient, SigC is degraded. Further work is required to identify the specific mechanism for this process.

Studies in *Myxococcus xanthus* have identified a copper-binding sigma factor, CorE, which contains a C-X-C motif as part of a cysteine-rich domain required for metal binding and function (148). SigC contains a C-G-C motif in the helix-turn-helix domain of region 4.2 (8). Alamar Blue assays were used to examine the viability of *M. tuberculosis* strains containing single amino acid mutations in this motif. Changing of any of these residues to alanine reduced viability of the bacteria in SMT medium containing TTM. This suggests a role for the C-G-C motif in SigC function. Future work, including metal-binding analysis and *in vitro* transcription analysis in the presence of copper will better determine the role of this region in SigC function and metal-sensing.

In summary, this work suggests a regulatory mechanism for *M. tuberculosis* SigC by copper. SigC is required for *M. tuberculosis* growth in copper-chelated conditions and the C-G-C motif is important for SigC function. In *M. tuberculosis,* SigC is stably

detected when copper is chelated from the media, but is degraded when copper ions are present. These data support a model in which SigC is stabilized in low-copper conditions, such as those found in steady-state eukaryotic cells, where *M. tuberculosis* will persist during a latent infection (210, 35). In this setting, SigC is available to initiate transcription of copper acquisition genes, for scavenging copper from the environment. The cytoplasmic copper pools will increase, as will copper-dependent aerobic respiration. Once enough copper ions enter the cytoplasm, SigC will be degraded to stop copper import. Future work investigating the role of SigC during chronic or latent infections, and the direct effects of copper ions on SigC folding and function will better characterize the role of SigC in copper import. Additional work to clarify the functions of the *PPE1-nrp* operon, and *ctpB* will solidify the role of this copper-acquisition mechanism in *M. tuberculosis.*

Chapter 4 of this dissertation focuses on co-enzyme B_{12} (Co-B_{12}) synthesis in *M. tuberculosis*. Co-B_{12} is a necessary cofactor for the following *M. tuberculosis* enzymes: methionine synthase, MetH; methylmalonyl-coA mutase, MutAB; and a class III ribonucleotide reductase, NrdZ (127). Despite encoding homologs for many Co-B_{12} biosynthetic genes, production of this co-enzyme has not been demonstrated for *M. tuberculosis* or any of the other closely-related tuberculous mycobacteria (6). In contrast, Co-B_{12} is readily produced by and detected in cell lysates of non-tuberculous mycobacteria such as *M. smegmatis* and *M. marinum*. Although there is limited evidence demonstrating production of the cofactor by *M. tuberculosis*, mRNA transcripts and/or peptide signatures of predicted Co-B_{12} biosynthetic pathway proteins have been detected in samples taken from distal lung infections of humans with TB and from the culture

filtrates from *M. tuberculosis* grown as stationary pellicles (211, 159). This suggests that *M. tuberculosis* may only synthesize the co-enzyme under specific conditions.

The Co-B_{12} biosynthetic pathway requires up to 30 enzymes, and varies across organisms. There are two archetypal pathways for Co-B_{12} synthesis. First, the early-cobalt insertion pathway is found in organisms such as *Salmonella* Typhimurium, which inserts cobalt in the second step of corrin-ring synthesis prior to modification and ring contraction of the tetrapyrrole (134). Second is the late-cobalt insertion pathway, characteristic of Co-B_{12}-producing organisms, like *Pseudomonas denitrificans*, which inserts cobalt as one of the last steps for corrin-ring synthesis (134). The genome of *M. tuberculosis* encodes annotated homologs to known Co-B_{12} biosynthetic genes (158). There is redundancy in the naming of Co-B_{12} biosynthetic enzymes between the pathways, and many of the enzymes from the two pathways are not mutually exclusive, even though the naming suggests otherwise (141). Therefore, enzymes annotated as late-insertion enzymes may share high similarity and identity to enzymes in the early-insertion pathway (141).

Previous work in our laboratory has shown that two genes from *M. tuberculosis* complement the function of annotated Co-B_{12} biosynthetic homologs from the aerobic Co-B_{12} producer *M. smegmatis*. The genes analyzed are annotated as *cobK* and *cobU* in both mycobacterial species and their predicted functions are not exclusive to either Co-B_{12} biosynthetic pathway (134, 155). The *M. tuberculosis* genome also encodes genes whose enzymes are predicted to function exclusively in the early-insertion pathway, such as a predicted homolog to the sirohydrochlorin-cobaltochelatase CbiX, responsible for inserting cobalt in the second step of corrin-ring synthesis (173). A homolog to this

enzyme is also present in the bovine intestinal pathogen *Mycobacterium avium* subsp. *paratuberculosis* and is upregulated along with other Co-B_{12} biosynthetic genes during nitrosative multi-stress (175). Hypoxyprobe (pimonidazole hydrochloride) staining of tissues from *M. tuberculosis* infected animals has confirmed hypoxic conditions within granulomas (64). Additionally, when a non-replicating persistent state is induced through oxygen depletion using the Wayne culture technique in *M. tuberculosis*, there is upregulation of the Co-B_{12} dependent ribonucleotide reductase NrdZ (161). It is also known that during infection *M. tuberculosis* uses fatty acids and cholesterol as a carbon source and, when required uses the Co-B_{12} dependent methylmalonyl-CoA mutase to assimilate propionate into succinate (29). Lastly, a screen of over 200 clinical isolates showed 17 strains with loss-of-function mutations in *cobN*, which is used by aerobic organisms for late-cobalt insertion, but found very few isolates with mutations in other Co-B_{12} biosynthetic genes (15). This information leads to the hypothesis that *M. tuberculosis* requires Co-B_{12} under hypoxic, fatty acid-rich conditions, such as those found in the granuloma and that the predicted Co-B_{12} biosynthetic genes of *M. tuberculosis* function through an early-cobalt insertion mechanism that is likely active when the bacteria are in this specific hypoxic niche.

Because the conditions found within the host are not easily replicated *in vitro*, and no tuberculous mycobacterial species has been shown to synthesize the cofactor aerobically, we first aimed to demonstrate that *M. tuberculosis* encodes genes whose enzymes function to synthesize Co-B_{12} through an early-cobalt-insertion mechanism, which is more characteristic of anaerobic-producing organisms. To assess the function of predicted Co-B_{12} biosynthetic genes from *M. tuberculosis*, we assayed *S.* Typhimurium

B_{12} auxotrophic mutants with specific blocks in the Co-B_{12} biosynthetic pathway. Each predicted *M. tuberculosis* homolog was expressed from an arabinose-inducible promoter in the corresponding *S.* Typhimurium mutant strain. Function was assessed by growing the strains on minimal Vogel-Bonner agar supplemented with arabinose. Growth of an *S.* Typhimurium mutant strain expressing a Co-B_{12} gene from *M. tuberculosis* indicated function of that specific gene in the Co-B_{12} biosynthetic pathway. Of the 19 genes tested using this approach, 16 functioned in Co-B_{12} synthesis. This included *Rv0259c* encoding the predicted sirohydrochlorin-cobaltochelatase, which suggests that *M. tuberculosis* is capable of performing early-cobalt insertion typically utilized by bacteria that can grow anaerobically. For two of the genes, no conditions tested resulted in B_{12} auxotrophy of the corresponding *S.* Typhimurium mutant. Additionally, for one of the *M. tuberculosis* genes, *Rv2065*, multiple attempts were made to synthesize the arabinose-inducible expression plasmid; however, all resulted in candidates with mutations, which suggests that leaky expression of this gene is toxic in *E. coli*. Homologs to some Co-B_{12} biosynthetic genes have yet to be identified, such as an equivalent to *S.* Typhimurium *cbiG*; however, these results indicate that the *M. tuberculosis* genome encodes many of the genes necessary for Co-B_{12} synthesis. While enzyme function is not a direct indication of cofactor production, the large number of enzymes with conserved functions suggests that *M. tuberculosis* requires these mechanisms within some niche, and that there may be tight regulation of Co-B_{12} synthesis by this organism. Continuing research to identify and assign a function to the remaining genes involved in Co-B_{12} synthesis, and to examine cofactor production by other mycobacterial strains, such as the progenitor

strain to all tuberculous mycobacteria, *M. canettii*, will further elucidate the exact mechanism of Co-B_{12} synthesis in *M. tuberculosis*.

To further examine Co-B_{12} synthesis, *M. tuberculosis* was grown in conditions that have previously led to increased transcription of mRNA or production of proteins predicted to be involved in Co-B_{12} biosynthesis by *M. tuberculosis* (159, 160). Bacteria were grown as stationary pellicles or forced into non-replicating persistence through slow oxygen depletion using the Wayne culture method (36). Cell extracts prepared from both types of cultures were assayed for Co-B_{12} production using an *S.* Typhimurium B_{12} auxotroph feeding assay, but the results did not demonstrate the presence of Co-B_{12}. It is possible that unidentified environmental factors are required for *M. tuberculosis* Co-B_{12} synthesis. For the Wayne cultures it is also possible that the low culture density and the cessation of bacterial replication resulted in an amount of Co-B_{12} that was below the limit of detection for the *S.* Typhimurium feeding assay.

In summary, these data demonstrate that *M. tuberculosis* encodes multiple genes functional in the Co-B_{12} biosynthetic pathway. Specifically, *Rv0259c* encodes a functional sirohydrochlorin-cobaltochelatase, which is common among anaerobic Co-B_{12} producing organisms, and is also present in the related pathogen *M. avium* subsp. *paratuberculosis* and is active during nitrosative stress (175). It is unlikely that the *M. tuberculosis* genome would maintain so many intact genes for an unused pathway. In fact, the only Co-B_{12} related gene that appears to be accumulating loss-of-function mutations in clinical isolates is *cobN*, which is responsible for aerobic cobalt insertion (15). This suggests that *M. tuberculosis* does not require Co-B_{12} synthesis under aerobic conditions, but has retained the means to synthesize the cofactor in hypoxic

environments, such as within the granuloma. It is in these hypoxic environments where *M. tuberculosis* may use the Co-B_{12} dependent ribonucleotide reductase NrdZ to replace the oxygen-dependent ribonucleotide reductase encoded by *nrdAB nrdEF* (179, 212, 213). In this environment, the main carbon sources available are cholesterol and other fatty acids; therefore, *M. tuberculosis* may also require Co-B_{12} as a cofactor for methylmalonyl-CoA mutase for assimilation of propionate into succinate (29, 14, 33). Additional experiments to identify and replicate the conditions necessary for *M. tuberculosis* synthesis of Co-B_{12} are needed to elucidate the complete pathway.

In conclusion, this body of work highlights two systems that have helped *M. tuberculosis* to become one of the world's most successful human pathogens. Chapter 3 showed that *M. tuberculosis* SigC is required under copper-limited conditions and levels of the protein are post-translationally impacted by copper availability. This adaptation may lead to better survival in the host where copper ion levels are highly variable depending on the specific niche. In a setting with little or no free copper ions, SigC is available to transcribe targets with roles in copper acquisition, which will allow for more efficient cellular respiration through copper-dependent mechanisms. When copper levels are sufficient, SigC will be degraded to prevent additional copper from entering the cell, and causing toxicity. In chapter 4, it was demonstrated that *M. tuberculosis* has genes which encode products functional in the early cobalt-insertion pathway for co-enzyme B_{12} synthesis, exemplified by *S.* Typhimurium. Specifically, *M. tuberculosis* encodes genes specific to this pathway and required for anaerobic corrin ring synthesis. This supports the potential for *M. tuberculosis* to synthesize this important cofactor in extremely low oxygen environments, such as within hypoxic granulomas. It is in this

setting where *M. tuberculosis* may need Co-B_{12} dependent enzymes, such as the oxygen-independent ribonucleotide reductase for genome repair and replication. Through the evolution of novel mechanisms such as those described here that *M. tuberculosis* has remained such a global health threat. Elucidation of unique components of metabolic pathways and nutrient-acquisition systems can ultimately lead to targeted vaccines and better antibiotics to aid in the eradication of tuberculosis.

REFERENCES

1. WHO. 2017. Global Tuberculosis Report 2017.
2. Daniel TM. 2006. The history of tuberculosis. Respir Med 100:1862–1870.
3. Sun R, Converse PJ, Ko C, Tyagi S, Morrison NE, Bishai WR. 2004. Mycobacterium tuberculosis ECF sigma factor sigC is required for lethality in mice and for the conditional expression of a defined gene set. Mol Microbiol 52:25–38.
4. Karls RK, Guarner J, McMurray DN, Birkness KA, Quinn FD. 2006. Examination of Mycobacterium tuberculosis sigma factor mutants using low-dose aerosol infection of guinea pigs suggests a role for SigC in pathogenesis. Microbiology 152:1591–1600.
5. Rodrigue S, Brodeur J, Jacques P-E, Gervais AL, Brzezinski R, Gaudreau L. 2007. Identification of mycobacterial sigma factor binding sites by chromatin immunoprecipitation assays. J Bacteriol 189:1505–1513.
6. Grosse-Siestrup BT. 2012. PhD thesis. Examination of the SigC regulon and cobalamin biosynthesis in Mycobacterium tuberculosis. The University of Georgia.
7. Harris NC, Sato M, Herman NA, Twigg F, Cai W, Liu J, Zhu X, Downey J, Khalaf R, Martin J, Koshino H, Zhang W. 2017. Biosynthesis of isonitrile lipopeptides by conserved nonribosomal peptide synthetase gene clusters in Actinobacteria. Proc

Natl Acad Sci 114:7025–7030.

8. Thakur KG, Joshi AM, Gopal B. 2007. Structural and biophysical studies on two promoter recognition domains of the extra-cytoplasmic function sigma factor sigma(C) from Mycobacterium tuberculosis. J Biol Chem 282:4711–4718.

9. Manganelli R, Voskuil MI, Schoolnik GK, Dubnau E, Gomez M, Smith I. 2002. Role of the extracytoplasmic-function sigma factor sigma(H) in Mycobacterium tuberculosis global gene expression. Mol Microbiol 45:365–374.

10. Chang A, Smollett KL, Gopaul KK, Chan BHY, Davis EO. 2012. Mycobacterium tuberculosis H37Rv sigC is expressed from two promoters but is not auto-regulatory. Tuberculosis (Edinb) 92:48–55.

11. Gruber K, Puffer B, Kräutler B. 2011. Vitamin B12-derivatives-enzyme cofactors and ligands of proteins and nucleic acids. Chem Soc Rev 40:4346–4363.

12. Karasseva V, Weiszfeiler JG, Lengyel Z. 1977. Synthesis of vitamin B12 by various species of mycobacteria. Zentralbl Bakteriol Orig A 239:514–520.

13. Warner DF, Savvi S, Mizrahi V, Dawes SS. 2007. A riboswitch regulates expression of the coenzyme B12-independent methionine synthase in Mycobacterium tuberculosis: implications for differential methionine synthase function in strains H37Rv and CDC1551. J Bacteriol 189:3655–3659.

14. Savvi S, Warner DF, Kana BD, McKinney JD, Mizrahi V, Dawes SS. 2008. Functional characterization of a vitamin B12-dependent methylmalonyl pathway in Mycobacterium tuberculosis: implications for propionate metabolism during growth on fatty acids. J Bacteriol 190:3886–3895.

15. Comas I, Coscolla M, Luo T, Borrell S, Holt KE, Kato-Maeda M, Parkhill J, Malla

B, Berg S, Thwaites G, Yeboah-Manu D, Bothamley G, Mei J, Wei L, Bentley S, Harris SR, Niemann S, Diel R, Aseffa A, Gao Q, Young D, Gagneux S. 2013. Out-of-Africa migration and Neolithic coexpansion of Mycobacterium tuberculosis with modern humans. Nat Genet 45:1176–1182.

16. Bos KI, Harkins KM, Herbig A, Coscolla M, Weber N, Comas I, Forrest SA, Bryant JM, Harris SR, Schuenemann VJ, Campbell TJ, Majander K, Wilbur AK, Guichon RA, Wolfe Steadman DL, Cook DC, Niemann S, Behr MA, Zumarraga M, Bastida R, Huson D, Nieselt K, Young D, Parkhill J, Buikstra JE, Gagneux S, Stone AC, Krause J. 2014. Pre-Columbian mycobacterial genomes reveal seals as a source of New World human tuberculosis. Nature 514:494–497.
17. Koch R. 1891. A further communication on a remedy for Tuberculosis. Br Med J 1:125–127.
18. Jagielski T, Minias A, van Ingen J, Rastogi N, Brzostek A, Żaczek A, Dziadek J. 2016. Methodological and clinical aspects of the molecular epidemiology of Mycobacterium tuberculosis and other mycobacteria. Clin Microbiol Rev 29:239–290.
19. Müller B, Dürr S, Alonso S, Hattendorf J, Laisse CJM, Parsons SDC, Helden PD Van, Zinsstag J. 2013. Zoonotic Mycobacterium bovis-induced Tuberculosis in humans. Emerg Infect Dis 19:899–908.
20. WHO. 2017. Roadmap for zoonotic tuberculosis 24.
21. Barry CE, Crick DC, Mcneil MR, Delivery C, Collins F. 2016. Targeting the formation of the cell wall core of M. tuberculosis. Infect Disord Drug Targets 7:182–202.

22. Brennan P. 2003. Structure, function, and biogenesis of the cell wall of Mycobacterium tuberculosis. Tuberculosis 83:91–97.

23. Camacho LR, Ensergueix D, Perez E, Gicquel B, Guilhot C. 1999. Identification of a virulence gene cluster of Mycobacterium tuberculosis by signature-tagged transposon mutagenesis. Mol Microbiol 34:257–267.

24. Goren MB, Brokl O, Schaefer WB. 1974. Lipids of putative relevance to virulence in Mycobacterium tuberculosis: correlation of virulence with elaboration of sulfatides and strongly acidic lipids. Infect Immun 9:142–149.

25. Camacho LR, Constant P, Raynaud C, Laneelle MA, Triccas JA, Gicquel B, Daffe M, Guilhot C. 2001. Analysis of the phthiocerol dimycocerosate locus of Mycobacterium tuberculosis. Evidence that this lipid is involved in the cell wall permeability barrier. J Biol Chem 276:19845–19854.

26. Rousseau C, Winter N, Pivert E, Bordat Y, Neyrolles O, Ave P, Huerre M, Gicquel B, Jackson M. 2004. Production of phthiocerol dimycocerosates protects Mycobacterium tuberculosis from the cidal activity of reactive nitrogen intermediates produced by macrophages and modulates the early immune response to infection. Cell Microbiol 6:277–287.

27. Yang X, Nesbitt NM, Dubnau E, Smith I, Sampson NS. 2009. Cholesterol metabolism increases the metabolic pool of propionate in Mycobacterium tuberculosis. Biochemistry 48:3819–3821.

28. Rocco CJ, Escalante-Semerena JC. 2010. In Salmonella enterica, 2-methylcitrate blocks gluconeogenesis∇. J Bacteriol 192:771–778.

29. Eoh H, Rhee KY. 2014. Methylcitrate cycle defines the bactericidal essentiality of

isocitrate lyase for survival of Mycobacterium tuberculosis on fatty acids. Proc Natl Acad Sci U S A 111:4976–4981.

30. Lee W, VanderVen BC, Fahey RJ, Russell DG. 2013. Intracellular Mycobacterium tuberculosis Exploits Host-derived Fatty Acids to Limit Metabolic Stress. J Biol Chem 288:6788–6800.

31. Tobin DM, Ramakrishnan L. 2008. Comparative pathogenesis of Mycobacterium marinum and Mycobacterium tuberculosis. Cell Microbiol 10:1027–1039.

32. Traag BA, Driks A, Stragier P, Bitter W, Broussard G, Hatfull G, Chu F, Adams KN, Ramakrishnan L, Losick R. 2010. Do mycobacteria produce endospores? Proc Natl Acad Sci 107:878–881.

33. Pandey AK, Sassetti CM. 2008. Mycobacterial persistence requires the utilization of host cholesterol. Proc Natl Acad Sci U S A 105:4376–4380.

34. VanderVen BC, Fahey RJ, Lee W, Liu Y, Abramovitch RB, Memmott C, Crowe AM, Eltis LD, Perola E, Deininger DD, Wang T, Locher CP, Russell DG. 2015. Novel inhibitors of cholesterol degradation in Mycobacterium tuberculosis reveal how the bacterium’s metabolism is constrained by the intracellular environment. PLoS Pathog 11:e1004679.

35. Neyrolles O, Hernández-Pando R, Pietri-Rouxel F, Fornès P, Tailleux L, Barrios Payán JA, Pivert E, Bordat Y, Aguilar D, Prévost M-C, Petit C, Gicquel B. 2006. Is adipose tissue a place for Mycobacterium tuberculosis persistence? PLoS One 1:e43.

36. Wayne LG, Hayes LG. 1996. An in vitro model for sequential study of shiftdown of Mycobacterium tuberculosis through two stages of nonreplicating persistence.

Infect Immun 64:2062–2069.

37. Shi L, Sohaskey CD, Kana BD, Dawes S, North RJ, Mizrahi V, Gennaro ML. 2005. Changes in energy metabolism of Mycobacterium tuberculosis in mouse lung and under in vitro conditions affecting aerobic respiration. Proc Natl Acad Sci U S A 102:15629–15634.

38. Muttucumaru DGN, Roberts G, Hinds J, Stabler RA, Parish T. 2004. Gene expression profile of Mycobacterium tuberculosis in a non-replicating state. Tuberculosis (Edinb) 84:239–246.

39. Singh A, Crossman DK, Mai D, Guidry L, Voskuil MI, Renfrow MB, Steyn AJC. 2009. Mycobacterium tuberculosis WhiB3 maintains redox homeostasis by regulating virulence lipid anabolism to modulate macrophage response. PLoS Pathog 5:e1000545.

40. Leistikow RL, Morton RA, Bartek IL, Frimpong I, Wagner K, Voskuil MI. 2010. The Mycobacterium tuberculosis DosR regulon assists in metabolic homeostasis and enables rapid recovery from nonrespiring dormancy. J Bacteriol 192:1662–1670.

41. Converse PJ, Karakousis PC, Klinkenberg LG, Kesavan AK, Ly LH, Allen SS, Grosset JH, Jain SK, Lamichhane G, Manabe YC, McMurray DN, Nuermberger EL, Bishai WR. 2009. Role of the dosR-dosS two-component regulatory system in Mycobacterium tuberculosis virulence in three animal models. Infect Immun 77:1230–1237.

42. Wayne LG, Lin KY. 1982. Glyoxylate metabolism and adaptation of Mycobacterium tuberculosis to survival under anaerobic conditions. Infect Immun

37:1042–1049.

43. Kerns PW, Ackhart DF, Basaraba RJ, Leid JG, Shirtliff ME. 2014. Mycobacterium tuberculosis pellicles express unique proteins recognized by the host humoral response. Pathog Dis 70:347–358.

44. Ojha AK, Baughn AD, Sambandan D, Hsu T, Trivelli X, Guerardel Y, Alahari A, Kremer L, Jacobs WR, Hatfull GF. 2008. Growth of Mycobacterium tuberculosis biofilms containing free mycolic acids and harbouring drug-tolerant bacteria. Mol Microbiol 69:164–174.

45. Kerns PW, Ackart DF, Basaraba RJ, Leid J, Mark E, Sciences B. 2014. Mycobacterium tuberculosis pellicles express unique proteins recognized by the host humoral response. Pathog Dis 70:347–358.

46. Sambandan D, Dao DN, Weinrick BC, Vilchèze C, Gurcha SS, Ojha A, Kremer L, Besra GS, Hatfull GF, Jacobs WR. 2013. Keto-mycolic acid-dependent pellicle formation confers tolerance to drug-sensitive Mycobacterium tuberculosis. MBio 4:e00222-13.

47. Pai M, Behr MA, Dowdy D, Dheda K, Divangahi M, Boehme CC, Swaminathan S, Spigelman M, Getahun H, Menzies D, Raviglione M. 2016. Tuberculosis. Nat Rev Dis Prim 2:1–23.

48. Armstrong JA. 1975. Phagosome-lysosome interactions in cultured macrophages infected with virulent tubercle bacilli. Reversal of the usual nonfusion pattern and observations on bacterial survival. J Exp Med 142:1–16.

49. Sturgill-Koszycki S, Schlesinger P, Chakraborty P, Haddix P, Collins H, Fok A, Allen R, Gluck S, Heuser J, Russell D. 1994. Lack of acidification in

Mycobacterium phagosomes produced by exclusion of the vesicular proton-ATPase. Science (80-) 263:678–681.

50. Wong D, Bach H, Sun J, Hmama Z, Av-Gay Y. 2011. Mycobacterium tuberculosis protein tyrosine phosphatase (PtpA) excludes host vacuolar-H+-ATPase to inhibit phagosome acidification. Proc Natl Acad Sci 108:19371–19376.

51. Bitter W, Houben ENG, Bottai D, Brodin P, Brown EJ, Cox JS, Derbyshire K, Fortune SM, Gao LY, Liu J, Van Pittius NCG, Pym AS, Rubin EJ, Sherman DR, Cole ST, Brosch R. 2009. Systematic genetic nomenclature for type VII secretion systems. PLoS Pathog 5:e1000507.

52. Sreejit G, Ahmed A, Parveen N, Jha V, Valluri VL, Ghosh S, Mukhopadhyay S. 2014. The ESAT-6 Protein of Mycobacterium tuberculosis Interacts with Beta-2-Microglobulin (β2M) Affecting Antigen Presentation Function of Macrophage. PLoS Pathog 10:e1004446.

53. Guinn KM, Hickey MJ, Mathur SK, Zakel KL, Grotzke JE, Lewinsohn DM, Smith S, Sherman DR. 2004. Individual RD1 -region genes are required for export of ESAT-6/CFP-10 and for virulence of Mycobacterium tuberculosis. Mol Microbiol 51:359–370.

54. Tufariello JM, Chapman JR, Kerantzas CA, Wong K-W, Vilchèze C, Jones CM, Cole LE, Tinaztepe E, Thompson V, Fenyö D, Niederweis M, Ueberheide B, Philips JA, Jacobs WR. 2016. Separable roles for *Mycobacterium tuberculosis* ESX-3 effectors in iron acquisition and virulence. Proc Natl Acad Sci 113:E348–E357.

55. Schaaf K, Smith SR, Duverger A, Wagner F, Wolschendorf F, Westfall AO,

Kutsch O, Sun J. 2017. Mycobacterium tuberculosis exploits the PPM1A signaling pathway to block host macrophage apoptosis. Sci Rep 7:42101.

56. Ernst JD. 2012. The immunological life cycle of tuberculosis. Nat Rev Immunol 12:581–591.

57. Hinchey J, Lee S, Jeon BY, Basaraba RJ, Venkataswamy MM, Chen B, Chan J, Braunstein M, Orme IM, Derrick SC, Morris SL, Jacobs WR, Porcelli SA. 2007. Enhanced priming of adaptive immunity by a proapoptotic mutant of Mycobacterium tuberculosis. J Clin Invest 117:2279–2288.

58. O'Garra A, Redford PS, McNab FW, Bloom CI, Wilkinson RJ, Berry MPR. 2013. The immune response in Tuberculosis. Annu Rev Immunol 31:475–527.

59. Danelishvili L, McGarvey J, Li Y, Bermudez LE. 2003. Mycobacterium tuberculosis infection causes different levels of apoptosis and necrosis in human macrophages and alveolar epithelial cells. Cell Microbiol 5:649–660.

60. Matthews K, Ntsekhe M, Syed F, Scriba T, Russell J, Tibazarwa K, Deffur A, Hanekom W, Mayosi BM, Wilkinson RJ, Wilkinson KA. 2012. HIV-1 infection alters CD4+memory T-cell phenotype at the site of disease in extrapulmonary tuberculosis. Eur J Immunol 42:147–157.

61. Harisinghani MG, McLoud TC, Shepard J-AO, Ko JP, Shroff MM, Mueller PR. 2000. Tuberculosis from head to toe. RadioGraphics 20:449–470.

62. Lönnroth K, Jaramillo E, Williams BG, Dye C, Raviglione M. 2009. Drivers of tuberculosis epidemics: the role of risk factors and social determinants. Soc Sci Med 68:2240–2246.

63. Cisneros JR, Murray KM. 1996. Corticosteroids in tuberculosis. Ann

Pharmacother 30:1298–1303.

64. Via LE, Lin PL, Ray SM, Carrillo J, Allen SS, Eum SY, Taylor K, Klein E, Manjunatha U, Gonzales J, Lee EG, Park SK, Raleigh JA, Cho SN, McMurray DN, Flynn JL, Barry CE. 2008. Tuberculous granulomas are hypoxic in guinea pigs, rabbits, and nonhuman primates. Infect Immun 76:2333–2340.

65. Capuano III S V, Croix D a, Pawar S, Zinovik A, Myers A, Lin PL, Fuhrman C, Klein E, Flynn JL, Bissel S. 2003. Experimental Mycobacterium tuberculosis infection of cynomolgus macaques closely resembles the various manifestations of human M. tuberculosis infection. Infect Immun 71:5831–5844.

66. Boehme CC, Nabeta P, Hillemann D, Nicol MP, Shenai S, Krapp F, Allen J, Tahirli R, Blakemore R, Rustomjee R, Milovic A, Jones M, O'Brien SM, Persing DH, Ruesch-Gerdes S, Gotuzzo E, Rodrigues C, Alland D, Perkins MD. 2010. Rapid molecular detection of tuberculosis and rifampin resistance. N Engl J Med 363:1005–1015.

67. Chakravorty S, Simmons AM, Rowneki M, Parmar H, Cao Y, Ryan J, Banada PP, Deshpande S, Shenai S, Gall A, Glass J, Krieswirth B, Schumacher SG, Nabeta P, Tukvadze N, Rodrigues C, Skrahina A, Tagliani E, Cirillo DM, Davidow A, Denkinger CM, Persing D, Kwiatkowski R, Jones M, Alland D. 2017. The New Xpert MTB/RIF Ultra: improving detection of Mycobacterium tuberculosis and resistance to rifampin in an assay suitable for Point-of-Care testing. MBio 8:e00812-17.

68. Andersen P, Munk ME, Pollock JM, Doherty TM. 2000. Specific immune-based diagnosis of tuberculosis. Lancet 356:1099–1104.

69. Nahid P, Dorman SE, Alipanah N, Barry PM, Brozek JL, Cattamanchi A, Chaisson LH, Chaisson RE, Daley CL, Grzemska M, Higashi JM, Ho CS, Hopewell PC, Keshavjee SA, Lienhardt C, Menzies R, Merrifield C, Narita M, O'Brien R, Peloquin CA, Raftery A, Saukkonen J, Schaaf HS, Sotgiu G, Starke JR, Migliori GB, Vernon A. 2016. Official American Thoracic Society/Centers for Disease Control and Prevention/Infectious Diseases Society of America Clinical Practice Guidelines: Treatment of Drug-Susceptible Tuberculosis. Clin Infect Dis 63:853–867.

70. World Health Organization WH, Global Tuberculosis Programme. 2016. WHO treatment guidelines for drug-resistant tuberculosis : 2016 update. Who 56.

71. Bloemberg, Guido, V., Gagneux, Sebastien., Bottger, Erik C. 2015. Acquired resistance to bedaquiline and delamanid in therapy for tuberculosis. N Engl J Med 373:1985–1986.

72. Colditz GA, Berkey CS, Mosteller F, Brewer TF, Wilson ME, Burdick E, Fineberg H V. 1995. The efficacy of bacillus Calmette-Guérin vaccination of newborns and infants in the prevention of tuberculosis: meta-analyses of the published literature. Pediatrics 96.

73. Fine PEM. 1995. Variation in protection by BCG: implications of and for heterologous immunity. Lancet 346:1339–1345.

74. Andersen P, Doherty TM. 2010. The success and failure of BCG — implications for a novel tuberculosis vaccine. Nat Rev Microbiol 3:656–662.

75. Gruber TM, Gross CA. 2003. Multiple sigma subunits and the partitioning of bacterial transcription space. Annu Rev Microbiol 57:441–466.

76. Cole ST, Brosch R, Parkhill J, Garnier T, Churcher C, Harris D, Gordon S V, Eiglmeier K, Gas S, Barry CE, Tekaia F, Badcock K, Basham D, Brown D, Chillingworth T, Connor R, Davies R, Devlin K, Feltwell T, Gentles S, Hamlin N, Holroyd S, Hornsby T, Jagels K, Krogh A, McLean J, Moule S, Murphy L, Oliver K, Osborne J, Quail MA, Rajandream MA, Rogers J, Rutter S, Seeger K, Skelton J, Squares R, Squares S, Sulston JE, Taylor K, Whitehead S, Barrell BG. 1998. Deciphering the biology of Mycobacterium tuberculosis from the complete genome sequence. Nature 393:537–544.

77. Francke C, Groot Kormelink T, Hagemeijer Y, Overmars L, Sluijter V, Moezelaar R, Siezen RJ. 2011. Comparative analyses imply that the enigmatic sigma factor 54 is a central controller of the bacterial exterior. BMC Genomics 12:385.

78. Rodrigue S, Provvedi R, Jacques P-E, Gaudreau L, Manganelli R. 2006. The sigma factors of Mycobacterium tuberculosis. FEMS Microbiol Rev 30:926–941.

79. Murakami KS, Masuda S, Darst SA. 2002. Structural basis of transcription initiation: RNA polymerase holoenzyme at 4 A resolution. Science 296:1280–1284.

80. Dombroski AJ, Walter WA, Gross CA. 1993. Amino-terminal amino acids modulate sigma-factor DNA-binding activity. Genes Dev 7:2446–2455.

81. Campbell EA, Muzzin O, Chlenov M, Sun JL, Olson CA, Weinman O, Trester-Zedlitz ML, Darst SA. 2002. Structure of the bacterial RNA polymerase promoter specificity σ Subunit. Mol Cell 9:527–539.

82. Sanderson A, Mitchell JE, Minchin SD, Busby SJW. 2003. Substitutions in the Escherichia coli RNA polymerase sigma70 factor that affect recognition of

extended -10 elements at promoters. FEBS Lett 544:199–205.

83. Campbell EA, Muzzin O, Chlenov M, Sun JL, Olson CA, Weinman O, Trester-Zedlitz ML, Darst SA. 2002. Structure of the bacterial RNA polymerase promoter specificity σ subunit. Mol Cell 9:527–539.

84. Sachdeva P, Misra R, Tyagi AK, Singh Y. 2010. The sigma factors of Mycobacterium tuberculosis: regulation of the regulators. FEBS J 277:605–626.

85. Manganelli R, Voskuil MI, Schoolnik GK, Smith I. 2001. The Mycobacterium tuberculosis ECF sigma factor sigmaE: role in global gene expression and survival in macrophages. Mol Microbiol 41:423–437.

86. He H, Hovey R, Kane J, Singh V, Zahrt TC. 2006. MprAB Is a stress responsive two-component system that directly regulates expression of sigma factors SigB and SigE in Mycobacterium tuberculosis. J Bacteriol 188:2134–2143.

87. Lee J-H, Karakousis PC, Bishai WR. 2008. Roles of SigB and SigF in the Mycobacterium tuberculosis Sigma Factor Network. J Bacteriol 190:699–707.

88. Williams EP, Lee J-H, Bishai WR, Colantuoni C, Karakousis PC. 2007. Mycobacterium tuberculosis SigF regulates genes encoding cell wall-associated proteins and directly regulates the transcriptional regulatory gene phoY1. J Bacteriol 189:4234–4242.

89. Manganelli R, Dubnau E, Tyagi S, Kramer FR, Smith I. 1999. Differential expression of 10 sigma factor genes in Mycobacterium tuberculosis. Mol Microbiol 31:715–724.

90. Lonetto MA, Brown KL, Rudd KE, Buttner MJ. 1994. Analysis of the Streptomyces coelicolor sigE gene reveals the existence of a subfamily of

eubacterial RNA polymerase sigma factors involved in the regulation of extracytoplasmic functions. Proc Natl Acad Sci 91:7573–7577.

91. Taranto MP, Vera JL, Hugenholtz J, De Valdez GF, Sesma F. 2003. Lactobacillus reuteri CRL1098 produces cobalamin. J Bacteriol 185:5643–5647.

92. Agarwal N, Woolwine SC, Tyagi S, Bishai WR. 2007. Characterization of the Mycobacterium tuberculosis sigma factor SigM by assessment of virulence and identification of SigM-dependent genes. Infect Immun 75:452–61.

93. Raman S, Hazra R, Dascher CC, Husson RN. 2004. Transcription regulation by the Mycobacterium tuberculosis alternative sigma factor SigD and its role in virulence†. J Bacteriol 186:6605–6616.

94. Manganelli R, Fattorini L, Tan D, Iona E, Orefici G, Altavilla G, Cusatelli P, Smith I. 2004. The extra cytoplasmic function sigma factor sigma(E) is essential for Mycobacterium tuberculosis virulence in mice. Infect Immun 72:3038–3041.

95. Dainese E, Rodrigue S, Delogu G, Provvedi R, Laflamme L, Brzezinski R, Fadda G, Smith I, Gaudreau L, Palù G, Manganelli R. 2006. Posttranslational regulation of Mycobacterium tuberculosis extracytoplasmic-function sigma factor sigma L and roles in virulence and in global regulation of gene expression. Infect Immun 74:2457–2461.

96. Gaudion A, Dawson L, Davis E, Smollett K. 2013. Characterisation of the mycobacterium tuberculosis alternative sigma factor SigG: Its operon and regulon. Tuberculosis 93:482–491.

97. Lee JH, Geiman DE, Bishai WR. 2008. Role of stress response sigma factor SigG in Mycobacterium tuberculosis. J Bacteriol 190:1128–1133.

98. Kaushal D, Schroeder BG, Tyagi S, Yoshimatsu T, Scott C, Ko C, Carpenter L, Mehrotra J, Manabe YC, Fleischmann RD, Bishai WR. 2002. Reduced immunopathology and mortality despite tissue persistence in a Mycobacterium tuberculosis mutant lacking alternative sigma factor, SigH. Proc Natl Acad Sci U S A 99:8330–8335.

99. Hu Y, Kendall S, Stoker NG, Coates ARM. 2004. The Mycobacterium tuberculosis sigJ gene controls sensitivity of the bacterium to hydrogen peroxide. FEMS Microbiol Lett 237:415–423.

100. Homerova D, Halgasova L, Kormanec J. 2008. Cascade of extracytoplasmic function sigma factors in Mycobacterium tuberculosis: Identification of a σJ-dependent promoter upstream of sigI. FEMS Microbiol Lett 280:120–126.

101. Wu CW, Schmoller SK, Sung JS, Talaat AM. 2007. Defining the stressome of Mycobacterium avium subsp. paratuberculosis in vitro and in naturally infected cows. J Bacteriol 189:7877–7886.

102. Veyrier F, Saïd-Salim B, Behr MA. 2008. Evolution of the mycobacterial SigK regulon. J Bacteriol 190:1891–1899.

103. Hahn M, Raman S, Anaya M, Husson RN. 2005. The Mycobacterium tuberculosis extracytoplasmic-function sigma factor SigL regulates polyketide synthases and secreted or membrane proteins and is required for virulence. J Bacteriol 187:7062–7071.

104. Agarwal N, Tyagi AK. 2006. Mycobacterial transcriptional signals: requirements for recognition by RNA polymerase and optimal transcriptional activity. Nucleic Acids Res 34:4245–57.

105. Raman S, Puyang X, Cheng TY, Young DC, Moody DB, Husson RN. 2006. Mycobacterium tuberculosis SigM positively regulates Esx secreted protein and nonribosomal peptide synthetase genes and down regulates virulence-associated surface lipid synthesis. J Bacteriol 188:8460–8468.

106. Cole ST, Eiglmeier K, Parkhill J, James KD, Thomson NR, Wheeler PR, Honoré N, Garnier T, Churcher C, Harris D, Mungall K, Basham D, Brown D, Chillingworth T, Connor R, Davies RM, Devlin K, Duthoy S, Feltwell T, Fraser A, Hamlin N, Holroyd S, Hornsby T, Jagels K, Lacroix C, Maclean J, Moule S, Murphy L, Oliver K, Quail MA, Rajandream MA, Rutherford KM, Rutter S, Seeger K, Simon S, Simmonds M, Skelton J, Squares R, Squares S, Stevens K, Taylor K, Whitehead S, Woodward JR, Barrell BG. 2001. Massive gene decay in the leprosy bacillus. Nature 409:1007–1011.

107. Waagmeester A, Thompson J, Reyrat J-M. 2005. Identifying sigma factors in Mycobacterium smegmatis by comparative genomic analysis. Trends Microbiol 13:505–509.

108. Park J-H, Roe J-H. 2008. Mycothiol regulates and is regulated by a thiol-specific antisigma factor RsrA and sigma(R) in Streptomyces coelicolor. Mol Microbiol 68:861–870.

109. Campbell EA, Tupy JL, Gruber TM, Wang S, Sharp MM, Gross CA, Darst SA. 2003. Crystal structure of Escherichia coli σE with the cytoplasmic domain of its anti-σ RseA. Mol Cell 11:1067–1078.

110. Wagner D, Maser J, Lai B, Cai Z, Barry CE, Höner K, David G, Bermudez LE, Iii CEB. 2005. Elemental Analysis of Mycobacterium avium-, Mycobacterium

tuberculosis-, and Mycobacterium smegmatis-containing phagosomes indicates pathogen-Induced microenvironments within the host cell's endosomal system. J Immunol 174:1491–1500.

111. Festa RA, Jones MB, Butler-Wu S, Sinsimer D, Gerads R, Bishai WR, Peterson SN, Darwin KH. 2011. A novel copper-responsive regulon in Mycobacterium tuberculosis. Mol Microbiol 79:133–148.

112. Liu T, Ramesh A, Ma Z, Ward SK, Zhang L, George GN, Talaat AM, Sacchettini JC, Giedroc DP. 2007. CsoR is a novel Mycobacterium tuberculosis copper-sensing transcriptional regulator. Nat Chem Biol 3:60–68.

113. Ward SK, Abomoelak B, Hoye EA, Steinberg H, Talaat AM. 2010. CtpV: A putative copper exporter required for full virulence of Mycobacterium tuberculosis. Mol Microbiol 77:1096–1110.

114. Wolschendorf F, Ackart D, Shrestha TB, Hascall-Dove L, Nolan S, Lamichhane G, Wang Y, Bossmann SH, Basaraba RJ, Niederweis M. 2011. Copper resistance is essential for virulence of Mycobacterium tuberculosis. Proc Natl Acad Sci U S A 108:1621–1626.

115. Piddington DL, Fang FC, Laessig T, Cooper AM, Orme IM, Buchmeier NA. 2001. Cu,Zn superoxide dismutase of Mycobacterium tuberculosis contributes to survival in activated macrophages that are generating an oxidative burst. Infect Immun 69:4980–4987.

116. Shi L, Jung Y-J, Tyagi S, Gennaro ML, North RJ. 2003. Expression of Th1-mediated immunity in mouse lungs induces a Mycobacterium tuberculosis transcription pattern characteristic of nonreplicating persistence. Proc Natl Acad

Sci 100:241–246.

117. Linder M, Hazegh-Azam M. 1996. Copper biochemistry and molecular biology. Am J Clin Nutr 63:797–811.

118. Rae TD, Schmidt PJ, Pufahl RA, Culotta VC, O'Halloran T V. 1999. Undetectable intracellular free copper: The requirement of a copper chaperone for superoxide dismutase. Science (80-) 284:805–808.

119. Bertinato J, L'Abbé MR. 2004. Maintaining copper homeostasis: regulation of copper-trafficking proteins in response to copper deficiency or overload. J Nutr Biochem 15:316–322.

120. Minot GR, Murphy WP. 1926. Treatment of pernicious anemia by a special diet. JAMA J Am Med Assoc 87:470–476.

121. Hodgkin, Dorothy Crowfoot, F.R.S., Kamper, Jennifer, Lindsey, June, MacKay, Maureen, Pickworth, Jenny, Robertson, J.H. Shoemaker, Clara Brink, White, J.G., Prosen, R.J. TKN. 1957. The Structure of Vitamin B12 I. An outline of the crystallographic investigation of vitamin B12. Proc R Soc London 228–263.

122. Warren MJ, Raux E, Schubert HL, Escalante-Semerena JC. 2002. The biosynthesis of adenosylcobalamin (vitamin B12). Nat Prod Rep 19:390–412.

123. Raux E, Schubert HL, Warren* MJ. 2000. Biosynthesis of cobalamin (vitamin B12): a bacterial conundrum. Cell Mol Life Sci 57:1880–1893.

124. Jeong J, Park J, Park J, Kim J. 2014. Processing of glutathionylcobalamin by a bovine B12 trafficking chaperone bCblC involved in intracellular B12 metabolism. Biochem Biophys Res Commun 443:173–178.

125. Mancia F, Keep NH, Nakagawa A, Leadlay PF, McSweeney S, Rasmussen B,

secke PB, Diat O, Evans PR. 1996. How coenzyme B12 radicals are generated: the crystal structure of methylmalonyl-coenzyme A mutase at 2 å resolution. Structure 4:339–350.

126. Cheong CG, Escalante-Semerena JC, Rayment I. 2001. Structural investigation of the biosynthesis of alternative lower ligands for cobamides by nicotinate mononucleotide: 5,6-dimethylbenzimidazole phosphoribosyltransferase from Salmonella enterica. J Biol Chem 276:37612–37620.

127. Young DB, Comas I, de Carvalho LPS. 2015. Phylogenetic analysis of vitamin B12-related metabolism in Mycobacterium tuberculosis. Front Mol Biosci 2:1–14.

128. Drennan CL, Matthews RG, Ludwig ML. 1994. Cobalamin-dependent methionine synthase: the structure of a methylcobalamin-binding fragment and implications for other B12-dependent enzymes. Curr Opin Struct Biol 4:919–929.

129. Ferla MP, Patrick WM. 2014. Bacterial methionine biosynthesis. Microbiology 160:1571–1584.

130. Moosa A. 2012. PhD Thesis. Molecular mechanisms of transport and metabolism of vitamin B 12 in mycobacteria. University of the Witwatersrand, Johannesburg.

131. Chowdhury S, Thomas MG, Escalante-Semerena JC, Banerjee R. 2001. The coenzyme B12 analog 5′-deoxyadenosylcobinamide-GDP supports catalysis by methylmalonyl-CoA mutase in the absence of trans-ligand coordination. J Biol Chem 276:1015–1019.

132. Blakley RL. 1965. Cobamides and ribonucleotide reduction. I. Cobamide stimulation of ribonucleotide reduction in extracts of lactobacillus leichmannii. J Biol Chem 240:2173–2180.

133. Banerjee R, Ragsdale SW. 2003. The many faces of vitamin B12: catalysis by cobalamin-dependent enzymes. Annu Rev Biochem 72:209–247.

134. Warren MJ, Escalante-Semerena JC. 2008. Biosynthesis and use of cobalamin (B12). EcoSal Plus 1.

135. Van Bibber M, Bradbeer C, Clark N, Roth JR. 1999. A new class of cobalamin transport mutants (btuF) provides genetic evidence for a periplasmic binding protein in Salmonella typhimurium. J Bacteriol 181:5539–41.

136. Wuerges J, Garau G, Geremia S, Fedosov SN, Petersen TE, Randaccio L. 2006. Structural basis for mammalian vitamin B12 transport by transcobalamin. Proc Natl Acad Sci U S A 103:4386–4391.

137. Gopinath K, Venclovas C, Ioerger TR, Sacchettini JC, McKinney JD, Mizrahi V, Warner DF. 2013. A vitamin B_{12} transporter in Mycobacterium tuberculosis. Open Biol 3:120175.

138. Woodson JD, Escalante-Semerena JC. 2004. CbiZ, an amidohydrolase enzyme required for salvaging the coenzyme B12 precursor cobinamide in archaea. Proc Natl Acad Sci U S A 101:3591–3596.

139. Gray MJ, Escalante-Semerena JC. 2009. The cobinamide amidohydrolase (cobyric acid-forming) CbiZ enzyme: a critical activity of the cobamide remodelling system of Rhodobacter sphaeroides. Mol Microbiol 74:1198–1210.

140. Gray MJ, Escalante-Semerena JC. 2009. In vivo analysis of cobinamide salvaging in Rhodobacter sphaeroides strain 2.4.1. J Bacteriol 191:3842–51.

141. Rodionov DA, Vitreschak AG, Mironov AA, Gelfand MS. 2003. Comparative genomics of the vitamin B12 metabolism and regulation in prokaryotes. J Biol

Chem 278:41148–41159.

142. Raux E, Thermes C, Heathcote P, Rambach A, Warren MJ. 1997. A role for Salmonella typhimurium cbiK in cobalamin (vitamin B12) and siroheme biosynthesis. J Bacteriol 179:3202–3212.

143. Leech HK, Raux-Deery E, Heathcote P, Warren MJ. 2002. Production of cobalamin and sirohaem in Bacillus megaterium: an investigation into the role of the branchpoint chelatases sirohydrochlorin ferrochelatase (SirB) and sirohydrochlorin cobalt chelatase (CbiX). Biochem Soc Trans 30:610–613.

144. Debussche L, Couder M, Thibaut D, Cameron B, Crouzet J, Blanche F. 1992. Assay, purification, and characterization of cobaltochelatase, a unique complex enzyme catalyzing cobalt insertion in hydrogenobyrinic acid a,c-diamide during coenzyme B12 biosynthesis in Pseudomonas denitrificans. J Bacteriol 174:7445–7451.

145. White C, Lee J, Kambe T, Fritsche K, Petris MJ. 2009. A role for the ATP7A copper-transporting ATPase in macrophage bactericidal activity. J Biol Chem 284:33949–33956.

146. Ward SK, Abomoelak B, Hoye EA, Steinberg H, Talaat AM. 2010. CtpV: a putative copper exporter required for full virulence of Mycobacterium tuberculosis. Mol Microbiol 77:1096–1110.

147. Allen BW. 1998. Mycobacteria: General Culture Methodology and Safety Considerations, p. 15–30. *In* Mycobacteria Protocols. Humana Press, New Jersey.

148. Marcos-Torres FJ, Perez J, Gomez-Santos N, Moraleda-Munoz A, Munoz-Dorado J. 2016. In depth analysis of the mechanism of action of metal-dependent sigma

factors: Characterization of CorE2 from Myxococcus xanthus. Nucleic Acids Res 44:5571–5584.

149. Gómez-Santos N, Pérez J, Sánchez-Sutil MC, Moraleda-Muñoz A, Muñoz-Dorado J. 2011. Core from Myxococcus xanthus is a Copper-Dependent RNA polymerase sigma factor. PLoS Genet 7.

150. Thakur KG, Gopal B. 2005. Crystallization and preliminary X-ray diffraction studies of two domains of a bilobed extra-cytoplasmic function sigma factor SigC from Mycobacterium tuberculosis. Acta Crystallogr Sect F Struct Biol Cryst Commun 61:779–781.

151. Worawan, M., Zenner, C. Z., Ogden KL. 2008. Removal efficiency and binding mechanisms of copper and copper-EDTA complexes using polyethyleneimine. Environ Sci Technol 42:2124–2129.

152. Farhana A, Guidry L, Srivastava A, Singh A, Hondalus MK, Steyn AJC. 2010. Reductive stress in microbes: Implications for understanding mycobacterium tuberculosis disease and persistenceAdvances in Microbial Physiology.

153. Jacques J-F, Rodrigue S, Brzezinski R, Gaudreau L, Artsimovitch I, Svetlov V, Anthony L, Burgess R, Landick R, Beaucher J, Rodrigue S, Jacques P, Smith I, Brzezinski R, Gaudreau L, Cole S, Brosch R, Parkhill J, DeMaio J, Zhang Y, Ko C, Young D, Bishai W, Dye C, Scheele S, Dolin P, Pathania V, Raviglione M, Ghosh P, Ishihama A, Chatterji D, Gruber T, Gross C, Jacques P, Gervais A, Cantin M, Lucier J, Dallaire G, Drouin G, Gaudreau L, Goulet J, Brzezinski R, Kenney T, Churchward G, Lohrke S, Nechaev S, Yang H, Severinov K, Jin S, Manganelli R, Voskuil M, Schoolnik G, Smith I, Manganelli R, Voskuil M,

Schoolnik G, Dubnau E, Gomez M, Smith I, Manganelli R, Provvedi R, Rodrigue S, Beaucher J, Gaudreau L, Smith I, Mencia M, Monsalve M, Rojo F, Salas M, Mukherjee K, Nagai H, Shimamoto N, Chatterji D, Paget M, Helmann J, Peck M, Gaal T, Fisher R, Gourse R, Long S, Predich M, Doukhan L, Nair G, Smith I, Raman S, Song T, Puyang X, Bardarov S, Jacobs W, Husson R, Raman S, Hazra R, Dascher C, Husson R, Roberts E, Clark A, McBeth S, Friedman R, Snapper S, Melton R, Mustafa S, Kieser T, Jacobs W, Song T, Dove S, Lee K, Husson R, Steffen P, Ullmann A, Sun R, Converse P, Ko C, Tyagi S, Morrison N, Bishai W, Tang H, Severinov K, Goldfarb A, Ebright R. 2006. A recombinant Mycobacterium tuberculosis in vitro transcription system. FEMS Microbiol Lett 255:140–7.

154. Jeong J, Park J, Park J, Kim J. 2014. Processing of glutathionylcobalamin by a bovine B12 trafficking chaperone bCblC involved in intracellular B12 metabolism. Biochem Biophys Res Commun 443:173–178.

155. Vitreschak AG, Rodionov DA, Mironov AA, Gelfand MS. 2003. Regulation of the vitamin B12 metabolism and transport in bacteria by a conserved RNA structural element. RNA 9:1084–1097.

156. Warner DF, Savvi S, Mizrahi V, Dawes SS. 2007. A riboswitch regulates expression of the coenzyme B12-independent methionine synthase in Mycobacterium tuberculosis: implications for differential methionine synthase function in strains H37Rv and CDC1551. J Bacteriol 189:3655–3659.

157. Griffin JE, Pandey AK, Gilmore SA, Mizrahi V, McKinney JD, Bertozzi CR, Sassetti CM. 2012. Cholesterol catabolism by Mycobacterium tuberculosis

requires transcriptional and metabolic adaptations. Chem Biol 19:218–227.

158. Kapopoulou A, Lew JM C ST. 2011. The MycoBrowser portal: a comprehensive and manually annotated resource for mycobacterial genomes. Tuberc Jan 91(1):8–13.

159. Rachman H, Strong M, Ulrichs T, Grode L, Schuchhardt J, Mollenkopf H-J, Kosmiadi GA, Eisenberg D, Kaufmann. 2006. Unique Transcriptome Signature of Mycobacterium tuberculosis in Pulmonary Tuberculosis. Infect Immun 74:1233–1242.

160. Målen H, Berven FS, Fladmark KE, Wiker HG. 2007. Comprehensive analysis of exported proteins from Mycobacterium tuberculosis H37Rv. Proteomics 7:1702–1718.

161. Voskuil MI, Visconti KC, Schoolnik GK. 2004. Mycobacterium tuberculosis gene expression during adaptation to stationary phase and low-oxygen dormancy. Tuberculosis (Edinb) 84:218–227.

162. Debussche L, Thibaut D, Cameron B, Crouzet J, Blanche F. 1993. Biosynthesis of the corrin macrocycle of coenzyme B12 in Pseudomonas denitrificans. J Bacteriol 175:7430–7440.

163. Moore SJ, Lawrence AD, Biedendieck R, Deery E, Frank S, Howard MJ, Rigby SEJ, Warren MJ. 2013. Elucidation of the anaerobic pathway for the corrin component of cobalamin (vitamin B12). Proc Natl Acad Sci 110:14906–14911.

164. Escalante-Semerena JC. 2007. Conversion of cobinamide into adenosylcobamide in bacteria and archaea. J Bacteriol 189:4555–60.

165. Moore SJ, Warren MJ. 2012. The anaerobic biosynthesis of vitamin B12. Biochem

Soc Trans 40:581–586.

166. Woodson JD, Zayas CL, Escalante-Semerena JC. 2003. A New Pathway for Salvaging the Coenzyme B12 Precursor Cobinamide in Archaea Requires Cobinamide-Phosphate Synthase (CbiB) Enzyme Activity. J Bacteriol 185:7193–7201.

167. Gray MJ, Tavares NK, Escalante-Semerena JC. 2008. The genome of Rhodobacter sphaeroides strain 2.4.1 encodes functional cobinamide salvaging systems of archaeal and bacterial origins. Mol Microbiol 70:824–836.

168. Datsenko KA, Wanner BL. 2000. One-step inactivation of chromosomal genes in Escherichia coli K-12 using PCR products. Proc Natl Acad Sci U S A 97:6640–6645.

169. Vogel HJ, Bonner M. 1956. Acetylornithinase purification. J Biol Chem 218:97–106.

170. Price-Carter M, Tingey J, Bobik TA, Roth JR. 2001. The alternative electron acceptor tetrathionate supports B12-dependent anaerobic growth of Salmonella enterica serovar typhimurium on ethanolamine or 1,2-propanediol. J Bacteriol 183:2463–2475.

171. Crouzet J, Cameron B, Cauchois L, Rigault S, Rouyez MC, Blanche F, Thibaut D, Debussche L. 1990. Genetic and sequence analysis of an 8.7-kilobase Pseudomonas dentrificans fragment carrying eight genes involved in transformation of precorrin-2 to cobyrinic acid. J Bacteriol 172:5980–5990.

172. Goldman BS, Roth JR. 1993. Genetic structure and regulation of the cysG gene in Salmonella typhimurium. J Bacteriol 175:1457–1466.

173. Beck R, Raux E, Thermes C, Rambach A, Warren M. 1997. CbiX: a novel metal-binding protein involved in sirohaem biosynthesis in Bacillus megaterium. Biochem Soc Trans 25:77S.

174. Raux E, Lanois A, Warren MJ, Rambach A, Thermes C. 1998. Cobalamin (vitamin B12) biosynthesis: identification and characterization of a Bacillus megaterium cobI operon. Biochem J 335:159–66.

175. Cossu A, Sechi LA, Zanetti S, Rosu V. 2012. Gene expression profiling of Mycobacterium avium subsp. paratuberculosis in simulated multi-stress conditions and within THP-1 cells reveals a new kind of interactive intramacrophage behaviour. BMC Microbiol 12:87.

176. Raux E, Lanois A, Levillayer F, Warren MJ, Brody E, Rambach A, Thermes C. 1996. Salmonella typhimurium cobalamin (vitamin B12) biosynthetic genes: functional studies in S. typhimurium and Escherichia coli. J Bacteriol 178:753–767.

177. Kajiwara Y, Santander PJ, Roessner CA, Pé Rez LM, Scott AI. 2006. Genetically Engineered Synthesis and Structural Characterization of Cobalt-Precorrin 5A and -5B, Two New Intermediates on the Anaerobic Pathway to Vitamin B 12 : Definition of the Roles of the CbiF and CbiG Enzymes. J Am Chem Soc 128:9971–9978.

178. Boritsch EC, Supply P, Honoré N, Seeman T, Stinear TP, Brosch R. 2014. A glimpse into the past and predictions for the future: The molecular evolution of the tuberculosis agent. Mol Microbiol 93:835–852.

179. Gopinath K, Moosa A, Mizrahi V, Warner DF. 2013. Vitamin B 12 metabolism in

mycobacterium tuberculosis 1405–1418.

180. Deery E, Schroeder S, Lawrence AD, Taylor SL, Seyedarabi A, Waterman J, Wilson KS, Brown DG, Geeves M a., Howard MJ, Pickersgill RW, Warren MJ. 2012. An enzyme-trap approach allows isolation of intermediates in cobalamin biosynthesis. Nat Chem Biol 8:933–940.

181. Roth JR, Lawrence JG, Rubenfield M, Kieffer-Higgins S, Church GM. 1993. Characterization of the cobalamin (vitamin B12) biosynthetic genes of Salmonella typhimurium. J Bacteriol 175:3303–3316.

182. Debuscche L, Thibaut D, Cameron B, Crouzet J, Blanche F. 1990. Purification and characterization of cobyrinic acid a,c-diamide synthase from Pseudomonas denitrificans. J Bacteriol 172:6239–6244.

183. Heldt D, Lawrence a D, Lindenmeyer M, Deery E, Heathcote P, Rigby SE, Warren MJ. 2005. Aerobic synthesis of vitamin B12: ring contraction and cobalt chelation. Biochem Soc Trans 33:815–819.

184. Fonseca M V, Escalante-Semerena JC. 2000. Reduction of cob(III)alamin to cob(II)alamin in Salmonella enterica serovar typhimurium LT2. J Bacteriol 182:4304–4309.

185. Taga ME, Larsen NA, Howard-Jones AR, Walsh CT, Walker GC. 2007. BluB cannibalizes flavin to form the lower ligand of vitamin B12. Nature 446:449–453.

186. Campbell GRO, Taga ME, Mistry K, Lloret J, Anderson PJ, Roth JR, Walker GC. 2006. Sinorhizobium meliloti bluB is necessary for production of 5,6-dimethylbenzimidazole, the lower ligand of B12. Proc Natl Acad Sci U S A 103:4634–9.

187. Blanche F, Maton L, Debussche L, Thibaut D. 1992. Purification and characterization of Cob(II)yrinic acid a,c-diamide reductase from Pseudomonas denitrificans. J Bacteriol 174:7452–7454.

188. Escalante-Semerena JC, Suh SJ, Roth JR. 1990. cobA function is required for both de novo cobalamin biosynthesis and assimilation of exogenous corrinoids in Salmonella typhimurium. J Bacteriol 172:273–280.

189. Suh S-J, Escalante-Semerena JC. 1993. Cloning, sequencing and overexpression of cob A which encodes ATP:corrinoid adenosyltranferase in Salmonella typhimurium. Gene 129:93–97.

190. Galperin MY, Grishin N V. 2000. The synthetase domains of cobalamin biosynthesis amidotransferases cobB and cobQ belong to a new family of ATP-dependent amidoligases, related to dethiobiotin synthetase. Proteins 41:238–47.

191. Brushaber KR, O'Toole GA, Escalante-Semerena JC. 1998. CobD, a Novel Enzyme with L-Threonine-O-3-phosphate Decarboxylase Activity, Is Responsible for the Synthesis of (R)-1-Amino-2-propanol O-2-Phosphate, a Proposed New Intermediate in Cobalamin Biosynthesis in Salmonella typhimurium LT2. J Biol Chem 273:2684–2691.

192. Zayas CL, Claas K, Escalante-Semerena JC. 2007. The CbiB protein of Salmonella enterica is an integral membrane protein involved in the last step of the de novo corrin ring biosynthetic pathway. J Bacteriol 189:7697–7708.

193. O'Toole GA, Escalante-Semerena JC. 1995. Purification and Characterization of the Bifunctional CobU Enzyme of Salmonella typhimurium LT2: Evidence for a CobU-GMP Intermediate. J Biol Chem 270:23560–23569.

194. Trzebiatowski JR, O'Toole GA, Escalante-Semerena JC. 1994. The cobT Gene of Salmonella typhimurium Encodes the NaMN: 5,6-Dimethylbenzimidazole Phosphoribosyltransferase Responsible for the Synthesis of Nl-(5-Phospho-x-D-Ribosyl)- 5,6-Dimethylbenzimidazole, an Intermediate in the Synthesis of the Nucleotide Loop o. J Bacteriol 176:3568–3575.

195. Crofts TS, Seth EC, Hazra AB, Taga ME. 2013. Cobamide structure depends on both lower ligand availability and CobT substrate specificity. Chem Biol 20:1265–1274.

196. Chan CH, Newmister SA, Talyor K, Claas KR, Rayment I, Escalante-Semerena JC. 2014. Dissecting cobamide diversity through structural and functional analyses of the base-activating CobT enzyme of Salmonella enterica. Biochim Biophys Acta 1840:464–475.

197. Zayas CL, Escalante-Semerena JC. 2007. Reassessment of the late steps of coenzyme B12 synthesis in Salmonella enterica: evidence that dephosphorylation of adenosylcobalamin-5'-phosphate by the CobC phosphatase is the last step of the pathway. J Bacteriol 189:2210–2218.

198. Watkins HA, Baker EN. 2010. Structural and functional characterization of an RNase HI domain from the bifunctional protein Rv2228c from Mycobacterium tuberculosis. J Bacteriol 192:2878–2886.

199. Maggio-Hall L a, Escalante-Semerena JC. 1999. In vitro synthesis of the nucleotide loop of cobalamin by Salmonella typhimurium enzymes. Proc Natl Acad Sci U S A 96:11798–803.

200. O'Toole GA, Escalante-Semerena JC. 1993. cobU-dependent assimilation of

nonadenosylated cobinamide in cobA mutants of Salmonella typhimurium. J Bacteriol 175:6328–6336.

201. Roof DM, Roth JR. 1989. Functions required for vitamin B12-dependent ethanolamine utilization in Salmonella typhimurium. J Bacteriol 171:3316–3323.

202. O'Toole GA, Rondon MR, Escalante-Semerena JC. 1993. Analysis of mutants of Salmonella typhimurium defective in the synthesis of the nucleotide loop of cobalamin. J Bacteriol 175:3317–3326.

203. Grabau C, Roth JR. 1992. A Salmonella typhimurium cobalamin-deficient mutant blocked in 1-amino- 2-propanol synthesis. J Bacteriol 174:2138–2144.

204. O'Toole GA, Trzebiatowski JR, Escalante-Semerena JC. 1994. The cobC gene of Salmonella typhimurium codes for a novel phosphatase involved in the assembly of the nucleotide loop of cobalamin. J Biol Chem 269:26503–26511.

205. Thomas MG, Escalante-Semerena JC. 2000. Identification of an Alternative Nucleoside Triphosphate: 5'-Deoxyadenosylcobinamide Phosphate Nucleotidyltransferase in Methanobacterium thermoautotrophicum Delta H. J Bacteriol 182:4227–4233.

206. Dussurget O, Stewart G, Neyrolles O, Pescher P, Young D, Marchal G. 2001. Role of Mycobacterium tuberculosis copper-zinc superoxide dismutase. Infect Immun 69:529–33.

207. Ulrichs T, Kaufmann SHE. 2006. New insights into the function of granulomas in human tuberculosis. J Pathol 208:261–269.

208. Fine-Coulson K, Reaves BJ, Karls RK, Quinn FD. 2012. The role of lipid raft aggregation in the infection of type II pneumocytes by Mycobacterium

tuberculosis. PLoS One 7:e45028.

209. Fine-Coulson K, Giguère S, Quinn FD, Reaves BJ. 2015. Infection of A549 human type II epithelial cells with Mycobacterium tuberculosis induces changes in mitochondrial morphology, distribution and mass that are dependent on the early secreted antigen, ESAT-6. Microbes Infect 1–9.

210. Hernández-Pando R, Jeyanathan M, Mengistu G, Aguilar D, Orozco H, Harboe M, Rook GAW, Bjune G. 2000. Persistence of DNA from Mycobacterium tuberculosis in superficially normal lung tissue during latent infection. Lancet 356:2133–2138.

211. Målen H, Berven FS, Fladmark KE, Wiker HG. 2007. Comprehensive analysis of exported proteins from Mycobacterium tuberculosis H37Rv. Proteomics 7:1702–1718.

212. Dawes SS, Warner DF, Tsenova L, Timm J, McKinney JD, Kaplan G, Rubin H, Mizrahi V. 2003. Ribonucleotide reduction in Mycobacterium tuberculosis: function and expression of genes encoding class Ib and class II ribonucleotide reductases. Infect Immun 71:6124–6131.

213. Voskuil MI. 2004. Mycobacterium tuberculosis gene expression during environmental conditions associated with latency. Tuberculosis (Edinb) 84:138–143.